20th NRB
2015 FINLAND

20th International Northern Research Basins Symposium and Workshop

Kuusamo, Finland, August 16–21, 2015

Proceedings

Editors: Johanna Korhonen and Esko Kuusisto

Proceedings

20th International Northern Research Basins Symposium and Workshop

Kuusamo, Finland – August 16–21, 2015

Editors:

Johanna Korhonen and Esko Kuusisto

Finnish Environment Institute (SYKE)

Proceedings
20th International Northern Research Basins Symposium and Workshop
Kuusamo, Finland – August 16–21, 2015

Contact:
Johanna Korhonen
Finnish Environment Institute (SYKE)
P.O. Box 140
00251 Helsinki
FINLAND
johanna.korhonen@ymparisto.fi

www.syke.fi/20thnrb

ISBN 978-952-11-4512-4

ISBN 978-952-11-4513-1 (PDF)

Cover design: Erika Várkonyi

Table of Contents

Preface

It is a pleasure to host the 20th International Northern Research Basins (NRB) Symposium and Workshop in Kuusamo, which is one of the snowiest places in Finland. Kuusamo is renowned for its natural beauty, it is a region of fells and forests in an almost untouched wilderness adorned by lakes, rivers and rapids. In addition, Kuusamo is one of the most well-known nature photography locations in Europe.

In 1975, the International Hydrological Program (IHP) National Committees of Canada, Denmark/Greenland, Finland, Norway, Sweden, the USA and the USSR established the IHP working group on Northern Research Basins. The overall objective of the NRB working group is to encourage research in hydrological basins at northern latitudes where snow, ice and frozen ground have a dominant role in the hydrological cycle. In 1992, Iceland joined the group and Russia took over the responsibilities of the former USSR. In addition, countries with polar research programs are eligible for associate membership. The objectives of the NRB Working Group have evolved over the years as follows:

1. To gain a better understanding of hydrologic processes, particularly those in which snow, ice, and frozen ground have a major influence on the hydrological regime, and to determine the relative importance of each component of the water balance.
2. To provide data for the development and testing of transposable models which may be applied to regional, national, and international water and land resource programs.
3. To relate hydrologic processes to the chemical and biological evolution of northern basins.
4. To assess and predict the effect of human activities on the hydrologic regime in northern environments.
5. To encourage the exchange of personnel (technicians, scientists, research officers, and others) among participating countries.
6. To provide information for the improvement and standardization of measurement techniques and network design in northern regions.
7. To encourage exchange of information on a regular basis, and
8. To set up task forces to promote research initiatives on topics of special interest to northern research basins.

Nineteen productive symposia/workshops have been held to date:

Edefors, Sweden (1975); Fairbanks, USA (1977); Québec City, Canada (1979); Ullensvang, Norway (1982); Vierumäki, Finland (1984); Houghton, USA (1986); Ilulissat, Greenland (1988); Abisco, Sweden (1990); Whitehorse-Dawson-Inuvik, Canada (1992); Spitsbergen, Norway (1994); Prudhoe Bay-Fairbanks, USA (1997); Reykjavik-Kirkjubærjarklaustur, Iceland (1999); Saariselkä-Murmansk, Finland/Russia (2001); Kangerlussuaq, Greenland/Denmark (2003); Luleå-Kvikkjokk, Sweden (2005): Karelia, Russia (2007); Eastern Arctic, Canada (2009); Bergen-Geiranger-Loen-Fjærland-Voss, Norway (2011); South-central Alaska, USA (2013).

I am a veteran of the first 13 NRB symposia/workshops, after that I have not participated any of them. It is a great pleasure to be back in the 20th NRB, which will also celebrate the forty year history of these events. It is therefore good time to have a look at the history – and set new milestones for future research.

Forty years ago no one was talking on climate change, with the exception of some speculations on a new "Little Ice Age" being ahead of us, because of a slight cooling trend. No one could anticipate the huge technical development in measuring techniques, satellite technology, data transmission and storage, etc.

The future challenges are plentiful. In Finland the main challenge right now is the diminishing of financial resources; direct budget funding for research institutes and universities is decreasing and competition on funding is hard. This is affecting both water research and particularly monitoring. The future of hydrological networks is very uncertain. New techniques will help to some extent – if there is money to continue this development. However, in-situ observations are still needed in the future for validation and calibration of new methods.

The main subject of the 20th International NRB Symposium and Workshop is "The value of hydrological information". As in all previous NRB symposia/workshops, general sessions on aspects related to snow, ice and frozen ground are included in the program. These sessions include e.g. papers related to "Climate change impacts on arctic environment", "New techniques in northern hydrological studies" and "Role of snow and ice in northern hydrology".

Acknowledgments

The organizers of the 20th International NRB Symposium and Workshop would like to thank the following organizations for their contributions and sponsorship:

- Ministry of Agriculture and Forestry (MMM)
- Maa- ja vesitekniikan tuki ry.
- Maj and Tor Nessling Foundation
- Nordic Association for Hydrology (NHF)
- Federation of Finnish Learned Societies
- Finnish Association for Geophysicists

Without the generous support of these organizations, this event would not have occurred. Special recognition is given to all who helped with the production of this symposium and workshop. Graphic designer Erika Varkonyi created the logo and symposium visual materials, designed proceedings cover and did layout. Undergraduate student Noora Haavisto joined the organizers this summer and assisted organizing of the symposium. Financial Services team at SYKE and financial officer Mika Visuri have helped with registration fee payments and sorting out finances and all the fiscal matters for the event. Secretarial personnel at SYKE have assisted with travel arrangements. The work of all these individuals is extremely appreciated.

On behalf of the 20th International NRB organizing committee,

Esko Kuusisto and Johanna Korhonen

THE ORGANIZING COMMITTEE FOR THE 20TH INTERNATIONAL NRB:

Johanna Korhonen (Chair & Finland Chief delegate)
Head of hydrological monitoring, Freshwater Centre, Finnish Environment Institute
Dr. Esko Kuusisto
Leading hydrologist, Freshwater Centre, Finnish Environment Institute
Prof. Matti Leppäranta
Department of Physics, University of Helsinki
Prof. Harri Koivusalo
Aalto University, Water Resources Engineering
Prof. Björn Klöve,
Oulu University, Water Resources and Environmental Engineering Laboratory
Dr. Riku Paavola
Director of Oulanka research station, University of Oulu

List of Participants

CANADA:

Barrett, David
University of Victoria
3800 Finnerty Road
V8P 5C2 Victoria BC, CANADA
dcbarrett@gmail.com

Carey, Sean
McMaster University, Geography and Earth Sciences
1280 Main Street West
L8S4K1 Hamilton ON, CANADA
careysk@mcmaster.ca

Janowicz, Richard
Yukon Water Resources Branch
Box 2703
Y1A 2C6 Whitehorse YT, CANADA
richard.janowicz@gov.yk.ca

Newton, Brandi
University of Victoria
3406 - 2371 Lam Circle
V8N6K8 Victoria BC, CANADA
bwnewton@uvic.ca

Prowse, Terry
W-CIRC/Environment Canada
3800 Finnerty Road
V8P 5C2 Victoria BC, CANADA
terry.prowse@ec.gc.ca

Woo, Caroline
1280 Main Street West
L8S4K1 Hamilton ON, CANADA
woo@mcmaster.ca

Woo, Ming-ko
McMaster University
1280 Main Street West
L8S4K1 Hamilton ON, CANADA
woo@mcmaster.ca

CHINA:

Wen, Lijuan
Cold and Arid Regions Environmental and Engineering Research Institute, Chinese Academy of Sciences
Lanzhou, Gansu, 73000, CHINA
wlj@lzb.ac.cn

Yang, Fang
Water Conservancy and Civil Engineering College, Inner Mongolia Agricultural University
Hohhot 010018, CHINA
ffff.yyyy@sina.com

Yang, Yu
Department of Basic Sciences, Shenyang Institute of Engineering
Puchang Road 18
110136 Shenyang, CHINA
yangyang-0606@hotmail.com

ESTONIA:

Pedusaar, Tiia
Estonian Environmental Agency/Hydrology Department
Mustamäe tee 33
10616 Tallinn, ESTONIA
tiia.pedusaar@envir.ee

FINLAND:

Akanegbu, Justice
Water Resources and Environmental Engineering, University of Oulu
P. O. Box 4300
90014 Oulu, FINLAND
justice.akanegbu@oulu.fi

Haavisto, Noora
Freshwater Centre, Finnish Environment Institute (SYKE)
P.O. Box 140
00251 Helsinki, FINLAND
noora.haavisto@ymparisto.fi

Irannezhad, Masoud
Water Resources and Environmental Engineering, University of Oulu
P. O. Box 4300
90014 Oulu, FINLAND
masoud.irannezhad@oulu.fi

Klöve, Björn	Water Resources and Environmental Engineering, University of Oulu P. O. Box 4300 90014 Oulu, FINLAND bjorn.klove@oulu.fi
Koivusalo, Harri	Water Resources Engineering, Aalto University P. O. Box 15200 00076 Aalto, FINLAND harri.koivusalo@aalto.fi
Korhonen, Johanna	Freshwater Centre, Finnish Environment Institute (SYKE) P.O. Box 140 00251 Helsinki, FINLAND johanna.korhonen@ymparisto.fi
Koskela, Jarkko	Freshwater Centre, Finnish Environment Institute (SYKE) P.O. Box 140 00251 Helsinki, FINLAND jarkko.j.koskela@ymparisto.fi
Kuusisto, Esko	Freshwater Centre, Finnish Environment Institute (SYKE) P.O. Box 140 00251 Helsinki, FINLAND esko.kuusisto@ymparisto.fi
Leppänen, Leena	Arctic Research Centre, Finnish Meteorological Institute Tähteläntie 62 99600 Sodankylä, FINLAND leena.leppanen@fmi.fi
Leppäranta, Matti	Department of Physics, University of Helsinki P.O. Box 48 00014 Helsinki, FINLAND matti.lepparanta@helsinki.fi
Meriö, Leo-Juhani	Water Resources and Environmental Engineering, University of Oulu P. O. Box 4300 90014 Oulu, FINLAND leo.juhani.merio@gmail.com

Mäkinen, Risto
Freshwater Centre, Finnish Environment Institute (SYKE)
P.O. Box 140
00251 Helsinki, FINLAND
risto.p.makinen@ymparisto.fi

Paavola, Riku
Oulanka research station, University of Oulu
Liikasenvaarantie 134
93999 Kuusamo, FINLAND
riku.paavola@oulu.fi

Ronkainen, Iina
Finnish Meteorological Institute
P.O. BOX 503
00101 Helsinki, FINLAND
iina.ronkainen@fmi.fi

Rätti, Osmo
Arctic Centre, University of Lapland
P. O Box 122
96101 Rovaniemi, FINLAND
osmo.ratti@ulapland.fi

ICELAND:

Thorsteinsson, Thorsteinn
Icelandic Meteorological Office
Bústaðavegi 7- 9
108 Reykjavik, ICELAND
thor@vedur.is

NORWAY:

Marchand, Wolf-Dietrich
Sweco Norge AS
Professor Brochs gate 2
7030 Trondheim, NORWAY
wolf.marchand@sweco.no

Sand, Knut
Statkraft Energi
Sluppenveien 6
N-7005 Trondheim, NORWAY
knut.sand@statkraft.com

RUSSIA:

Lebedeva, Liudmila
Melnikov Permafrost Institute
Merzlotnaya 36
677010 Yakutsk, RUSSIA
lyudmilaslebedeva@gmail.com

Semenova, Olga
St. Petersburg State University
7-9, Universitetskaya nab.
199034 St. Petersburg, RUSSIA
omakarieva@gmail.com

SWEDEN:

Bengtsson, Lars
Water Resources Engineering, Lund University
Box 117
22107 Lund, SWEDEN
lars.bengtsson@tvrl.lth.se

Gustafsson, David
Swedish Meteorological and Hydrological Institute
Folkborgsvägen 17
601 76 Norrköping, SWEDEN
david.gustafsson@smhi.se

Hammarberg, Ola
VDM AB
Fröjavägen 10F
83247 Frösön, SWEDEN
ola.hammarberg@vdmab.se

UNITED STATES OF AMERICA:

Feiccabrino, James
Water Resources Engineering, Lund University
108 E State Street
Montpelier, Vermont 05602, USA
james.feiccabrino@googlemail.com

Ihli, Katherine
InterWorks Consulting
15621 SnowMan Road
Loveland, Colorado 80538, USA
interworksconsulting@msn.com

Liston, Glen	Colorado State University Mail Code 1375 Fort Collins, Colorado 80523, USA glen.liston@colostate.edu
Plumb, Edward	National Weather Service, NOAA 930 Koyukuk Drive, Room 351 Fairbanks, Alaska 99775, USA edward.plumb@noaa.gov
Stuefer, Sveta	University of Alaska Fairbanks, Department of Civil & Environmental Engineering 306 Tanana Drive, Duckering Room 463 Fairbanks, Alaska 99775-5860, USA sveta.stuefer@alaska.edu

Application of hydrologic information transfer for hydrograph prediction in boreal catchment: Kitkajärvi catchment, Kuusamo, Finland

Justice O. Akanegbu*, Bjørn Kløve

Water resources and environmental engineering, University of Oulu, Oulu, 90014, FINLAND
**justice.akanegbu@oulu.fi*

ABSTRACT
In this study, major hydrological signatures governing runoff events in 5 gauged catchments surrounding Kitkajärvi catchment located in northern Finland where investigated. These signatures were employed in catchment classifications and comparisons which will enable easy transfer of hydrologic information from the gauged catchments to the ungauged sub-catchments discharging into Kitkajärvi. The studied catchments were chosen based on their close proximity, and physical characteristics which is similar, to that of Kitkajärvi sub-catchments. Runoff signatures in these catchments were studied and compared in other to establish the most significant signatures governing runoff from these catchments. Identifying such signatures will be useful to find optimal parameters for conceptual rainfall-runoff models, such as HBV, which will be transferrable to the ungauged catchments.

KEYWORDS
Hydrological information transfer; boreal catchments; runoff

1. INTRODUCTION
Kitkajärvi catchment is located in Kuusamo region in Northeast Finland. The catchment encompasses the whole watersheds of Ala-Kitka, Yli-Kitka and Posio lakes. A total of 38 sub-catchments with areas greater than 5 km^2 drains into these lakes. The main problem faced when carrying out studies, such as water quality modelling, on these lakes is that none of the 38 sub-catchments draining into the lakes are gauged for runoff measurements.

The objectives of this study is to investigate and establish the major hydrologic signatures governing runoff from catchments located in northern Finland with a focus on investigating the applicability of hydrologic information transfer using conceptual hydrologic model HBV in these catchments.

Catchment classification and conceptual model parameter regionalization studies have been widely carried out on large scale catchments across the globe but little have been done on small scale catchments. Sawicz et al. (2011) carried out study on catchments in eastern part of USA where he employed the use of hydrologic signatures related to catchment functionality in classifying 280 catchments spanning the eastern half of USA. Merz and Blöschl (2004) studied the connection between catchment attributes and spatial proximity on regionalization of a lumped conceptual rainfall-runoff model parameters. According to their findings, spatial proximity is a prefer substitute of unknown controls on runoff dynamics than catchment attributes hence, their recommendation of using average parameters of nested neighbours and regionalisation by Kriging as best parameter regionalization methods.

2. METHODS

The study employs the comparison of hydrological signatures governing runoff from gauged catchments in close proximity with Kitkajärvi watershed in other to establish their similarity and correlation of their functionality with catchment attributes. Their runoff response characteristics were studied using hydrological signatures governing flows as highlighted by Sawicz et al. (2011). These signatures include runoff ratio (R_{QP}), slope of flow duration curve (S_{FDC}), base flow index (BFI) and snow day ratio (R_{SD}).

3. RESULTS

From the preliminary results obtained so far after evaluating the catchments based on their runoff ratio, base flow index and flow duration curve, the runoff ratio of the 5 catchments studied range from 0.6 to 0.8 with catchments with significant lake percentage having the highest runoff ratio (table 1). The base flow index range from 0.3 to 0.7 with catchments with higher percentage of lake having higher base flow index (table 1). The flow duration curve for the catchments depicts overland flow as the major contributor to stream flows from the catchments as shown in figures 1 & 2.

Table 1. Comparison of catchment attributes in relation to runoff signatures

Catchment	Area km2	Land use %						Runoff Ratio	Base flow Index
		Slope	Forest	Wetland	Lake	Agric.	Urban		
Ylijoen	56.27	9.92	81.22	15.62	1.78	1.38	0	0.68	0.3
Kursunjoen	27.6	8.17	92.2	4.69	1.52	1.18	0.41	0.64	0.433
Vaarajoen	19.3	7.41	85.18	5.69	8.16	0.73	0.25	0.81	0.492
Kuolionjoen alaosan	104.9	8.2	79.32	8.15	9.6	2.89	0	0.74	0.619
Vuotungin	161.9	7.12	80.56	2.27	12.86	4.31	0	0.71	0.739

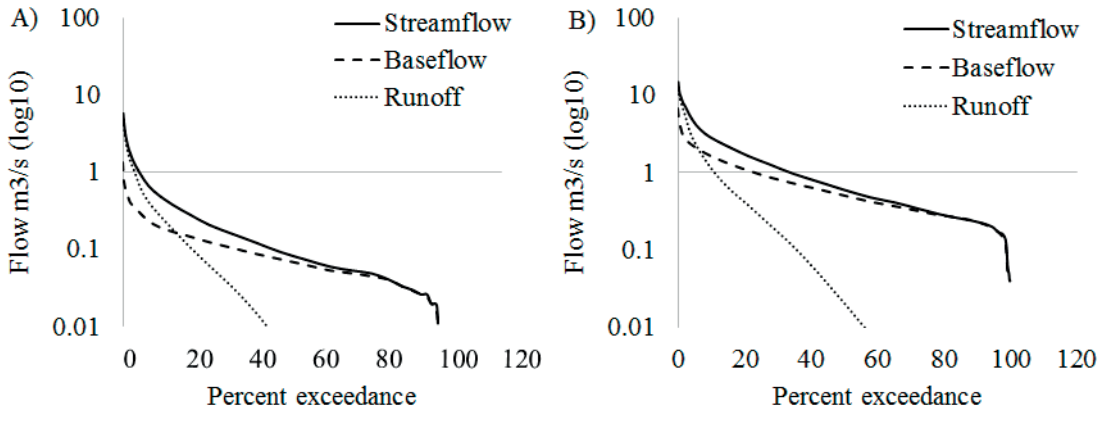

Figure 1. Flow duration curve for A) Kursunjoen catchment, B) Kuolionjoen alaosan catchment

4. DISCUSSION AND CONCLUSION

The high runoff ratios recorded from the catchments shows that streamflow is the dominant process through which water exits from the catchments while evaporation process is low. The low base flow index recorded in catchments with low lake percentage indicates that overland flow is the major contributor to streamflow in the catchments rather than base flow. Further analysis will be conducted to determine the correlation between these signatures such as base flow index with catchment physical attributes such as lake percentage. The study is still on-going and further investigations will be done in other catchments to be able to establish factors on which similarity measures of the catchments will be based. This will allow for catchment grouping which will enable hydrological information transfer between catchments of similar hydrologic characteristics.

5. LIST OF REFERENCES

Merz, R. & Blöschl, G. 2004 Regionalisation of catchment model parameters. *Journal of Hydrology*. 287(2004), 95–123.

Sawicz, K., Wagener, T., Sivapalan, M., Troch, P.A., & Carrillo, G. 2011 Catchment classification: empirical analysis of hydrologic similarity based on catchment function in the eastern USA. *Hydrology and Earth System Sciences.* 15, 2895–2911.

A cross sectional study of rain/snow threshold changes from the North Sea across the Scandinavian Mountains to the Bay of Bothnia

James M. Feiccabrino

Water Resources Engineering, Lund University, Lund S-221 00, SWEDEN
**James.Feiccabrino@googlemail.com*

ABSTRACT

Rain/snow threshold studies are typically conducted at large (country to global) or small (watershed) scales to find parameters that best mimic nature or improve runoff model output. However, this study considers how rain/snow threshold values are influenced by landscape geography in a cross sectional area from the North Sea over the Scandinavian Mountains to the Bay of Bothnia. Twelve years of meteorological observations from 4-5 stations in each of the west to east geographical landscapes; North Sea, exposed coast, protected fjords, windward flat, Windward intermountain valley, leeward intermountain valley, leeward hills, leeward flat, and Bothnian Coast; are compared for changes in single and dual air, dew point, and wet bulb temperature thresholds as well as affects of warm/cold air temperature advection.

Earth's surface temperature affects near surface temperatures. This temperature influence decreases with height. Therefore, rain/snow temperature threshold values for the entire season could be different than threshold values for observations with and without snow cover and for different sea surface temperatures at coastal and ocean stations. Total misclassified precipitation for thresholds under these different surface conditions and thresholds for geographical landscapes are compared.

Wet-bulb temperature thresholds resulted in the least misclassified precipitation for both the Norwegian (14.59 to 12.85%), and Swedish datasets (9.82 to 8.56%), and the least misclassified precipitation for 8 of 9 landscape datasets, all with the same single and dual temperature threshold values. Air temperature rain/snow thresholds changed with geography. However, snow cover, temperature advection, and sea surface temperature allowed negligible decreases in landscape misclassified precipitation.

KEYWORDS

precipitation phase; snow; snow model; temperature threshold; hydrology; geographic landscape

1. INTRODUCTION

Topography and warm/cold ocean currents affect local to regional climates most notably in average air temperature and precipitation totals. Expanding on this, could regional surface based factors such as warming from open water or cooling from a snowpack affect the probability of snow determined using surface weather observations?

Within cold regions precipitation falling as rain or snow can have affects on many different aspects of life such as transportation safety on roads, strength or thickness of sea ice (Lundberg and Feiccabrino, 2009), runoff in rivers, or water storage in reservoirs for electricity production, drinking, or recreation. Models for these purposes use a precipitation phase determination scheme (PPDS) to assign precipitation values to a liquid (rain) or solid

(snow) phase. Most PPDS use; surface air temperature (T_A) (e.g. USACE, 1956), surface dew point temperature (T_D) (e.g. Marks et al., 2013), surface wet bulb temperature (T_W) (e.g. Matsuo et al., 1981), or a surface air temperature and relative humidity (RH) relationship (e.g. Ye et al., 2013).

There are two main kinds of PPDS schemes, single temperature threshold schemes (T_{RS}) and duel threshold schemes using a rain (T_R) and snow (T_S) temperature threshold with decrease in snow fraction (SF) between T_S and T_R.

Of note, surface based PPDS methods do not account for microphysical processes e.g. evaporation, sublimation, freezing and melting occurring in the lower atmosphere (Thériault and Stewart, 2010). These processes are calculation intensive requiring detailed atmospheric information often not included in surface (hydrological) models (Harder and Pomeroy, 2013).

A surface based PPDS relies heavily on the assumption of constant atmospheric conditions, such as, a set decrease in air temperature with height (e.g. the CHRM model using - 7.5˚C/km lapse rate) (Fang et al., 2013). This particular assumption is not ideal when a snowpack (open water) conductively cools (warms) near surface air but has little affect on temperatures a couple hundred meters above the ground. The atmospheric height, to which temperatures are modified by surface heating/cooling is partly determined, by the period of time a body of air spends over a heating/cooling source.

A warm bias of +0.7°C for T_{RS} was found by Dai (2008) over oceans (1.9°C) compared to land (1.2°C). Stewart (1992) found precipitation phase transitions to commonly occur near coastlines caused by open water transferring heat to the near surface atmosphere, therefore increasing melt energy. Wind could then carry this heat over the near coastal regions. The stronger the wind, the further inland (predominant wind) or offshore the air heated by the ocean can be transported.

Frontal and air mass boundaries will also affect the PPDS assumption of average atmospheric conditions (Feiccabrino et al., 2012) and can be identified by cold/warm air advection at the surface.

Air forced to rise over terrain causes orographically enhanced precipitation. Increased precipitation rates force the atmospheric melting layer to deepen due to increased energy requirements to melt the snow. The melting layer deepening lowers the 0˚C isotherm and snow elevations compared to upwind (Minder et al., 2011). This change in atmospheric conditions might therefore affect rain/snow threshold values. The amount of change in the snow elevation and thickness of the melting layer depends on the geometry of the terrain and the melting layer properties (Minder et al., 2011).

The purpose of this study is to determine; 1.) if station locations can be classified into geographic landscapes where PPDS schemes (T_A, T_D, and T_W) have similar T_{RS}, T_S and T_R values, 2.) if these values noticeably change by landscape, and 3.) if these landscape T_{RS}, T_S and T_R values are effected by sea surface temperature (SST), presence of a snowpack, or warm/cold air advection.

2. METHODS

Two datasets built from free of charge public data available online from the Norwegian and Swedish meteorological institutes are used in this study. The weather stations were assigned to the geographic landscapes of North Sea ocean platforms, exposed coast, protected fjords, windward flat, and windward intermountain valleys in Norway, and leeward intermountain

valleys, leeward hills, leeward flat, and Bothnian Coast in Sweden. Station locations (Figure 1), elevation, and observation sample size are given in Tables 1 and 2.

The Norwegian meteorological data consisted of automated surface weather observations for 06, 12, and 18 UTC reporting; date, time, T_A to 0.1˚C, world meteorological organization (WMO) present weather code, *RH* in %, SST for ocean and coastal stations, snow depth reported once a day for all inland stations, and atmospheric pressure. Some stations reported T_D (more common after 2010), and there were no reported T_W values. There was also an inconsistency or a lack of liquid precipitation totals available for either 6, 12, or 24hour time periods preceding an observation.

Table 1. Norwegian weather stations with location, elevation, observation period, and numbers of total observations, precipitation observations, and precipitation observations between October and May with a T_A between -3 and 5°C (with percentage).

MET. STATION NAME	Map #	Lat (N)	Long (E)	Ele (m)	Start Date	End Date	Total # Obs	Total # Precip	Total # -3 to 5°C
NORTH SEA OCEAN PLATFORMS							**51258**	**6990**	**2368 (34%)**
Ormen Lange	1	63.56	5.23	40	Dec10’	Dec12’	1295	335	93 (28%)
Draugen	2	64.35	7.78	55	Mar98’	Feb13’	12987	1322	414 (31%)
Heidrun	3	65.32	7.32	68	Mar98’	Feb13’	19248	3378	1177 (35%)
Norne	4	66.02	8.09	33	Mar98’	Feb13’	17728	1955	684 (35%)
EXPOSED COAST							**86869**	**7685**	**2839 (37%)**
Buholmråsa Fyr	5	64.40	10.45	18	Mar98’	Feb13’	21850	1067	264 (25%)
Nordøyan Fyr	6	64.80	10.55	33	Mar98’	Feb13’	21314	2424	909 (38%)
Sklinna Fyr	7	65.20	11.00	23	Mar98’	Feb13’	21826	1152	516 (45%)
Myken	8	66.76	12.49	17	Mar98’	Feb13’	21879	3042	1150 (38%)
PROTECTED FJORDS							**47984**	**5087**	**2236 (44%)**
Hjelvik-Myrbø	9	62.60	7.23	35	May98’	Feb09’	5757	751	302 (40%)
Tingvoll-Hanem	10	62.84	8.30	69	Mar98’	Nov08’	11691	2157	970 (45%)
Trondheim-Voll	11	63.41	10.45	127	Mar98’	Feb13’	21885	560	271 (48%)
Finnøy Hamarøy	12	68.00	15.61	53	Mar98’	Mar06’	8651	1619	693 (43%)
WINDWARD FLAT							**56372**	**11381**	**5138 (45%)**
Selbu-Stubbe	13	63.21	11.12	242	Mar98’	Nov06’	9517	1800	801 (45%)
Verdal-Reppe	14	63.78	11.68	81	Mar98’	Feb13’	16418	3786	1593 (42%)
Høylandet-Drageidet	15	64.56	12.18	29	Jan99’	Jun07’	8864	1596	815 (51%)
Bardufoss	16	69.06	18.54	76	Mar98’	Feb13’	21573	4199	1929 (46%)
WINDWARD INTERMOUNTAIN VALLEYS							**50183**	**8179**	**3878 (47%)**
Råros Lufthavn	17	62.58	11.35	625	Jan05’	Feb13’	11334	1601	623 (39%)
Nordli - Holand	18	64.45	13.72	433	Mar98’	Feb13’	16089	3664	1771 (48%)
Fiplingvatn	19	65.29	13.53	370	Mar98’	Feb13’	8852	2042	1153 (56%)
Saltdal	20	66.77	15.59	81	Sep99’	May12’	13908	872	331 (38%)

The Swedish Meteorological data consisted of hourly automated surface weather observations reporting; date, time T_A to 0.1˚C, WMO present weather code (Every 3 hours before Aug 2010), *RH* in % and hourly liquid precipitation total. Most of the stations did not report a co-located daily snow depth, or atmospheric pressure.

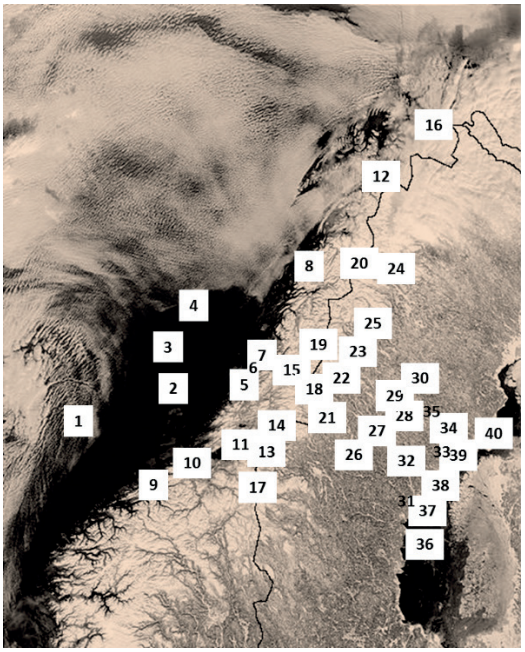

Figure 1. Swedish and Norwegian weather station locations plotted over a cropped down visible satellite image of the Scandinavian Peninsula from February 19 2003. (modified from Descloitres, 2003)

Table 2. Swedish stations with location, elevation, observation period, and numbers of total observations, precipitation observations, and precipitation observations between October and May with a T_A between -3 and 5°C (with percentage).

MET STATION NAME	Map #	LAT (N)	LON (E)	ELE (m)	Start Date	End Date	Total # Obs	Total # Precip	Total # -3 to 5°C
LEEWARD INTERMOUNTAIN VALLEYS							**345801**	**30546**	**9986 (33%)**
Korsvattnet	21	63:84	13.50	717	Mar98’	Jul10’	105940	9845	3561 (36%)
Gäddede	22	64:51	14.22	550	Jan08’	Jul10’	21151	1647	581 (35%)
Gielas	23	65:33	15.07	577	Mar98’’	Jul10’	95904	7358	2326 (32%)
Mierkenis	24	66.68	16.11	614	Mar98’	Jul10’	101697	9572	2756 (29%)
Hemavan	25	65.81	15.10	492	Jan08’	Jul10’	21109	2124	762 (36%)
LEEWARD HILLS							**540526**	**31043**	**9406 (30%)**
Föllinge	26	63:68	14.61	362	Mar98’	Jul10’	108453	5749	1784 (31%)
Hallhåxåsen	27	63:77	15.33	375	Mar98’	Jul10’	108406	6281	1891 (30%)
Hoting	28	64:09	16.24	241	Mar98’	Jul10’	107271	6191	1959 (32%)
Gubbhögen	29	64:22	15.56	310	Mar98’	Jul10’	108569	6365	1992 (31%)
Vilhelmina	30	64:58	16.84	348	Mar98’	Jul10’	107827	6457	1780 (28%)
LEEWARD FLAT							**538951**	**30301**	**10008 (33%)**
Torpshammar	31	62:49	16.28	99	Mar98’	Jul10’	108084	5103	1796 (35%)
Krångede	32	63:15	16.17	220	Mar98’	Jul10’	107837	6438	2115 (33%)
Hemling	33	63:65	18.55	182	Mar98’	Jul10’	108216	6021	2118 (35%)
Fredrika	34	64:08	18.37	327	Mar98’	Jul10’	107590	6587	2055 (31%)
Åsele	35	64:17	17.32	307	Mar98’	Jul10’	107224	6152	1924 (31%)
BOTHNIAN COAST							**475116**	**20104**	**8650 (43%)**
Kuggören	36	61:70	17.53	8	Mar98’	Jul10’	108346	4189	1860 (44%)
Brämön	37	62:23	17.66	20	Mar98’	Jul10’	107169	4438	1945 (44%)
Lungö	38	62:64	18.09	17	Mar98’	Jul10’	105655	4576	1950 (43%)
Järnäsklubb	39	63:44	19.86	6	Mar98’	Jul10’	108011	4935	2063 (42%)
Holmön	40	63.82	20.70	2	May05’	Jul10’	45935	1966	832 (42%)

For the analysis, T_D was calculated using Eq. 1, a common formula;

$$TD = \left(\frac{RH}{100}\right)^{0.125} * (112 + 0.9 * TA) + 0.1 * TA - 112 \quad \text{Eq 1}$$

The Swedish data lacking atmospheric pressure, forced T_W to be calculated using an empirical formula (Stull, 2011) rather than the common formula that requires air pressure;

$$TW = TA \operatorname{atan}[0.151977(RH + 8.313659)^{.5}] + \operatorname{atan}(TA + RH) - \operatorname{atan}(RH - 1.676331) + 0.00391838(RH)^{1.5} \operatorname{atan}(0.023101RH) - 4.686035 \quad \text{Eq 2}$$

Since many Norwegian observations lacked a liquid precipitation measurement, the threshold temperature analysis was conducted by separating weather observations into non-precipitation or liquid, solid, frozen, and mixed phase precipitation events indicated by the WMO present weather code. Precipitation events were therefore equal unit-less quantities regardless of phase or intensity.

Datasets for precipitation events occurring between -3 and 5°C were built for each country, geographic landscape, and individual weather station to determine single and dual T_A, T_D, and T_W thresholds. The determined threshold temperature is the T_{RS}, or T_S and T_R combination that results in the lowest error (observed rain classified as snow + observed snow classified as rain). Single thresholds were found first. Linear T_S and T_R combinations were then tested for 1, 2, 3, and 4°C spreads with the T_{RS} set as the 50% value, then offset plus and minus 0.5°C from the T_{RS} value.

For ocean and coastal landscapes, a further analysis was conducted dividing the dataset amongst soil surface temperature (SST) values to determine if SST has any affect on T_{RS}. In similar analysis, the Norwegian observations reporting a snow depth were divided into groups of 2cm or less snow depth and 15cm and greater snow depth to determine if the presence of a thick snowpack has an affect on T_{RS} values.

Finally, Norwegian observations with a 1.5°C or greater increase in T_A from the observation 6hrs before were categorized as warm air advection (WAA) observations, while observations with a 1.5°C or greater decrease in T_A were categorized as cold air advection (CAA) observations.. Swedish stations were analysed at both 3 and 6 hour intervals for warm and cold air advection.

3. RESULTS

Threshold values for the two countries and geographical landscapes are found in Table 3 and the results for the individual Norwegian and Swedish stations are presented in Table 4. The T_A values are always ≥ T_W values which are always ≥ T_D values.

For Norway (Tables 3 and 4) T_W is the most consistent threshold value having every landscape T_{RS}, T_S, and T_R values = the country values. Wet-bulb PPDS resulted in the least error for all landscapes with both single and dual thresholds with the exception of the Fjords T_{RS} analysis where T_A had 0.73% less error. The dual threshold misclassified precipitation averaged a 1% decrease in misclassified precipitation for T_A (-0.5%), T_D (-0.97%) and T_W (-1.45%) compared to single threshold values.

Table 3. Country and geographical landscape single (T_{RS}) and dual (T_S and T_R) air (TA), dew point (TD) and wet-bulb (TW) temperature thresholds with percent misclassified error (% Er), and difference in error (Δ% Er) between the country and landscape threshold temperatures.

	Single Temperature Thresholds (T_{RS})						Dual Temperature Thresholds ($T_S - T_R$)					
Location	T_A °C	% Er	T_D °C	% Er	T_W °C	% Er	T_A °C	% Er	T_D °C	% Er	T_W °C	% Er
Country Threshold	% Er	Δ %Er	% Er	Δ %Er	% Er	Δ %Er	% Er	Δ %Er	% Er	Δ %Er	% Er	Δ %Er
Norway	**1.0**	**14.6%**	**0.0**	**16.7%**	**0.5**	**12.9%**	**0.5 – 1.5**	**14.1%**	**-0.5 – 0.5**	**15.8%**	**0.0 – 1.0**	**11.4%**
North Sea	2.0	17.2%	-0.5	19.2%	0.5	16.8%	1.5 – 2.5	16.5%	-1.0 – 0.0	19.0%	0.0 – 1.0	16.0%
	21.3%	4.1%	20.5%	1.3%			20.9%	4.4%	19.6%	0.6%		
Exposed Coast	1.5	14.9%	-0.5	17.6%	0.5	14.3%	1.0 – 2.0	13.9%	-1.0 – 0.0	16.6%	0.0 – 1.0	13.0%
	15.8%	0.9%	19.2%	1.6%			15.4%	1.5%	17.8%	1.2%		
Protected Fjords	1.0	10.7%	0.5	15.1%	0.5	11.4%	0.5 – 1.5	10.4%	0.0 – 1.0	14.2%	0.0 – 1.0	10.1%
			15.3%	0.2%					14.8%	0.6%		
Windward Flat	1.0	13.3%	0.0	16.0%	0.5	12.5%	0.5 – 1.5	13.0%	-0.5 – 0.5	15.1%	0.0 – 1.0	11.1%
Windward Mtn. Valleys	1.5	12.8%	0.0	14.4%	0.5	11.9%	1.0 – 2.0	11.8%	0.0 – 1.0	13.2%	0.0 – 1.0	10.0%
	13.7%	0.9%					12.9%	1.1%	13.5%	0.3%		
Sweden	**1.5**	**9.8%**	**0.5**	**11.0%**	**0.5**	**8.6%**	**1.0 – 2.0**	**10.2%**	**0.0 – 1.0**	**10.8%**	**0.0 – 1.0**	**8.7%**
Leeward Mtn. Valleys	1.5	8.5%	0.5	10.4%	0.5	7.4%	1.0 – 2.0	9.0%	0.0 – 1.0	10.2%	0.0 – 1.0	7.7%
Leeward Hills	1.0	9.0%	0.0	10.5%	0.5	7.8%	1.0 – 2.0	9.5%	0.0 – 1.0	10.4%	0.0 – 1.0	7.9%
	9.3%	0.3%	10.6%	0.1%								
Leeward Flat	1.0	9.5%	0.5	10.4%	0.5	8.0%	1.0 – 2.0	9.9%	0.0 – 1.0	10.2%	0.0 – 1.0	8.2%
	9.6%	0.1%										
Bothnian Coast	1.0	11.5%	0.5	12.7%	0.5	11.3%	0.5 – 1.5	12.2%	0.0 – 1.0	12.6%	0.0 – 1.0	11.3%
	12.2%	0.7%					12.5%	0.3%				

For Sweden (Tables 3 and 4) T_W was the most consistent threshold value with every geographical threshold matching the country threshold for T_{RS} (0.5°C), T_S (0.0°C), and T_R (1.0°C). The single threshold values often resulted in slightly less error than dual thresholds for T_A, T_D, and T_W. As in Norway T_D resulted in the highest errors in both single and dual threshold methods.

3.1 Influence of Snow Cover on Air Temperature Thresholds

The decrease in a geographic landscape error resulting from the use of two T_{RS} values 1.) T_{RS} for exposed ground (Snow Depth ≤2cm) and 2.) T_{RS} for snow covered ground (Snow depth ≥ 15cm) was minimal (Table 5). The largest decrease in total error of 0.12% from 13.16% to 13.04% occurred in the windward flat landscape indicates that the presence of snow cover is not a major factor in PPDS error.

3.2 Influence of Sea Surface Temperature on Air Temperature Thresholds

The decrease in landscape error resulting from the use of different T_{RS} values calculated for 1°C (Table 6) and 2°C (Table 7) SST intervals was greater than the change due to snow cover (Table 5) but was still less than 0.50% for all analysed datasets.

3.3 Influence of Cold and Warm Air Advection on Air Temperature Thresholds

The decrease in a landscape error resulting from the use of T_{RS} values calculated for warm and cold air advection resulted in minimal decreases in total error. Of note, 8 of 12 CAA T_{RS} values were = geographic landscape T_{RS} compared to 2 WAA T_{RS} values.

Table 4. Norwegian and Swedish station air and wet-bulb single temperature thresholds (T_{RS}) at 0.5°C with misclassified precipitation error (%Er) and the difference between stations T_{RS} error and geological landscape/country T_{RS} error (ΔEr).

		Single Temperature Threshold % Error					
		Air Temperature Thresholds			Wet-bulb Temperature Thresholds		
Geo. Landscape	Station #	Station T_{RS} / %Er	Geo %Er /ΔEr	Country %Er / ΔEr	Station T_{RS} / %Er	Geo %Er /ΔEr	Country %Er / ΔEr
North Sea Ocean Platforms (TA = 2.0, TW = 0.5)	1	1.5°C 12.0%	13.0% 1.0%	13.0% 1.0%	0.5°C 11.9%		
	2	2.0°C 24.5%		30.5% 6.0%	1.0°C 19.5%	21.9% 2.4%	21.9% 2.4%
	3	2.0°C 15.9%		19.2% 3.3%	0.5°C 16.5%		
	4	2.0°C 15.5%		20.5% 5.0%	0.5°C 13.6%		
Exposed Coast (TA = 1.5, TW = 0.5)	5	1.5°C 16.2%		17.3% 1.1%	0.0°C 16.0%	19.0% 3.0%	19.0% 3.0%
	6	2.0°C 15.6%	16.5% 0.9%	17.5% 1.0%	0.5°C 15.7%		
	7	1.0°C 13.8%	15.2% 1.4%		0.5°C 11.5%		
	8	1.5°C 13.1%		14.9% 1.8%	0.5°C 13.5%		
Protected Fjords (TA = 1.0, TW = 0.5)	9	1.5°C 15.6%	18.3% 2.7%	18.3% 2.7%	1.0°C 16.6%	18.8% 2.2%	18.8% 2.2%
	10	1.0°C 9.0%			0.5°C 9.2%		
	11	1.0°C 13.0%			0.0°C 14.3%	15.0% 0.7%	15.0% 0.7%
	12	1.0°C 8.7%			1.0°C 9.0%	9.8% 0.8%	9.8% 0.8%
Windward Flat (TA = 1.0, TW = 0.5)	13	1.0°C 12.9%			-0.5°C 12.5%	16.1% 3.6%	16.1% 3.6%
	14	1.5°C 12.4%	12.9% 0.5%	12.9% 0.5%	0.5°C 10.7%		
	15	0.5°C 15.5%	17.3% 1.8%	17.3% 1.8%	0.0°C 14.1%	15.6% 1.5%	15.6% 1.5%
	16	1.0°C 12.1%			0.0°C 10.8%	11.2% 0.4%	11.2% 0.4%
Windward Intermountain Valleys (TA = 1.5, TW = 0.5)	17	1.5°C 15.0%		16.6% 1.6%	0.5°C 12.6%		
	18	1.5°C 11.2%		11.3% 0.1%	0.5°C 9.8%		
	19	1.5°C 15.2%		16.4% 1.2%	1.0°C 13.0%	15.4% 2.4%	15.4% 2.4%
	20	1.5°C 8.6%		11.7% 3.1%	0.0°C 7.0%	9.2% 2.2%	9.2% 2.2%
Leeward Intermountain Valleys (TA = 1.5, TW = 0.5)	21	1.5°C 7.2%			0.5°C 7.0%		
	22	1.0°C 8.7%	17.0% 8.3%	17.0% 8.3%	0.5°C 14.2%		
	23	1.5°C 7.0%			0.5°C 7.1%		
	24	1.5°C 8.4%			0.5°C 6.5%		
	25	1.0°C 9.8%	12.5% 2.7%	12.5% 2.7%			
Leeward Hills (TA = 1.0, TW = 0.5)	26	1.0°C 9.5%		10.0% 0.5%	0.5°C 7.5%		
	27	1.5°C 8.0%	9.2% 1.2%		0.5°C 8.7%		
	28	1.5°C 8.4%	8.8% 0.4%		0.5°C 6.9%		
	29	1.0°C 8.7%		9.6% 0.9%	0.0°C 7.4%	7.5% 0.1%	7.5% 0.1%
	30	1.0°C 9.1%		10.8% 1.7%	0.0°C 7.8%	8.6% 0.8%	8.6% 0.8%
Leeward Flat (TA = 1.0, TW = 0.5)	31	1.0°C 11.2%		11.4% 0.2%	0.5°C 10.1%		
	32	1.5°C 10.3%	12.6% 2.3%		0.5°C 10.0%		
	33	1.0°C 8.9%		9.7% 0.8%	0.5°C 7.6%		
	34	1.0°C 6.1%		7.6% 1.5%	0.5°C 5.2%		
	35	1.0°C 8.4%		9.1% 0.7%	0.5°C 7.1%		
Bothnian Coast (TA = 1.0, TW = 0.5)	36	1.5°C 11.3%	12.0% 0.7%		1.0°C 11.3%	11.4% 0.1%	11.4% 0.1%
	37	1.5°C 10.0%	11.8% 1.8%		0.5°C 11.5%		
	38	1.0°C 11.7%		14.4% 2.7%	0.5°C 12.3%		
	39	1.0°C 11.4%		12.0% 0.6%	0.5°C 10.5%		
	40	1.0°C 9.4%		14.9% 5.5%	0.5°C 10.5%		

Table 5. Single air temperature thresholds, for observations with and without a snowpack including misclassified precipitation (error), total error, and the resulting decrease in landscape/country error.

Country or Geographical Landscape (T_A)	Snow Depth 0-2CM		Snow Depth ≥ 15CM		Total % Error / Δ T_A Error % (Table 3)
	T_A	Δ Error	T_A	Δ Error	
Norway (1.1°C)	1.3°C	-0.52%	1.1°C		14.33% / -0.04%
Fjords (1.0°C)	1.0°C		0.9°C	-0.56%	10.54% / -0.11%
Windward Flat (1.1°C)	1.3°C	-1.18%	1.1°C		13.04% / -0.12%
Intermountain Valley (1.4°C)	1.3°C	-0.37%	1.4°C		12.30% / -0.03%

Table 6. Single air temperature thresholds, for observations in a geographic landscape with a given sea surface temperature (SST) including misclassified precipitation (error) for that SST, total landscape error and the resulting decrease in landscape error due to the SST analysis.

Landscape (T_A)	SST ≥ 10°C	9°C	8°C	7°C	6°C	Total % Error / Δ T_A Error % (Table 3)
	T_A / % Error	T_A / % Error	T_A / % Error	T_A / % Error	T_A / % Error	
Ocean (1.8°C)	2.2°C/ 19.12%	2.2°C/ 18.90%	1.8°C/ 16.31%	1.7°C/ 16.73%	2.1°C/ 15.87%	16.60% / -0.30%

Table 7. Single air temperature thresholds, for observations in a geographic landscape with a given sea surface temperature (SST) including misclassified precipitation (error) for that SST, total landscape error, and the resulting decrease in landscape error due to SST analysis.

Country or Landscape (T_A)	SST ≥ 10°C	8-10°C	6-8°C	4-6°C	2-4°C	Total % Error / Δ T_A Error % (Table 3)
	T_A / % Error	T_A / % Error	T_A / % Error	T_A / % Error	T_A / % Error	
Norway (1.1°C)	1.8°C/ 17.00%	1.8°C/ 17.00%	1.7°C/ 16.75%	1.7°C/ 15.47%	1.2°C/ 11.29%	13.91% / -0.46%
Sea Coast (1.0°C)	1.8°C/ 12.50%	2.0°C/ 20.00%	1.5°C/ 16.81%	1.7°C/ 15.58%	1.2°C/ 11.35%	14.39% / -0.28%

Table 8. Single air temperature thresholds, for observations in a geographic landscape with warm and cold air advection including misclassified precipitation (error) for warm and cold air advection, total landscape error, and the resulting decrease in landscape error due to temperature advection analysis.

Country or Landscape (T_A)		CAA Observations			WAA Observations			Total % Error / Δ T_A Error % (Table 3)	
		T_A (n %)	%Error	Δ Error	T_A (n %)	%Error	Δ Error	CAA	WAA
Norway (1.1°C)		1.1°C (15)	14.00%		1.9°C (12)	15.11%	-0.73%		14.29% / -0.08%
Ocean Platforms (1.8°C)		1.8°C (21)	18.01%		3.1°C (06)	16.91%	-5.15%		16.60% / -0.30%
Sea Coast (1.0°C)		1.2°C (20)	14.55%	-02.65%	2.1°C (08)	15.31%	-1.33%	14.14% / -0.53%	14.57% / -0.10%
Fjords (1.0°C)		1.0°C (13)	11.76%		1.0°C (11)	13.50%			
Windward Flat (1.1°C)		1.1°C (15)	11.33%		1.5°C (15)	14.08%	-0.64%		13.06% / -0.10%
Windward Mtn. (1.4°C)		1.4°C (11)	11.84%		2.0°C (15)	13.44%	-1.50%		12.09% / -0.24%
Sweden (1.3°C)	3hr	1.3°C (07)	8.64%		1.5°C (08)	11.07%	-0.76%		9.50% / -0.06%
	6hr	1.3°C (14)	8.78%		1.4°C (18)	10.94%	-0.31%		9.50% / -0.06%
Leeside Mtns. (1.5°C)	3hr	1.5°C (08)	7.42%		1.9°C (09)	9.76%	-1.41%		8.33% / -0.13%
	6hr	1.5°C (16)	7.57%		1.7°C (19)	9.70%	-0.67%		8.33% / -0.13%
Leeside Hills (1.2°C)	3hr	1.3°C (08)	6.93%	-0.43%	1.5°C (09)	10.97%	-0.50%	8.74% / -0.03%	8.73% / -0.04%
	6hr	1.3°C (15)	8.12%	-0.14%	1.4°C (19)	10.82%	-0.16%	8.75% / -0.02%	8.74% / -0.03%
Leeside Flat (1.3°C)	3hr	1.3°C (07)	9.89%		1.5°C (09)	12.02%	-0.21%		9.17% / -0.02%
	6hr	1.3°C (13)	9.96%		1.3°C (21)	10.81%			
Bothnian Coast (1.1°C)	3hr	1.1°C (05)	8.86%		1.4°C (04)	8.82%	-2.41%		11.15% / -0.11%
	6hr	1.2°C (10)	7.97%	-0.24%	1.4°C (12)	11.92%	-0.48%	11.23% / -0.03%	11.20% / -0.06%

4. DISCUSSION

The use of geographical landscapes to determine appropriate rain/snow thresholds for a PPDS is not necessary if using T_W. Though there was slight local variance in T_W threshold values, mainly on windward and leeward mountain stations, the local values never differed by more than 0.5°C from the landscape values (Table 4), and all landscape and country values had the same T_{RS} (0.5°C), T_S (0.0°C), and T_R (1.0°C) (Table 3).

However, the use of geographical landscapes for T_A thresholds is very useful. In close agreement with Dai's (2008) study, the T_{RS} on ocean platforms was found to be 1.8°C. Coastal stations and Fjords had a T_{RS} of 1.0°C, this was followed by a slow increase in T_{RS} to 1.1°C at windward flat stations to 1.4 and 1.5°C for windward and leeward mountain valley stations with a slight decline to 1.2 and 1.3°C for leeside hills and flat stations with a return to 1.1°C in the Bothnian Bay landscape (Tables 3, 4, and 8). The higher T_{RS} for ocean stations is thought to be caused by the surface heating influence caused by the ocean. It is not as strong

at the coastal stations or fjords due to a cooler land influence and the water being more shallow allowing greater seasonal variation. The water in the Bothnian Bay has little affect on the T_{RS} for the Bothnain Coast landscape due to cooler SST than the North Atlantic, and being generally downwind during storms.

The complicated terrain in windward and leeward mountain valley landscapes may be the cause of both the increased variation in station T_A and T_D threshold values (Tables 3 and 4), and a slight increase in landscape T_A. Had the stations been located on mountain tops, or on upsloping windward hills instead of near villages in river valleys the results may have been closer to those found by Marks et al. (2013) where T_D produced a more accurate T_{RS} for PPDS than T_A, both near 0.0°C. Using valley stations increases the depth of dry (unsaturated) air between the station elevation and cloud height. The CHRM model lapse rate of - 7.5˚C/km (Fang et al., 2013) is a fair estimate of the unsaturated warming of air from the cloud level to the ground. With the mountain valley T_{RS}, snow would only have to fall through a 200m dry warm layer to reach the ground. This can occur without a complete melt.

It was surprising that adjusting T_A based T_{RS} values for the surface conditions of SST, and the presence or lack of snow cover resulted in such small decreases in landscape misclassified precipitation (Tables 5, 6, and 7). However, SST is still the most likely reason for much warmer geographical landscape air temperature T_{RS} values for the ocean stations compared to coastal or inland stations. For inland stations the ground temperatures could be freezing, so the presence or lack of snow cover may not matter much.

Assigning a separate air temperature T_{RS} value to observations with strong warm and cold air advection resulted in little to no reduction in misclassified precipitation contrary to the results from Feiccabrino et al. (2012) where separating CAA reduced error by 23%. This is most likely due to vast differences in study areas. The original air mass boundary study (Feiccabrino et al., 2012) took place in a continental climate. In a continental climate surface and upper air fronts are similar in that both upper and surface warm fronts precede *WAA* and cold fronts precede *CAA*. Over the Scandinavian Peninsula both warm and cold upper air fronts will advect surface air warmed by the Atlantic, therefore making it difficult to identify frontal types based on surface air advection.

5. CONCLUSION

Surface precipitation phase determination, in 8 of 9 Scandinavian landscapes, had less misclassified precipitation using a wet-bulb temperature (T_W) than dew point temperature (T_D) or air temperature (T_A). Importantly, T_W in all landscapes had the same single and dual temperature threshold values.

Using different T_A threshold values for geographical landscapes is a viable option for decreasing misclassified precipitation error in surface precipitation phase determination for large scale studies.

Using different geographical landscape T_A thresholds for observations separated by ranges of; sea surface temperature, snow cover, or warm/cold air advection resulted in minimal decreases in landscape misclassified precipitation over the Scandinavian Peninsula.

6. REFERENCES

Dai, A. 2008 Temperature and pressure dependence of the rain-snow phase transition over land and ocean. *Geophys. Res. Lett*. 35(12), L12802 http://dx.doi.org/10.1029/2008GL033295.

Descloitres, J. 2003. MODIS Land Rapid Response Team at NASA GSFC public domain image, Febuary 19, 2003. Available online: http://visibleearth.nasa.gov/view.php?id=65200 11 June 2015.

Fang, X., Pomeroy, J.W., Ellis, C.R., MacDonald, M.K., DeBeer, C.M. & Brown, T. 2013 Multi-variable evaluation of hydrological model predictions for a headwater basin in the Canadian Rocky Mountains. *Hydrol. Earth Syst. Sci*. 17(4), 1635-1659 http://dx.doi.org/10.5194/hessd-9-12825-2012.

Feiccabrino, J., Gustafsson, D. & Lundberg, A. 2012 Improving surface based precipitation phase determination through air mass boundary identification. *Hydrol. Res.* 43(3), 179-191.

Harder, P. & Pomeroy, J. 2013 Estimating precipitation phase using a psychrometric energy balance method. *Hydrol. Process*. 27(13), 1901-1914 http://dx.doi.org/10.1002/hyp.9799.

Lundberg, A. & Fieccabrino, J. 2009 Sea ice growth, modeling of precipitation phase, Proc. *20th International Conference on Port and Ocean Engineering under Arctic Conditions*.

Marks, D., Winstral, A., Reba, M., Pomeroy, J. & Kumar, M. 2013 An evaluation of methods for determining during-storm precipitation phase and the rain/snow transition elevation at the surface in a mountain basin. *Adv. Water Resour*. 55, 98-110 http://dx.doi.org/10.1016/j.advwatres.2012.11.012.

Matsuo, T., Sato, Y. & Sasyo, Y. 1981 Relationship between types of precipitation on the ground and surface meteorological elements. *J Meteorol. Soc. Jpn*. 59(4), 462-475.

Minder, J.R., Durran, D.R. & Roe, G.H. 2011 Mesoscale controls on the mountainside snow line. *J. Atmos. Sci*. 68(9), 2107-2127 http://dx.doi.org/10.1175/JAS-D-10-05006.1.

Stewart, R.E. 1992 Precipitation types in the transition region of winter storms. *Bull. Am. Meteorol. Soc.* 73(3), 287-296 http://dx.doi.org/10.1175/1520-0477(1992)073<0287:PTITTR>2.0.CO;2.

Stull, R. 2011 Wet-Bulb temperature from relative humidity and air temperature. *J. Appl. Meteorol. Climatol.* 50, 2267–2269.

Thériault, J.M. & Stewart, R.E. 2010 A parameterization of the microphysical processes forming many types of winter precipitation. *J. Atmos. Sci.* 67(5), 1492-1508 http://dx.doi.org/10.1175/2009JAS3224.1.

United States Army Corps of Engineers (USACE) 1956 *Snow hydrology*, Summary report of the snow investigations., North Pacific Division, Portland, OR, pp. 437.

Ye, H., Cohen, J. & Rawlins, M. 2013 Discrimination of solid from liquid precipitation over northern Eurasia using surface atmospheric conditions. *J. Hydrometeorol*. 14(4), 1345-1355 http://dx.doi.org/10.1175/JHM-D-12-0164.1.

FLUSH: 3D hydrological model for agricultural water management in high latitude areas

Koivusalo, H.[1*], Turunen, M.[1], Salo, H.[1], Haahti. K.[1], Nousiainen[2], R., Warsta, L.[1]

[1]*Department of Civil and Environmental Engineering, Aalto University School of Engineering, P.O. Box 15300, FI-00076 Aalto, Finland.*
[2]*Natural Resources Institute Finland (Luke), Vakolantie 55, FI-03400 Vihti, Finland*
**harri.koivusalo@aalto.fi*

ABSTRACT
Crop cultivation in high latitudes is constrained by short growing season and long dormant season with snow and frozen ground conditions. These hydrological characteristics enhance generation of large runoff volumes during periods of low evapotranspiration demand in autumn and rapid snowmelt during spring. Runoff leads to elevated loads of sediment and nutrients to surface waters. Cultivated fields in many northern regions are clay soils with distinctive hydraulic and load generation properties. FLUSH is a recently developed hydrological and solute transport computation platform for simulating year-round hydrological processes in agricultural fields and catchments. The subsurface flow and transport model is fully 3D and overland flow scheme is 2D. FLUSH is supplied with routines for describing water, heat and erosion processes in structured soils such as clay. The model is built with snow energy balance and soil heat transport schemes and augmented with a ditch network model, which facilitates extension of modeling scale from fields to small catchments. This paper demonstrates application of FLUSH to simulate water balance over seven years in two agricultural field sections in Gårdskulla Gård in southern Finland. A series of six periods outside of the growing season was simulated and the periods were classified in terms of the North Atlantic Oscillation (NAO) index. Runoff generation and drainage processes during mild (positive NAO index) and cold (negative NAO index) periods were investigated. The water balance simulations revealed key hydrological characteristics of cultivated fields, which paves the way for the design of efficient agricultural water management.

KEYWORDS
Water balance, hydrological modelling, NAO index, runoff, subsurface drains, agriculture, clay soil

1. INTRODUCTION

Agricultural water management in high-latitude areas is challenged by short growing season and long dormant season with low net radiation, cold temperatures, and low evapotranspiration demand. Runoff generation potential in northern areas is clearly higher during the period from autumn to spring than during summer. In snow-affected regions the winter and spring runoff patterns are strongly modified by cycles of snow accumulation and melt (Su et al. 2011; Jamieson et al. 2003; Turunen et al. 2015). High runoff volumes in cultivated areas with exposed bare soil surface lead to generation of sediment and nutrient loads to surface waters (e.g. Su et al. 2011; Puustinen et al. 2007). In future, the projected climate warming and increasing precipitation levels can worsen the ecological status of surface waters by leading to sustained periods of increased runoff and loads from cultivated areas especially in the high latitude areas (Hägg et al. 2013; Huttunen et al. 2015; Puustinen et al. 2007).

Agricultural water management in northern areas is challenged by the difficulties to effectively control load generation that occurs outside of the growing season. Several programs of water protection have been implemented but oftentimes the results of water protection measures from the point of view of the quality of receiving waters have been disappointing (Stålnacke et al. 2014; Ekholm et al. 2015). Experimental and modeling studies in cultivated fields have provided basic understanding of runoff and load generation processes in pollution source areas, but the detailed understanding of cold region hydrological processes and their implications on runoff and load generation under changing climatic conditions is incomplete (e.g. Kane 2005).

Hydrological computation routines, coupled with snow and frozen soil process description are available to tackle the issues of agricultural water management (e.g. Arnold et al. 1993; Larsson and Jarvis 1999; Luo et al. 2000; Kroes et al. 2008; Warsta et al. 2012). One-dimensional models can unveil the basic seasonal processes in the vertical distribution of water stored in snow and soil. However, one-dimensional models do not provide optimal support for assessment of water protection measures, because the measures are effectively two- or three-dimensional structures (Mohanty et al. 1998; Gärdenäs et al. 2006; Hintikka et al. 2008). The recent development of 3D hydrological models that include wintertime process descriptions (e.g. Refsgaard et al. 2010; Šimůnek and Šejna 2011; Warsta et al. 2012) supports more spatially diverse simulation of the field sections, including spatial distribution of soil properties and agricultural water management systems, such as open ditches and subsurface drainage networks.

The objective of this study was to demonstrate the application of FLUSH model (Warsta 2011; Warsta 2013a; Warsta 2013b) for simulating the hydrology of cultivated field sections located in southern Finland. The simulations covered a period of seven years in the experimental field of Gårdskulla Gård, where the past measurement campaigns of Äijö et al. (2014) have provided an extensive hourly data set of two field sections. The more specific objective was to demonstrate the variability of water outflow from the fields during series of dormant seasons with variable winter meteorological conditions. The long-term data and the model simulations supported data-based detection of water balance and its characteristics in winters with warm and cool weather patterns quantified by the NAO index (NOAA-NWS 2015).

2. SITE DESCRIPTION AND DATA

The study site of Gårdskulla Gård is situated in southern Finland (60°10'32"N, 24°10'17"E, Figure 1) in a coastal agricultural area of clay soils and mildly undulating topography. The climate in the area is characterised by the mean hourly air temperature of 6 °C and mean annual precipitation of 700 mm during the study years from 2008 to 2014. The setup of the experimental field includes two field sections with slopes of 1% and 5% (Figure 1). Soils within the fields belong to Vertic Luvic Stagnosols (Turunen et al. 2015).

The experimental setup, drainage design, soil characteristics and hydrometeorological measurements are documented in detail in Turunen et al. (2015) and Vakkilainen et al. (2008), while only a brief summary is provided here. Subsurface drain discharge and tillage layer runoff in the two sections (Figure 1) were measured with the frequency of 15 min using automated systems, and groundwater table level, snow water equivalent (SWE) and frost depth were manually observed weekly/biweekly during field visits from 2008 to 2014. The spacing of the subsurface drains (plastic pipes with a diameter of 0.05 m) was 16 m and the drain depth was 1 m in both field sections. The area of the monitored subsurface drain network was 5.7 ha in the flat section 1 and 4.7 ha in the steep section 2 (Figure 1). Shallow

subsurface drains were installed at the depth of 0.4 m in the lowest parts of the sections to collect tillage layer runoff. The tillage layer runoff measurement system recorded both surface runoff and the subsurface runoff flowing horizontally at the top soil layer that was regularly disturbed by the tillage operations. The tillage layer runoff measurement system collected runoff from an area of 3.3 ha in section 1 and 3.0 ha in section 2. The details of the measurements and data processing are described by Turunen et al. (2015).

Precipitation was recorded on site with a 15 min interval using a RAINEW 111 tipping bucket rain gauge (RainWise Inc., Bar Harbor, ME, USA). The form of precipitation was described as a function of air temperature and rainfall and snowfall were corrected with coefficients of 1.05 and 1.3, respectively. Other meteorological records were compiled from the weather stations of the Finnish Meteorological Institute (Turunen et al. 2015). For this study the dataset in Turunen et al. (2015) was extended with two years forming a total record of seven years of hourly hydrometeorological data. The data on the North Atlantic Oscillation (NAO) index were compiled from NOAA-NWS (2015) as monthly values over the study years.

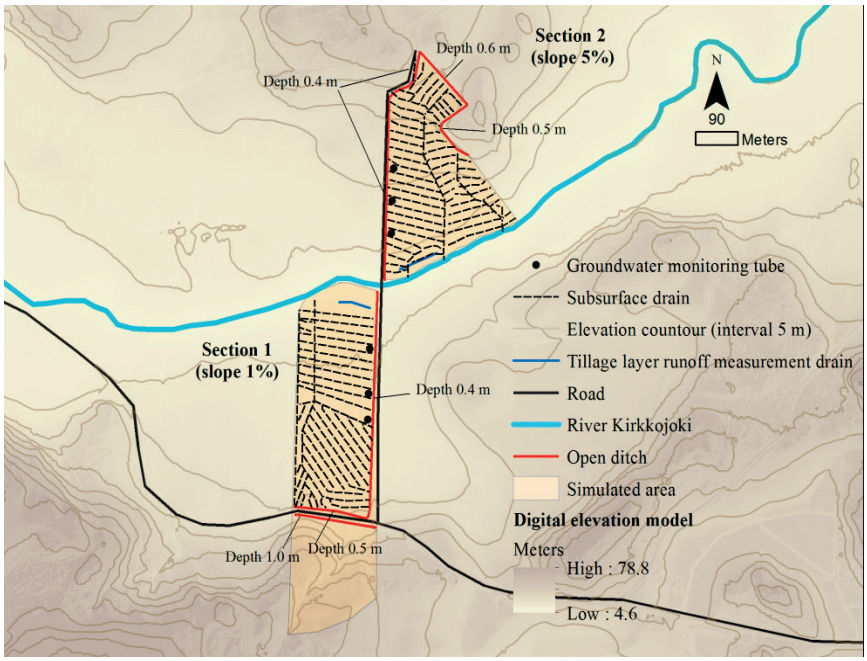

Figure 1. Location of the Gårdskulla Gård experimental field and layout of two monitored field sections.

3. THE HYDROLOGICAL MODEL AND ITS PARAMETERISATION

FLUSH is a distributed and dynamic hydrological model, which simulates subsurface water flow in 3D and overland flow in 2D (Warsta 2011; Warsta et al. 2013a). Due to the 3D approach, FLUSH is able to describe all dominant water balance components, and the model can take into account the spatial differences in soil hydraulic properties, drainage systems and land-use. The numerical solutions of the governing differential equations of overland and soil water flow are built on the finite volume method. The model simulates water flow with dual-permeability approach by dividing the subsurface computational domain into soil matrix and macropores. Water flow in both pore systems is computed with the Richards equation, and soil water retention characteristics and unsaturated hydraulic conductivities are described with

the van Genuchten (1980) schemes. Water exchange between the pore systems is calculated as a function of soil hydraulic properties and pressure difference (Gerke and van Genuchten 1993). In addition to static macropores, the model can take into account the dynamic soil macroporosity changes due to shrinkage and swelling with the approach of Kroes et al. (2008).

In order to support allow simulations throughout all seasons, Warsta et al. (2012) augmented the model with winter-time hydrological process descriptions through an energy-balance based snow model (Koivusalo et al. 2001) and a frozen soil description. The model simulates accumulation, melt and sublimation of snow, dynamics of snow and soil temperature, as well as soil freezing and thawing. Currently soil frost does not affect soil hydraulic parameters in the model.

Measured meteorological data and pre-computed series of potential evapotranspiration are given to the model as hourly input. Actual evapotranspiration is calculated by distributing the potential evapotranspiration vertically to the soil according to root mass distribution and by reducing potential evapotranspiration in too dry or wet soil moisture conditions (Feddes et al. 1978). Root depths, soil hydraulic parameters, digital elevation map, soil layer depths, and drainage systems parameters and locations are required as model input files. Dynamic changes in soil hydraulic parameters (e.g. macroporosity and depression storage) can be input to the model as time series. Model removes water from the simulated domain via surface runoff, drain discharge, groundwater outflow, seepage to open ditches and evapotranspiration. The drainage systems are described as sink terms in the model, and calculation of subsurface drainage fluxes is based on the Darcy's law. FLUSH includes computational descriptions for soil erosion and transport of suspended solids and solutes (Warsta et al. 2013b; Salo et al. 2015), as well as ditch hydraulic processes (Haahti et al. 2014).

The model parameterization in this study was based on the five-year simulations (2008-2012) of Turunen et al. (2015), who calibrated and validated a limited number of snow, drainage and soil parameters to match the model simulations against measurements of snow water equivalent, as well as subsurface drain discharge and tillage layer runoff series of the two sections in Gårdskulla Gård. The simulations of Turunen et al (2015) were extended in this study to cover two additional years (2008-2014). The boundary conditions of the downslope end of the modeled field sections were set as the observed water level of the Kirkkojoki stream flowing between the field sections (Figure 1). The upper boundary condition of field section 1 was a no-flow interface, but the simulated area of the field section 2 was extended south of the field section to account for the hydrological connection between the uphill areas and the field section. According to Turunen et al. (2015) exclusion of this hydrological connection in the model calibration resulted in biased and likely too small subsoil macroporosity in field section 1, and in this study the macroporosity in the soil layers beneath drain depth in section 1 was set to similar value as in field section 2 (0.08 %), i.e. it was assumed that both sections have similar subsoil structure. The bottom and the sides of the field sections were treated as no-flow boundaries. The boundary conditions in the ditches were prescribed as fixed water levels without using the hydraulic computation routine. For the analyses of water balance in this study, the modeled actual evapotranspiration in the field sections, the modeled drain discharge from the gauged drainage networks, the modeled tillage layer runoff, and the simulated groundwater flow entering the Kirkkojoki stream through subsurface pathways were quantified as daily time series based on the hourly computation results from 1 January 2008 to 31 December 2014.

4. RESULTS AND DISCUSSION

Figure 2 presents the calibration and extended validation results of the model in terms of annual accumulated drain discharge and tillage layer runoff in the two field sections of the Gårdskulla Gård experimental field. The modified efficiency of Legates and McCabe (1999), as used by Turunen et al. (2015), between the daily measured and simulated drain discharge during the calibration period (2008-2010) was 0.53 and 0.59 for the field sections with slopes of 1% and 5%, respectively. The corresponding coefficients for the drain discharge during the validation period were 0.38 and 0.41. The modified efficiency for tillage layer runoff during the calibration was 0.48 (slope 1%) and 0.61 (slope 5%), and the corresponding values for the validation were 0.49 and 0.51. The measured fraction of tillage layer runoff from the total drain discharge was 9-19%. There were spring periods with strikingly clear difference between the modeled tillage layer runoff and the measurements in April 2010 in the flat field section (Figure 2a) and in March 2012 in the steep field section (Figure 2b). These differences may be attributed to soil frost conditions (Turunen et al. 2015).

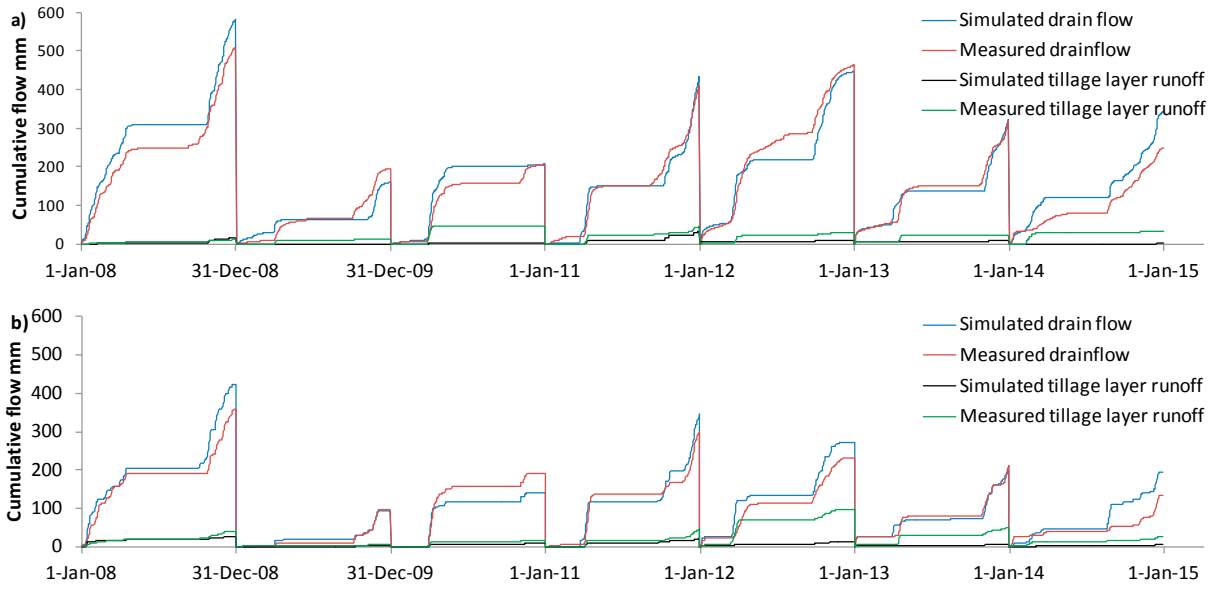

Figure 2. Measured and simulated annual accumulated series of drain discharge and tillage layer runoff in field sections 1 (a) and 2 (b). The years 2008-2010 are the model calibration period (see Turunen et al. 2015) and the years 2011-2014 are the validation period.

The annual water balance for the seven calendar years (Figure 3) reveals how precipitation in both field sections is divided into two major components: evapotranspiration and subsurface drain discharge. Evapotranspiration has a strong annual pattern, which dominates the growing season water balance (May-August) when all runoff components are low. Subsurface drain discharge is the major outflow component and it is the distinct hydrological feature outside the growing season (September-April). In contrast to evapotranspiration, subsurface drain discharge shows strong variability between different years. The major difference between the field sections is the lower level of subsurface drain discharge and the higher level of the secondary drainage to the main stream from section 2 with a higher slope. The secondary drainage occurs as groundwater flow through the saturated soil layers into the main stream between the field sections. Even though the soil in Gårdskulla fields is clay, the volume of tillage layer runoff remains low due to relatively high hydraulic conductivity of the macroporous clay soil, and moderately low precipitation and snowmelt intensities.

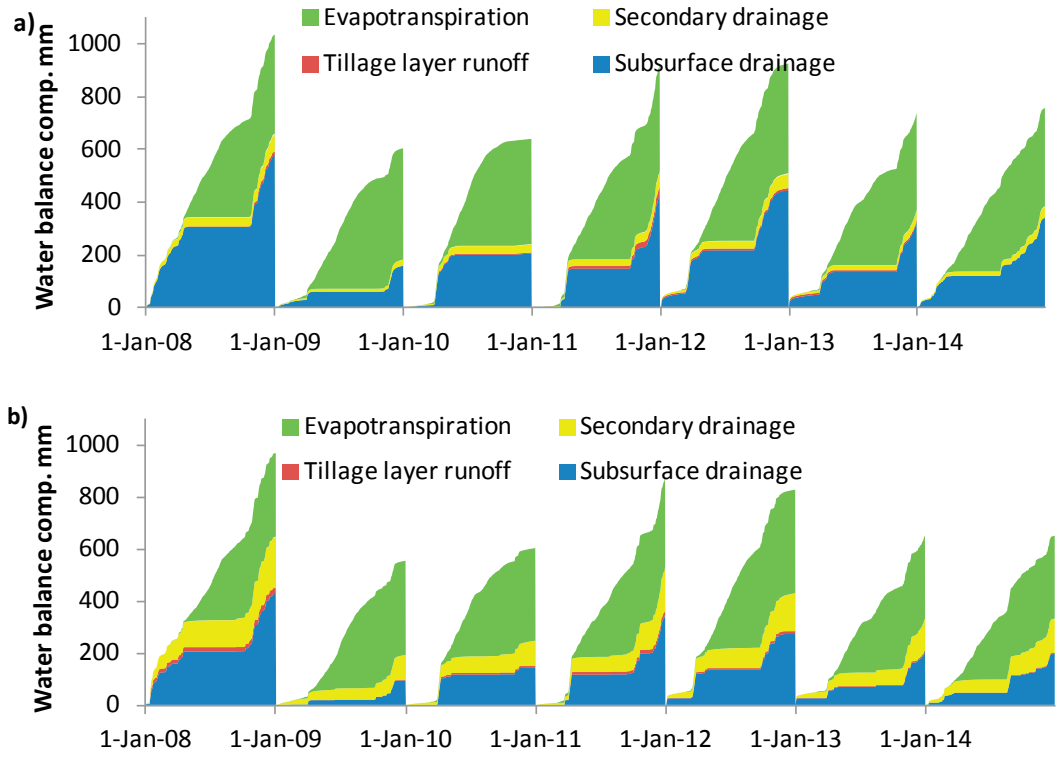

Figure 3. Cumulative water balance components from 2008 to 2014 in Gårdskulla Gård for the flat field section 1 (a, slope 1%) and the steep field section 2 (b, slope 5%).

The long computation period contained a large range of meteorological conditions, which led to winter periods with both plenty of snow (max winter SWE up to 176 mm) and with little snow (max SWE down to 22 mm). In order to classify the dormant periods, NAO indices were averaged from monthly values published by NOAA-NWS (2015) for the periods from September to April during the years 2008-2014. The mean September-April air temperature during the study years was strongly related to NAO with clearly higher values during the three periods when the mean NAO index was above zero and lower values when the NAO index was negative (Figure 4a). The precipitation sums reflect NAO less clearly, but the September-April periods with higher precipitation sums tend to occur simultaneously with positive NAO index. Figure 4b illustrates how the two major outflow components, the subsurface drain discharge and the secondary drainage flow, reflect the changes in NAO index. When the three years with positive NAO index are compared against the three years with negative NAO index, the subsurface drain discharge sum from the two field sections shows an increase of 46% and the secondary drain flow sum increases 30%. These changes can be set against the impact of slope on the fraction of the water outflow components: When slope increases from 1% to 5%, the subsurface drain discharge decreases 32% and secondary drain flow increases 99%. The highest levels of subsurface drain flows occurred in the flat field section during the years with mild winter and positive NAO index. The totals of tillage layer runoff were clearly lower than the subsurface flow components. The tillage layer runoff was not related to the NAO index as the other outflow components were, but it was dependent on the occurrence of occasional high intensity rainfall and snowmelt events.

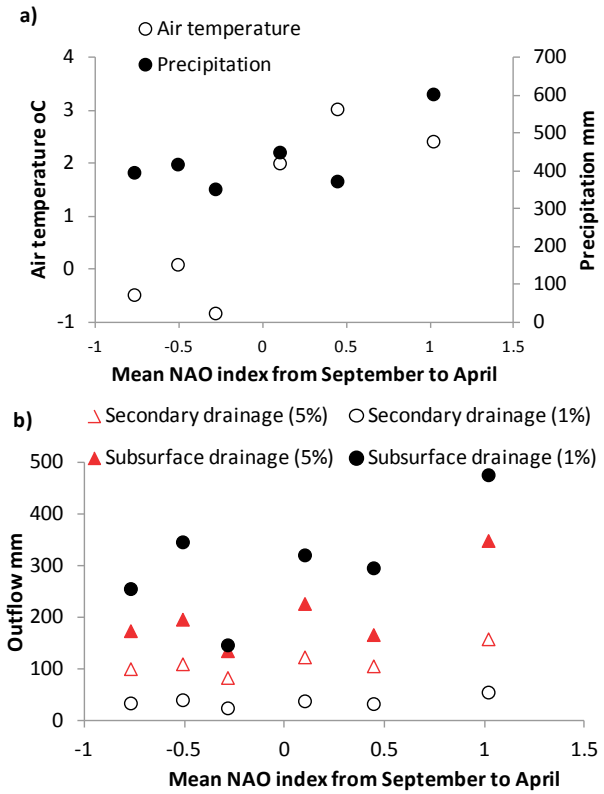

Figure 4. Mean air temperature and total precipitation (a) and subsurface drainage components (b) in the two fields of Gårdskulla Gård during periods from September to April with different mean values of the NAO index in 2008-2014.

The distribution of daily intensities of subsurface drain discharge showed a clear dependency on both NAO and the slope of the field sections as shown in Figure 5. The highest intensities of subsurface drain discharge were more or less the same, which is explained by the capacity of the drainage system. The modelled subsurface drain discharge is bound to a maximum level due to the entrance resistance computation scheme (Warsta et al. 2013). The moderate range of subsurface drain discharge intensities (0-4 mm/d in Figure 5a) was clearly lower in periods with negative NAO compared to the periods of positive NAO. This reflects the sustained generation of subsurface drain discharge during warm winters. In cold winters with negative NAO, subsurface flows were lower, because water was stored in the snowpack. The highest flows occurred during spring snowmelt, which is a short period of runoff generation compared to the sustained generation of runoff during mid-winter rain and intermittent snowmelt periods in mild winters (positive NAO). In contrast to the subsurface drain discharge, the highest intensities of tillage layer runoff were clearly affected by the slope of the field section with the highest intensities in the steep section. The impact of NAO and weather conditions on tillage layer runoff was not visible mainly because the number of tillage layer runoff events was small.

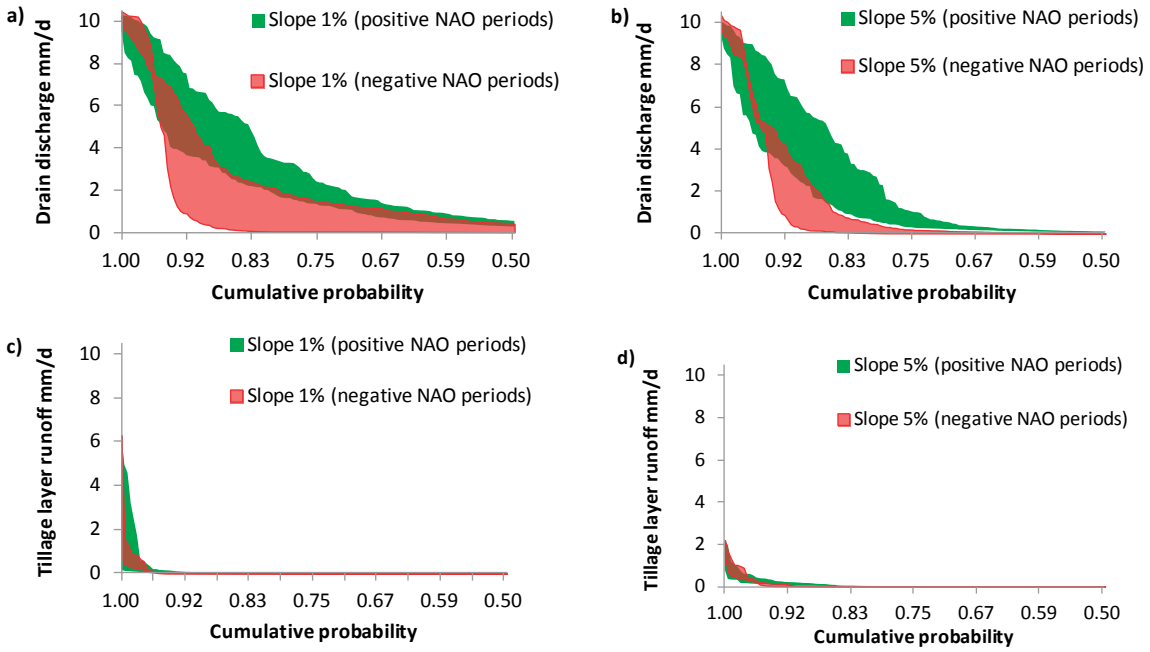

Figure 5. Upper 50% cumulative distribution of daily subsurface drain discharge intensities during the periods with positive and negative NAO index for the section with 1 % slope (a) and 5 % slope (b), and cumulative distribution of daily tillage layer runoff intensities during the years with positive and negative NAO index for the section with 1 % slope (c) and 5 % slope (d) in the Gårdskulla Gård experimental field during 2008-2014. Both shaded areas represent three periods of positive or negative NAO index.

5. CONCLUSIONS

The application of FLUSH to produce a holistic quantification of water balance components in an agricultural field was demonstrated through an investigation over a period of seven years in clayey field sections of Gårdskulla Gård. In the studied high-latitude conditions, evapotranspiration was the dominant water component during the growing seasons from May to August, whereas drain discharge dominated the water balance during the dormant periods from September to April. Drain discharge volumes showed a large variability between different years compared with the annual evapotranspiration with less variation. The increasing slope of the field area decreased the volume of subsurface drain discharge, which was compensated by an increase in groundwater outflow from the field area to the main stream. The variability of water outflow components between the years was largely related to the weather patterns outside of the growing season. Mild periods with positive NAO had the highest outflow volumes, which occurred throughout the dormant season. The difference of drain discharge and groundwater outflow caused by mild and cold periods was nearly as high as the impact of local slope (1 or 5%) on the runoff components. Tillage layer runoff occurring in the near surface layers of the field was low and depended more on the occasional intensities of high rainfall and snowmelt instead of the periodical weather patterns. Understanding and quantifying the water balance through periods of changing weather patterns is crucial for gaining improvements in agricultural water management and control of nutrient and sediment loads. The NAO index provides a convenient way to categorize winter conditions, which reflect runoff and load generation potential in cultivated areas in Nordic latitudes.

6. ACKNOWLEDGEMENTS

The study was funded by the Aalto University School of Engineering, the Finnish Drainage Research Foundation, the Ministry of Agriculture and Forestry and Maa- ja vesitekniikan tuki ry. We acknowledge CSC – IT Center for Science Ltd. for the allocation of computational resources.

7. REFERENCES

Äijö, H., Myllys, M., Nurminen, J., Turunen, M., Warsta, L., Paasonen-Kivekäs, M., Kor-pelainen, E., Salo, H., Sikkilä, M., Alakukku, L., Puustinen, M., 2014. PVO2-hanke, Salaojitustekniikat ja pellon vesitalouden optimointi. Salaojituksen tutkimusyhdistys ry:n tiedote 31. Finnish Field Drainage Association, Helsinki, Finland, pp. 105

Ekholm, P., Rankinen, K., Rita, H., Räike, A., Sjöblom, H., Raateland, A., Vesikko, L., Bernal, J.E.C., Taskinen, A., 2015. Phosphorus and nitrogen fluxes carried by 21 Finnish agricultural rivers in 1985–2006. Environmental Monitoring and Assessment 187, 1–17

Feddes RA,Kowalik PJ, ZaradnyH. 1978. Simulation of field water use and crop yield. Wageningen: Pudoc; 189 p.

Gärdenäs, A.I., Simunek, J., Jarvis, N., Genuchten, M.Th., 2006. Two-dimensional modelling of preferential water flow and pesticide transport from tile-drained field. Journal of Hydrology 329, 647–660.

Gerke, H.H., van Genuchten, M.T., 1993. A dual-porosity model for simulating the preferential movement of water and solutes in structured porous media. Water Resources Research 29, 305–319.

Haahti, K., Younis, B.A., Stenberg, L., Koivusalo, H. 2014. Unsteady flow simulation and erosion assessment in a ditch network of a drained peatland forest catchment in eastern Finland. Water Resources Management 28(14), 5175-5197.

Hägg, H.E., Lyon, S.W., Wällstedt, T., Mörth, C.-M., Claremar, B., Humborg, C., 2013. Future Nutrient Load Scenarios for the Baltic Sea Due to Climate and Lifestyle Changes. AMBIO 43, 337–351

Hintikka, S., Koivusalo, H., Paasonen-Kivekäs, M., Nuutinen, V., Alakukku, L., 2008.Role of macroporosity in runoff generation on a sloping subsurface drained clay field – a case study with MACRO model. Hydrological Research 39 (2), 143–155.

Huttunen, I., Lehtonen, H., Huttunen, M., Piirainen, V., Korppoo, M., Veijalainen, N., Viitasalo, M., Vehviläinen, B., 2015. Effects of climate change and agricultural adaptation on nutrient loading from Finnish catchments to the Baltic Sea. Science of The Total Environment 529, 168–181

Jamieson, A., Madramootoo, C.A., Engright, P., 2003. Phosphorus losses in surface and subsurface runoff from a snowmelt event on an agricultural field in Quebec. Canadian Biosystem Engineering 45, 1.1–1.7

Kane, D.L., 2005. High-latitude hydrology, what do we know? Hydrol. Process. 19, 2453–2454

Koivusalo, H., Heikinheimo, M., Karvonen, T., 2001. Test of a simple two-layer parameterisation to simulate the energy balance and temperature of a snow pack. Theorethical and Applied Climatology 70 (1–4), 65–79.

Kroes, J.G., van Dam, J.C., Groenendijk, P., Hendriks, R.F.A., Jacobs, C.M.J., 2008. SWAP version 3.2 – Theory description and user manual. Alterra-report 1649. Wageningen, The Netherlands, 262 pp.

Luo, W., Skaggs, R.W., Chescheir, G.M., 2000. DRAINMOD modifications for cold conditions. Transactions of the ASAE 43 (6), 1569-1582

Mohanty, B.P., Bowman, R.S., Hendrickx, J.M.H., Simunek, J., Van Genuchten, M.T.,1998. Preferential transport of nitrate to a tile drain in an intermittent-flood-irrigated field: model development and experimental evaluation. Water Resources Research 34 (5), 1061–1076.

NOAA-NWS. 2015. North Antaltic Oscillation (NAO). Climate Prediction Center, National Weather Service, National Oceanic and Atmospheric Administration, http://www.cpc.ncep.noaa.gov/products/precip/CWlink/pna/nao.shtml#current

Puustinen, M., Tattari, S., Koskiaho, J., Linjama, J., 2007. Influence of seasonal and annual hydrological variations on erosion and phosphorus transport from arable areas in Finland. Soil and Tillage Research 93, 44–55

Refsgaard, J.C., Storm, B., Clausen, T., 2010. Système Hydrologique Europeén (SHE): review and perspectives after 30 years development in distributed physically-based hydrological modelling. Hydrology research 41, 355–377

Salo, H., Warsta, L., Turunen, M., Paasonen-Kivekäs, M., Nurminen, J., & Koivusalo, H., 2015. Development and application of a solute transport model to describe field-scale nitrogen processes during autumn rains. Acta Agriculturae Scandinavica, Section B—Soil & Plant Science, 65(sup1), 30-43

Šimůnek, J. and Šejna M., 2011. HYDRUS – Software Package for Simulating the Two- and Three-dimensional Movement of Water, Heat and Multiple Solutes in Variably-Saturated Media. Technical manual. Version 2. PC-Progress, Prague, Czech Republic.

Stålnacke, P., Aakerøy, P.A., Blicher-Mathiesen, G., Iital, A., Jansons, V., Koskiaho, J., Kyllmar, K., Lagzdins, A., Pengerud, A., Povilaitis, A., 2014. Temporal trends in nitrogen concentrations and losses from agricultural catchments in the Nordic and Baltic countries. Agriculture, Ecosystems & Environment, Nitrogen losses from agriculture in the Baltic Sea region 198, 94–103

Su, J.J., van Bochove, E., Thériault, G., Novotna, B., Khaldoune, J., Denault, J.T., Zhou, J., Nolin, M.C., Hu, C.X., Bernier, M., Benoy, G., Xing, Z.S., Chow, L., 2011. Effects of snowmelt on phosphorus and sediment losses from agricultural watersheds in Eastern Canada. Agricultural Water Management 98, 867–876

Turunen, M., Warsta, L., Paasonen-Kivekäs, M., Nurminen, J., Alakukku, L., Myllys, M., Koivusalo, H., 2015. Effects of terrain slope on long-term and seasonal water balances in clayey, subsurface drained agricultural fields in high latitude conditions. Agricultural Water Management 150, 139–151

Vakkilainen, P., Alakukku, L., Myllys, M., Nurminen, J., Paasonen-Kivekäs, M., Peltomaa, R., Puustinen, M., Äijö, H., 2008. Pellon vesitalouden optimointi – Väliraportti 2008. Salaojituksen tutkimusyhdistys ry:n tiedote 29. Finnish Field Drainage Association, Helsinki, Finland, 100 pp.

van Genuchten, M.Th., 1980. A closed-form equation for predicting the hydraulic conductivity of unsaturated soils. Soil Science Society of America Journal 44, 892–898

Warsta, L., Turunen, M., Koivusalo, H., Paasonen-Kivekäs, M., Karvonen, T., Taski-nen, A., 2012. Modelling heat transport and freezing and thawing processes ina clayey, subsurface drained agricultural field. In: Proceedings of the 11th ICID Int. Drainage Workshop on Agricultural Drainage, Needs and Future Priorities, Cairo 23–27.9.2012, Egypt, pp.10.

Warsta, L., 2011. Modelling water flow and soil erosion in clayey, subsurface drained agricultural fields. Doctoral dissertation. Aalto University, School of Engineering, Department of Civil and Environmental Engineering, Espoo, Finland, 212 pp.

Warsta, L., Karvonen, T., Koivusalo, H., Paasonen-Kivekäs, M., Taskinen, A., 2013a.Simulation of water balance in a clayey, subsurface drained agricultural field with three-dimensional FLUSH model. Journal of Hydrology 476, 395–409

Warsta, L., Taskinen, A., Koivusalo, H., Paasonen-Kivekäs, M., Karvonen, T., 2013b.Modelling soil erosion in a clayey, subsurface-drained agricultural field with a three-dimensional FLUSH model. Journal of Hydrology 498, 132–143.

Usability of water temperature data from water level pressure transducers – a study on diurnal and vertical surface temperature variation in lakes and rivers

Johanna Korhonen[1*], Otso Seppälä[2], Jarkko J. Koskela[1]

[1]*Finnish Environment Institute (SYKE), P.O. Box 140, 00251 Helsinki, FINLAND*
[2]*Department of Civil and Environmental Engineering, Water Resources Engineering, Aalto University, FINLAND*
**johanna.korhonen@ymparisto.fi*

ABSTRACT

Lake surface temperatures can directly or indirectly influence physical, chemical, and biological processes in a lake and thus they are important information for researchers and experts. Water temperature is known for diurnal variation and vertical stratification in lakes during summer months in Finland. Pressure sensor measurements have become common for water level monitoring during recent decades and many of the devices are providing additional temperature information at the sensor's depth. Water temperature data gathered from pressure transducers installed in lakes and rivers were compared with official surface water temperature measured at 20 cm depth once a day. In this study diurnal and vertical variation of surface water temperature are analysed using data from eight different sites in Finland during the summer 2014. Study shows that pressure transducers provide additional temperature information which can be used for different purposes, but location and depth of the sensor have to be taken into account when using the data. The pressure transducer data could be in best use in the areas which do not have official temperature measurement sites nearby.

KEYWORDS

Surface water temperature; pressure transducer; variation; usability study; Finland

1. INTRODUCTION

The water temperature plays an important role in the energy balance of lakes and rivers through evaporation and advection. Water temperature has also an influence on the biological activity and growth of aquatic organisms in lakes. In summer season water temperature has also a major recreational role in northern latitudes where open water season is rather short. Main drivers affecting water temperature variation are meteorological variables like solar radiation, air temperature, wind speed, cloud cover, and relative humidity (Edinger et al 1968). Although mainly weather is affecting changes in water temperature, there is a response backwards. In Finland, large lakes play important microclimatic role especially in the spring and autumn when temperature difference between air masses and water bodies are large. Therefore lake water temperature is used as a data source for numerical weather prediction model HIRLAM in Finland (Rontu et al. 2012).

Since water temperature has an influence on many things, temperature data of lakes and rivers are frequently asked for different research projects and applications both at national level and globally. Lately a global database of water temperature data was established (Sharma et al. 2015). Temperature observations are used in Finland for example in the hydrological models

for lake evaporation calculation (Elo & Koistinen 2002) or for validation of satellite surface water observations (Kheyrollah Pour et al. 2014). Diurnal variations of surface water have already been studied in the 1970's and 1980's on Finnish lakes related to evaporation and heat balance studies (Elomaa, 1977; Järvinen & Huttula 1982).

There is a high demand for water temperature information in Finland especially in summertime and the official network is rather sparse. Pressure sensor measurements have become common for water level monitoring during recent decades and many of the devices are providing additional temperature information at the sensor's depth. In this study usability of temperature data derived from pressure transducers are investigated as an additional source of temperature data. This paper is mainly based on the Bachelor's Thesis by Seppälä (2015).

2. DATA AND METHODS

In Finland, systematic long-term surface water temperature monitoring in lakes and rivers has been carried out several decades by the Finnish Environment Institute. These temperatures have been measured once per day in the morning at 8 am at the depth of 20 cm (Korhonen, 2002). The surface water temperature network of lakes and rivers is rather sparse including only 34 sites in Finland in the year 2014. Most of the measuring sites are located in the southern or central part of the country. In the 20th century there used to be more measurement sites in the network but number of stations decreased remarkably in the 1990's due to budget cuts in monitoring. Measurements were done in the 20th century manually by an observer from the shore using a mercury thermometer. Later, measurements were done with a digital thermometer. In the 2000's automation of these measurements started with Finnish brand PVD designed for lake surface water measurements (Figure 1). In summer 2014 most of stations were equipped with floating automatic temperature sensors transmitting morning (8 am) values by SMS to the Finnish Environment Institute database. Newest versions of PVD devices make measurements every hour producing diurnal variation information.

Pressure transducers which are used for water level measuring measure simultaneously water temperature at the sensor depth. In this study water temperature information from OTT PLS pressure sensors were used. Water level transducers are measuring water temperature every 15 minutes. The Finnish Environment Institute had in year 2014 approximately 100 OTT pressure transducers in the field. They all provide water temperature information.

Data of official surface water temperature and pressure transducers were compared for eight different sites for the summer 2014. At three of study sites, pressure transducers were exactly in the same locations as official surface water temperature measurement within tens of meters distance. At three of study sites pressure sensors were installed in a limnigraph well, but not directly to the lake or river. Two of pressure sensor data sites did not have official temperature records in the same area. Data from near-by watershed were used for comparison. Information on sites used in this study is listed in the Table 1.

Figure 1. An example of floating PVD measuring surface water temperature.

Table 1. Sites included in this study. Compared official surface water temperature stations and water level stations with pressure transducer.

Site number in Figure 2.	Official water temperature site	Water level station	Distance between	Average pressure sensor depth during 2014	Remarks
1	Saimaa, Lauritsala	Saimaa, Lauritsala	< 500 m	1.47 m	Pressure sensor in the limnigraph well
2	Säkylän Pyhäjärvi	Säkylän Pyhäjärvi	< 500m	0.98 m	Pressure sensor in the limnigraph well
3	Kyyvesi	Kyyvesi	< 500 m	1.45 m	
4	Kallavesi	Kallavesi	< 20 m	1.57 m	
5	Oulankajoki	Kitkajoki	~10 km	1.39 m	Different river/ watershed
6	Inari, Nellim	Inari, Nellim	< 20 m	1.79 m	Pressure sensor in the limnigraph well
7	Kevojärvi	Muttusjärvi	~100 km	0.87 m	Different river/watershed
8	Kilpisjärvi	Kilpisjärvi	< 20 m	0.99 m	

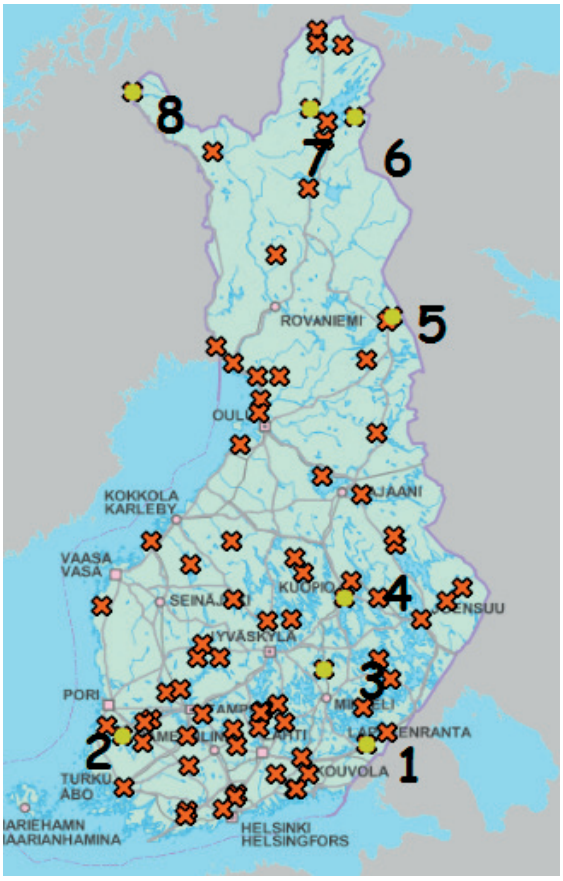

Figure 2. A map of official surface water temperature stations (orange crosses) in Finland and locations of OTT pressure transducers used in this study (yellow circles) for comparison.

3. RESULTS AND DISCUSSION

3.1 Comparison of water temperatures from pressure transducer and official surface water temperature observations

Temperature data from pressure transducers which were installed directly into a lake or a river did not differ remarkably from official surface water values, even though pressure sensors were in the deeper water layer. Differences were mostly under 2 degrees. In early summer when the warm surface layer is shallow there were more differences than during the late summer when water column was already warmed and the thermocline rather deep. During early summer depth of thermocline and upwelling of colder hypolimnion water caused mainly differences between official surface water temperature data and pressure sensor temperature data. At sites Kyyvesi, Kallavesi and Kilpisjärvi bias between different measurements were small (example Figure 3).

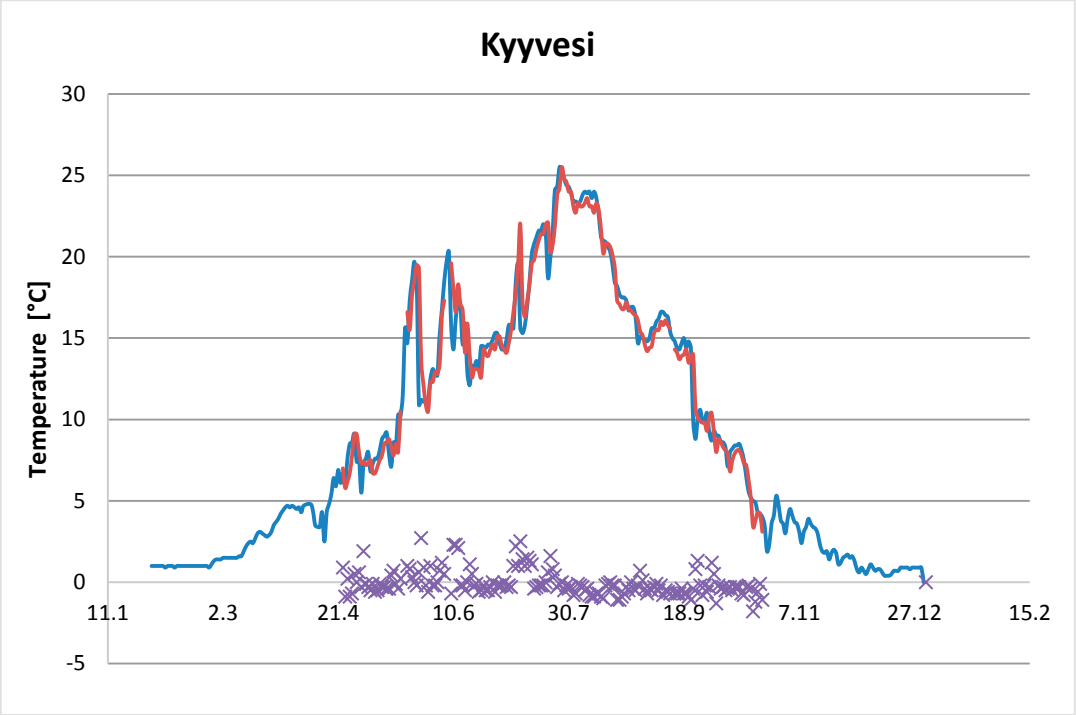

Figure 3. Water temperature of pressure transducer (8 AM) as blue line and the official surface water temperature as red line during the summer 2014. Difference was mainly below 2 Celsius degrees (purple crosses). Sensor is directly in the lake.

Some of water level pressure sensors are installed in the limnigraph well. In this case water temperature does not describe circumstances in the lake or river since there is no direct solar radiation influence to the well. Also at some cases tube connecting the limnigraph well to the lake or river can be under the thermocline and only hypolimnion water is accessing the well. As an example of limnigraph well temperature Figure 4. shows differences in Inari, Nellim. In the case of limnigraph well used for measuring water level automatically, transducer's temperature data of these observation sites cannot be used as reliable water temperature information. This means that when using pressure transducer temperature data, the exact installation location of device should be known. Data from limnigraph wells should not be used in any study as a lake or river water temperature information. At the moment there is no information in the database whether device is in the limnigraph well or not. This hinders the use of pressure transducers' water temperature data. In the future this information should be available.

Since the network of water temperature measurements is rather sparse in northern Finland, the use of pressure sensor's temperature data could bring more information. Some of the stations had to be compared with data from the different watershed, for example Kitkajoki (Figure 5). Differences were not very big and the course of water temperature during the summer were very similar.

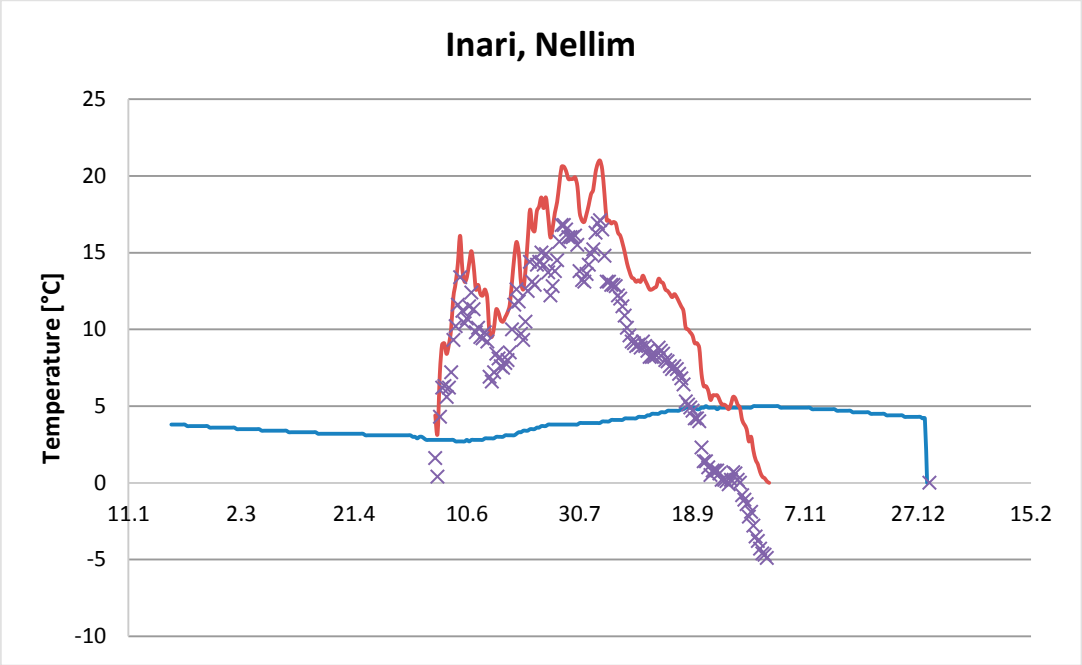

Figure 4. Example of water temperature data of pressure transducer located in the limnigraph well. Blue line is water temperature in the well, red line in the lake surface. Purple crosses show the difference between observations.

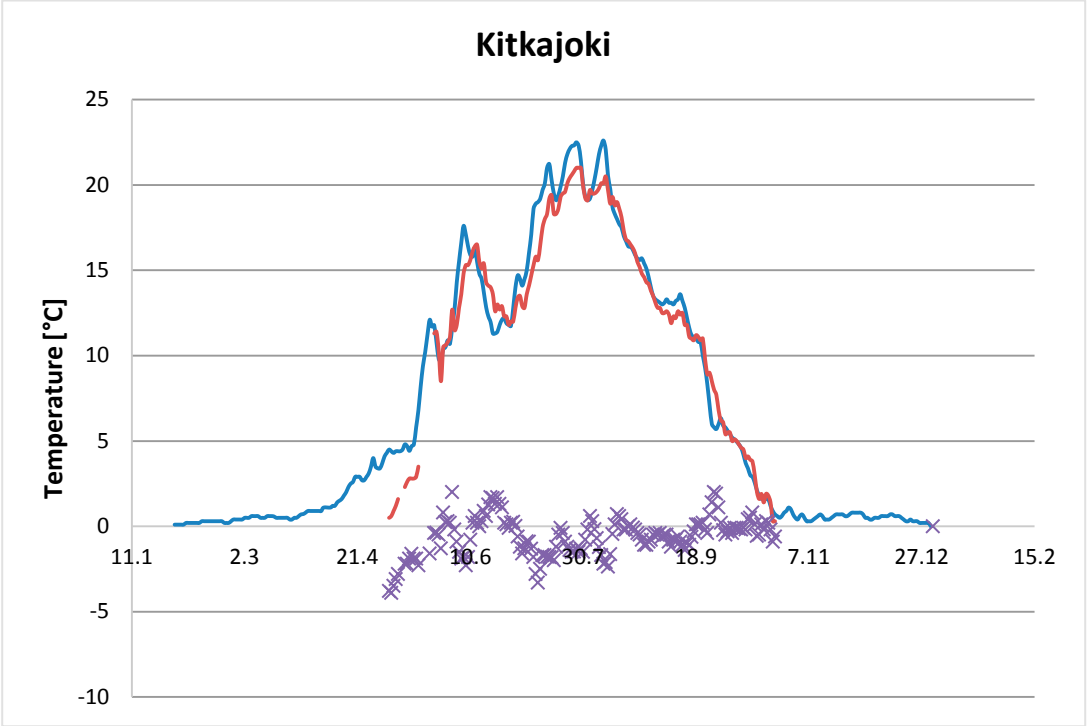

Figure 5. Example of water temperature differences from Kitkajoki pressure transducer compared with official surface water temperatures from other river (Oulankajoki) within 10 km distance.

3.2 Diurnal variation of water temperature

During the summer season surface water temperature has usually a diurnal variation and a vertical stratification, and the difference between morning and afternoon temperatures can be notable. Based on data used in this study, diurnal variation of water temperature was strongest during mid-summer months (July and August) in 2014 when there were most intense air temperature daily cycle. The minima of surface water temperature occurred usually night time or before sunrise and maxima during late afternoon or early evening. Based on the pressure transducer water temperature data, apparent diurnal water temperature variation is present in the sensor depth. In Kyyvesi, temperature variation cycle in July in 1.7 meters depth (Figure 6) was very similar to nearby surface water (Haukivesi 20 cm depth) station diurnal variation (Figure 7).

During summer 2014 only a couple of official surface water temperature devices logged temperatures for an hour interval. This allows to study diurnal variation of water temperature near the surface. As an example surface water temperature variation in July in lake Haukivesi observation site is presented in Figure 7. In early July weather was rather cool and there was no clear diurnal variation present. Later weather type changed to more typical summer weather with clear diurnal cycle. This was also seen from the water temperature data. In late July typical diurnal variation of surface water temperature was 1-3 Celcius degrees. The biggest change in surface water was cooling of water by 6 Celcius degrees in a day.

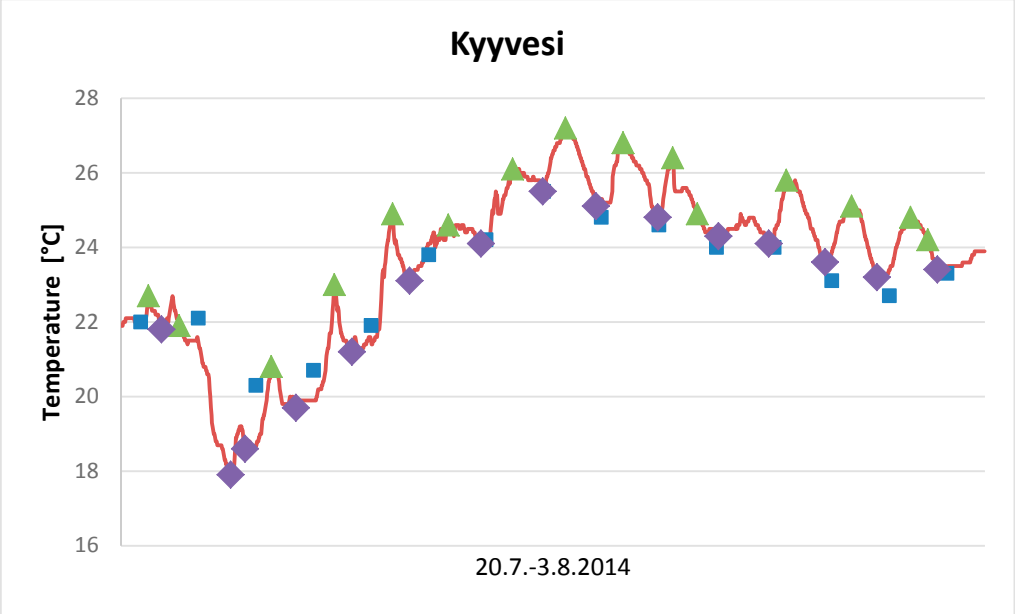

Figure 6. Diurnal variation of water temperature at 1.7 meters depth in July-August 2014 in Kyyvesi. Purple signs show minima of the day, green triangles maxima of the day. Blue squares indicate morning values of official water temperature site.

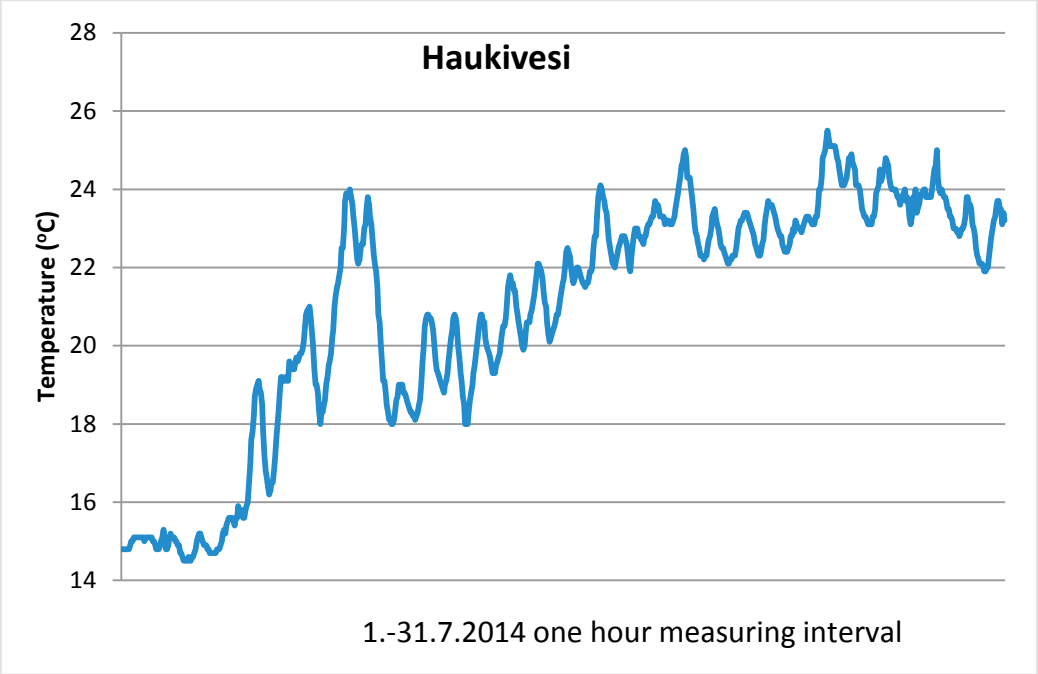

Figure 7. Hourly temperature information from one of the official surface water temperature sites (Haukivesi, near Kyyvesi) in July 2014.

Surface waters start usually to cool in early August (Korhonen 2002). During summer 2014 surface water maxima was recorded in most of the country in late July (23rd – 27th). A small diurnal variation persisted until end of the September. After that effect of solar radiation did not warm surface waters anymore during the day time.

Official daily surface water temperatures have been measured manually during the 20th century. Observers are guided to perform measurements in the morning at 8 AM, but there is no guarantee that all measurements during the decades are really done in the morning according the procedures. If measurements have been done sometimes during the late afternoon, there might be even 2-4 degree bias for higher than real values during the mid-summer time. Of course in the case of cooling period bias can be towards lower values. This might affect trend analysis of maximum values. Nowadays, since almost all sites have automatic measurements this kind of uncertainty is not present.

4. CONCLUSIONS

Study showed that pressure sensors which are situated directly in a lake or a river within 2 meter depth from the surface can provide usable information on surface water temperature in that specific area. Bias between 20 cm depth's official morning values and the values of pressure sensor's depth varied more in the early summer than during the late summer as was expected due to depth of thermocline. Usually difference was less than 2 degrees. In the late summer difference between 20 cm depth and pressure sensor's depth (1-2 m) was even smaller since both measurements were done in the same warm mixed surface layer. Even though pressure sensors are measuring deeper than just surface water they provide extra information, which can be used as input data for hydrological models and numerical weather prediction models, evaporation and heat budget calculations. These sensors also provide additional information for ecology research, fishing and recreational users. For this kind of use of data the accuracy of measurements is feasible. However, it is always advisable to first

evaluate data from each station with the nearby official surface water temperature stations depending on purposes of data use. Nevertheless, these pressure transducer data should not be used for long-term climate change studies since the depth and installing site of the sensor is not prearranged for water temperature measurements purposes and this might affect the results.

There is a significant diurnal fluctuation of water temperature in the surface water layer during warmest summer months when the air temperature is having clear diurnal variation and solar radiation is high. Actually, official surface water temperature values measured at 8 am are during warmest summer months (July and August) near the timing of lowest values of the day and temperatures in the afternoon can be even 2-4 degrees higher. This fact should be taken into account while using the official surface water temperatures for different purposes.

5. REFERENCES

Edinger, J., Duttweiler, D. & Geyer, J. 1968 The Response of Water Temperatures to Meteorological Conditions. *Water Resources Research* 4(5), 1137–1143.

Elo, A. & Koistinen, A., 2002 Evaluating temperature of lake surface and lake evaporation in Mäntyharju watershed area. *XXII Nordic Hydrological conference, Röros.* NHP Report no. 47. Nordic Hydrological Programme. 417-426.

Elomaa, E. 1977 Pääjärvi Presentative Basin Finland: Heat Balance of a Lake. *Fennia 149*.

Järvinen, J. & Huttula, T. 1982 Estimation of Lake Evaporation by Using Different Aerodynamical Equations. *Geophysica* 19(1): 87-99.

Kheyrollah Pour, H., Duguay, C., Solberg, S. & Rudjord, Ø. 2014 Impact of satellite-based lake surface observations on the initial state of HIRLAM. Part I: evaluation of remotely-sensed lake surface water temperature observations. *Tellus A2014,* 66, 21534.

Korhonen, J. 2002 *Water temperature conditions of lakes and rivers in Finland in the 20th century*. Finnish Environment 566. (In Finnish, summary in English). Finnish Environment Institute, Helsinki. 116 p.

Rontu, L., Eerola, K., Kourzaneva, E. & Vehviläinen, B. 2012 Data assimilation and parametrizations of lakes in HIRLAM. *Tellus A 2012,* 64, 17611.

Seppälä, O. 2015 *Järvien ja jokien veden lämpötilan vaihtelut - paineanturihavaintojen käytettävyystarkastelu. = Water temperature variations in lakes and rivers - usability study of pressure transducer temperature data*. Bachelor's Thesis, Aalto University. 36 p. (In Finnish only)

Sharma, S., Gray, D., Read, J., O'Reilly, C., Schneider, P., Qudrat, A. Gries, C., Stefanoff, S., Hampton, S., Hook,S. Lenters, J, Livingstone, D., McIntyre, P., Adrian, R., Allan, M. Anneville, O. Arvola, L.. Austin, J., Bailey, J., Baron, J., Brookes, J., Chen, Y., Daly, R., Dokulil, M., Dong, B., Ewing, K., de Eyto, E., Hamilton, D., Havens, K., Haydon, S., Hetzenauer, H., Heneberry, J., Hetherington, A., Higgins, S., Hixson, E., Lyubov R. Izmesteva, Jones, B., Kangur, K., Kasprzak, P., Köster, O., Kraemer, B., Kumagai, M., Kuusisto, E., Leshkevich, G., May, L., MacIntyre, S., Müller-Navarra, D., Naumenko, M., Noges, P., Noges, T., Niederhauser, P., North, R., Paterson, A., Plisnier, P-D., Rigosi, A. Rimmer, A., Rogora, M., Rudstam, L., Rusak, A., Salmaso, N., Samal, N., Schindler, D., Schladow, G., Schmidt, S., Schultz, T., Silow, E., Straile, D., Teubner, K., Verburg,P., Voutilainen, A., Watkinson, A., Weyhenmeyer, G., Williamson, C. & Woo, K. 2015 A global database of lake surface temperatures collected by in situ and satellite methods from 1985–2009. *Scientific data* 2, 150008.

Design floods for small forested and agricultural catchments in Finland

Jarkko J. Koskela* and Jarmo Linjama

Finnish Environment Institute, P.O.Box 140, FI-00251 Helsinki, FINLAND
**jarkko.j.koskela@ymparisto.fi*

ABSTRACT

Estimates of design floods for small catchments are often needed in planning of hydraulic structures such as culverts and bridges. As hydrological monitoring networks are always sparse with respect to areas were such structures are needed, it is a common practice to use a reference method to estimate these floods. In Finland general guidelines for design discharges of different structures in different areas have been updated regularly in the 2000's. Based on the land use and flood risks of the catchments design criteria can be a flood with a return period of 20 years ($HQ_{1/20}$), $HQ_{1/100}$ or even $HQ_{1/250}$ (Finnish Environment Institute 2015). In several sites it might be possible to get a reasonable estimate of the mean annual maximum discharge (MHQ) by using the available data but estimate e.g. for $HQ_{1/100}$ contains lots of uncertainties if the number of known annual maximum floods is small. Thus, it has been studied earlier whether some general guidelines could be given to estimate HQs for different return periods based on MHQ (Kaitera 1949; Niinivaara 1961; Mustonen 1968; Seuna 1982, 1983; Hyvärinen 1985). In the updated design guidelines for bridges and culverts, guidance for estimating the design floods for different return periods in unmonitored sites still refers to these relatively old publications and more importantly to hydrological data available until then.

This study aims to update this information and to find general guidelines for estimating design floods for small catchments in Finland. Runoff data from the monitoring network of so called small catchments that dates back from 1930's until today is utilized. A total of 38 catchments distributed all over Finland were selected for the analysis. On 7 sites the percentage of cultivated land is over 30 %. On the other hand, there are sites which are almost entirely forest and forested peatlands. The areas of the study catchments vary from 0.1 to 122 km² and they do not contain any lakes. The soil, vegetation and topography of the catchments vary. The highest percentage of agricultural land is in Hovi (100 %) while for example Teeressuonoja and Vähä-Askanjoki are entirely covered by forests and forested peatlands. The mean annual runoff in Finland is about 10 $ls^{-1}km^{-2}$, but in small basins without lakes the instantaneous runoff varies considerably. For example from zero in dry periods to 1900 $ls^{-1}km^{-2}$ after heavy rain on a cultivated small field catchment in Hovi.

Flood frequency analysis was carried out for the annual daily average runoff peaks for all the catchments. A visual inspection of the homogeneity, stationarity and independence of each time-series was performed in advance of the flood frequency analysis. Data was only accepted for the analysis if the flood peak time-series was considered to fulfil such assumptions. It was assumed that floods caused by snowmelt and heavy rain origin from a same distribution. It was not studied whether the timing of the floods in these catchments has changed. A 2-parameter Gumbel distribution was used for the flood frequency analysis in each catchment and method of moments was used as a method for the parameter estimation.

Results show high variability of design floods for the smallest catchments. For the catchments having areas smaller than 10 km^2 $HQ_{1/20}$ varies from 116 to 437 $ls^{-1}km^{-2}$, $HQ_{1/100}$ from 150 to 567 $ls^{-1}km^{-2}$ and $HQ_{1/250}$ from 170 to 641 $ls^{-1}km^{-2}$. The highest values were estimated for the entirely cultivated small (0.12 km^2) Hovi catchment and the lowest values for Teeressuonoja (0.69 km^2) which is fully covered with forests and forested peatlands. Both are located in southern Finland and very close to each other. For the larger catchments (> 10 km^2) variability was smaller. $HQ_{1/20}$ still varies from 126 to 347 $ls^{-1}km^{-2}$, $HQ_{1/100}$ from 166 to 436 $ls^{-1}km^{-2}$ and $HQ_{1/250}$ 188 up to 487 $ls^{-1}km^{-2}$.

The ratio between the HQs for different return periods and mean annual maximum discharge MHQ (HQ_{TR}/MHQ) also show some variability. $HQ_{1/20}$/MHQ varies from 1.5 to 2.0 (average 1.7), $HQ_{1/100}$/MHQ from 1.9 to 2.6 (average 2.2) and $HQ_{1/250}$/MHQ from 2.1 up to 3.0 (average 2.5). By being aware of the differences in the approaches, length of the available time-series and study catchments these values are relatively well in line with studies of Kaitera (1949), Niinivaara (1961), Mustonen (1968), Seuna (1983) and Hyvärinen (1985) which have been the base for HQ_{TR}/MHQ ratios in the guidelines given for planning of culverts and bridges in unmonitored sites.

Findings of the study can be utilized directly in the planning of hydraulic structures in unmonitored forested and agricultural small catchments in Finland. Results show high variability in design floods with respect the area of the catchment and land use. Thus, when using a reference site for estimating such floods a very careful selection of the best reference is of the essence. Otherwise floods may be under or overestimated and culverts and bridges are not optimally designed. The average ratios between the HQs for different return periods and mean annual maximum discharge showed only some small differences with the results of the studies made over 20 years ago.

KEYWORDS
Design flood; small catchments; flood frequency analysis; Finland

LIST OF REFERENCES
Finnish Environment Institute 2015 *Silta- ja rumpurakenteiden aukkomitoitus*. In preparation.

Hyvärinen, V. 1985 *River discharge in Finland*. Publications of the Water Research Institute 59, pp. 3-21. Helsinki.

Kaitera, P. 1949 *On the Melting of Snow in Springtime and its influence on the Discharge Maximum in Streams and Rivers in Finland*. Teknillisen korkeakoulun tutkimuksia N:o 1. Helsinki.

Mustonen, S. 1968 Ylivalumista pienillä järvettömillä valuma-alueilla. *Rakennustekniikka* 5: 244-246

Niinivaara, K. 1961 Ylivalumien todennäköisestä vaihtelusta Suomen päävesistöjen alueella. *Teknillinen aikakausilehti* 1961:18.

Seuna, P. 1982 *Frequency analysis of runoff of small basins*. Publications of the Water Research Institute 48. Helsinki.

Seuna, P. 1983 Pienet valuma-alueet – hydrologian tutkimusväline. *Rakennustekniikka* 5: 337-343.

Trends of breakup dates in Finnish lakes in 1963-2014

Esko Kuusisto

Finnish Environment Institute, Freshwater Centre
Mechelininkatu 34 B, Helsinki, FINLAND
**esko.kuusisto@environment.fi*

ABSTRACT

Long data series of freezing and breakup observations are available from the lakes in Finland. Some of these series were started already in the former half of the 19th century. In this study, the breakup dates during the last half-century have been analyzed from 51 lakes covering the whole country. A statistically significant linear trend (99.9%) towards an earlier breakup was detected on 40 lakes. Eight lakes had a trend with a significance of 99 per cent and the rest, three lakes with a significance of 95 per cent. In 70 per cent of the lakes, the shift towards an earlier breakup has been 10–14 days during the fifty-two year period. In 23 per cent, it has been 15–18 days. In southern and western parts of the country and in the former Oulu province the trends have been slightly stronger than elsewhere in the country. Smallest trends have occurred in Lapland.

KEYWORDS

Lake ice; Breakup; Climate change

1. INTRODUCTION

Millions of inland water bodies freeze over each winter. In February, the total extent of lake ice cover in the northern hemisphere probably exceeds two million square kilometers, in over fifty countries. On both hemispheres, there are also lakes which are perennially frozen; the summer thickness of ice is in excess of five meters in some Antarctic lakes. Even in Australia there are small lakes which seasonal ice cover (Green 2011).

In North America, seasonal lake ice cover can develop as far south as 33ºN, in Eurasia 26ºN. Among the fifteen largest lakes on the Earth, only four are not affected (Prowse & al. 2007). In high mountains, freezing lakes occur in a wide range of latitudes.

In Finland, the mean maximum ice volume in lakes was 18.6 km^3 in the period of 1961 – 1990, implying that 7.5 per cent of the lake water was in solid state (Kuusisto 1994). The nationwide average of maximum ice thickness was 55 cm in 1961–1990. Both extremes of the maximum thickness have been recorded after this period. In March 2003 it reached 67 cm nationwide, in March 2008 it remained as low as 42 cm.

Unlike river ice, lake ice is virtually unaffected by man's actions in watercourses and river basins. Only exceptionally do, e.g. thermal effluents, a road embankment or heavy regulation, alter lake ice conditions. Thus the nature's fingerprint in lake ice is very pure – a fact which offers many possibilities e.g. in climate change research.

2. BREAKUP DATA FROM FINNISH LAKES

In a country of 187 888 lakes, it is no wonder that long data series exist on lake ice variables – particularly because all those water bodies freeze every winter. The longest continuous observation series on break-up begins in 1822 (Lake Kallavesi), on freezing in 1833 (Lake Kallavesi) and on ice thickness in 1909 (Lake Muurasjärvi). – A much longer data series is available on the freeze-up of River Tornio, it starts as early as in 1693.

The Finnish Environment Institute has about 35 observation series of breakup dates covering the last hundred years. Without the unfortunate reorganization of the network in the 1990s, the number would be around 50.

From the lakes in northern Finland, there are rather few long breakup data series. The longest one north of the Arctic Circle is from Lake Inari, starting in 1923, but a satisfactory areal data coverage is available only since the early 1960s. This is one reason why the time period 1963–2014 was used in this study to detect the nationwide trends in breakup dates.

The total number of data series was 51. They covered the latitude range of 60º15'–69º45'N and longitude range of 20º49'–30º58'E. Thirty of the series were complete, ten had 1–3 and six 4–6 missing observations. The rest, five series, had longer gaps, which were filled using correlation with the closest available series.

The average breakup date varied from the 14th of April (Lake Lohjanjärvi) to the 17th of June (Lake Kilpisjärvi). The average range from the earliest to the latest date was 35 days, the largest being 47 days (Tammelan Pyhäjärvi), the shortest 28 days (Jerisjärvi and Lammasjärvi).

3. RESULTS

Linear regression analysis was applied to all data series. The results are shown in Fig. 1a. There is no question that the breakup has shifted towards an earlier date in the whole country. A statistically significant linear trend (99.9%) was detected in 40 lakes. Eight lakes had a trend with a significance of 99 per cent and the rest, three lakes with a significance of 95 per cent. In 70 per cent of the lakes, the shift towards an earlier breakup has been 10–14 days during the fifty-two year period. In 23 per cent, it has been 15–18 days. In southern and western parts of the country and in the former Oulu province the trends have been slightly stronger than elsewhere in the country. Smallest trends have occurred in Lapland.

Fig. 1b shows the largest and smallest trends, those of Säkylän Pyhäjärvi (18 days) and Kilpisjärvi (7 days). The first one is significant with the probability of 99.9 per cent, the latter with 95 per cent. Säkylän Pyhäjärvi is located in southwestern Finland, where the winters have been very mild during the last two decades. Kilpisjärvi is a tundra lake surrounded by the highest mountains in Finland, and its surface is 470 metres above sea level.

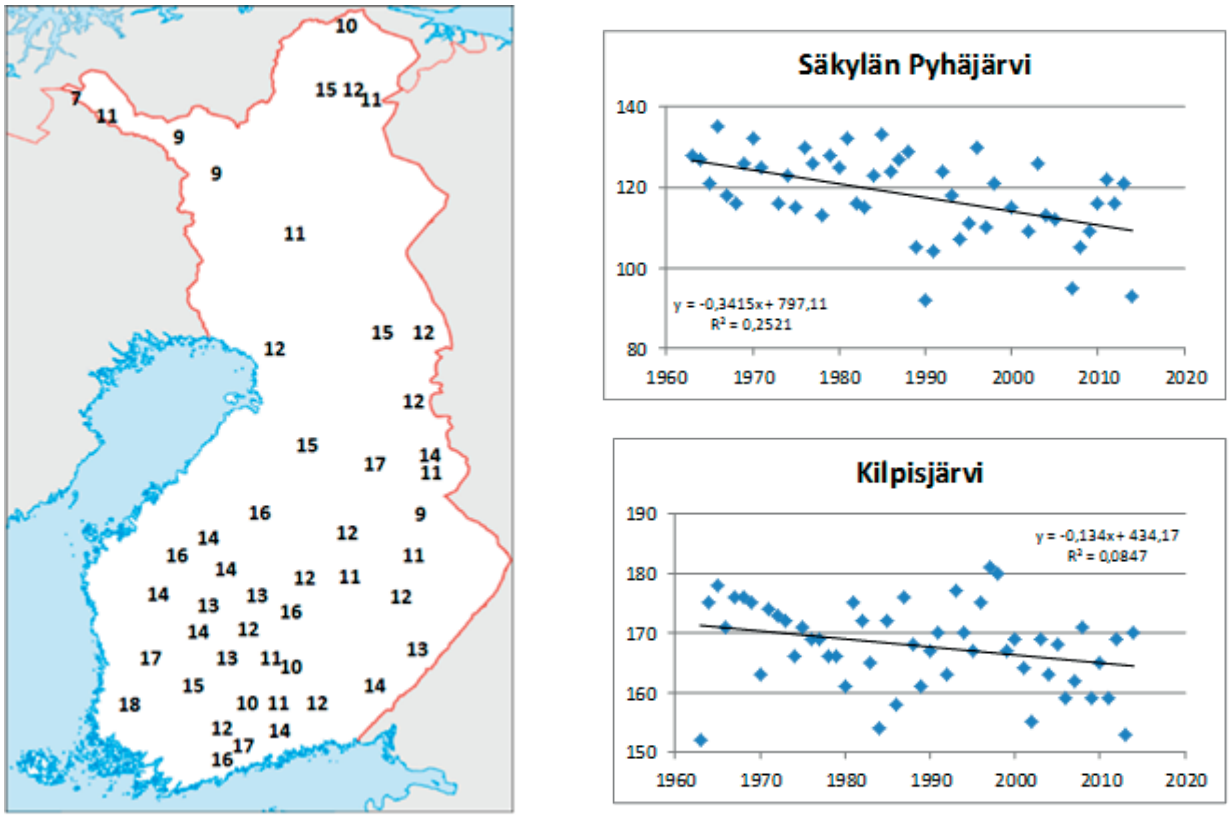

Fig. 1. a) The shift towards an earlier breakup in Finnish lakes in 1963-2014 (in days). b) The largest (Säkylän Pyhäjärvi) and smallest (Kilpisjärvi) trends towards an earlier breakup in that period.

4. EXTREME YEARS

By far the latest breakup during the observation history in Finland occurred in 1867. Even on the southern coast the lakes were still ice-covered at the end of May. In the Lake District, the breakup occurred on June the 15th –25th. In Southern and Central Finland, the difference to the second latest breakup is typically 2–3 weeks. In Lapland, the difference is smaller; in the Tornio river series (1693–2015) it is only six days.

The breakup of 1921 was probably the earliest for at least two centuries, perhaps even for a much longer period. Fig. 2 shows how long this record has stayed. In almost 60 per cent of the observation sites, it was valid until 2007. That spring one half of the remaining sites got a new record, and the two last springs have lowered the percentage close to ten.

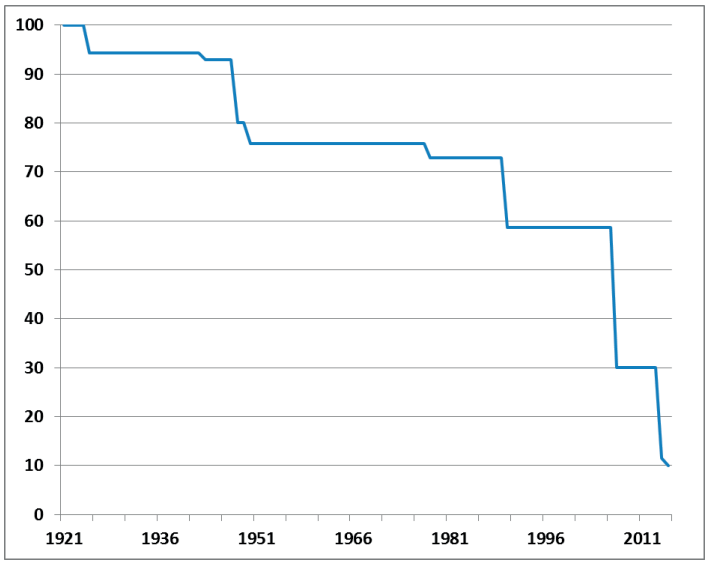

Figure 2. Percentage of the 1921 breakup being the earliest one in the whole data series of the lakes in Southern and Central Finland.

REFERENCES

Green, K. 2011. Interannual and seasonal changes in the ice cover of glacial lakes in the Snowy Mountains in Australia. Journal of Mountain Science 8, pp 655–663.

Kuusisto, E. 1994. The thickness and volume of lake ice in Finland in 1961–1990. Publications of the Water and Environment Research Institute 17, pp. 27–36.

Prowse, T. D. & al. 2007. River and lake ice. Chapter 8 in Global outlook for ice and snow, UNEP, pp. 201–214. Gallet J.C., F. Dominé, C. S. Zender, and G. Picard 2009 Measurement of the specific surface area of snow using infrared reflectance in an integrating sphere at 1310 and 1550 nm. *The Cryosphere.* vol. 3, 167-182.

The ice season of Lake Kilpisjärvi in the Finnish Arctic tundra

Matti Leppäranta[1]*, Elisa Lindgren[1], Kunio Shirasawa[2] and Ruibo Lei[3]

[1]*Department of Physics, University of Helsinki, Helsinki, 00014, FINLAND*
[2]*Institute of Low Temperature Science, Hokkaido University. Sapporo, 060-0819 JAPAN*
[3]*Polar Research Institute of China, Shanghai, 200136 CHINA*
**matti.lepparanta@helsinki.fi*

ABSTRACT
Recently an extensive research programme has been carried through on the ice cover geophysics in Lake Kilpisjärvi, located at 69°03'N 20°50'E, 473 m above sea level and about 60 km from the shore of the North Atlantic Ocean. The surface area of the lake is 37.1 km^2, and the maximum depth is 57 m. A two-year field study was performed in this lake in 2007–2009 with data collected of ice, snow and weather conditions with an automatic ice station in the lake. The heat budget together with ice structure, growth and melting was analysed. It was dominated by the radiation balance, and turbulent heat fluxes were large before freeze-up in fall, but in the ice season they were small except that occasionally sensible heat flux was large. In 2012–2013 the focus was in the solar radiation budget and ice melting in May–June. Long-term ice phenology time series of Lake Kilpisjärvi, available from 1952, show mean freezing and breakup dates of November 8th and June 18th, respectively. The freezing date has delayed by 2.3 days per decade but the ice breakup date does not show a significant change.

KEYWORDS
Arctic lake, ice formation, ice thickness, ice melting, field data, climatology

1. INTRODUCTION
In the Fennoscandian Arctic tundra, lakes are frozen for 7–8 months annually. Their ice sheets consist of congelation ice and snow-ice with snow cover on top, and the annual maximum thickness of ice is close to one meter. Ice grows from November to April and melts during May and June. The ice cover weakens turbulence and mixing in the water body and as well stabilizes the temperature structure. The polar night lasts two months in this region, and due to the snow cover the lakes are dark for 3–4 months each winter. For the past decades, most mid-latitude lakes show later freeze-up and earlier ice breakup (e.g., Magnuson et al. 2000) but for Arctic lakes there is less data.

The primary motivation of recent research of tundra lakes has been to better understand the interaction with the atmosphere and the ecology and fishery of these lakes (Kirillin et al. 2012). The coupling between atmosphere and Lake Kilpisjärvi is significant in weather forecasting (Yang et al. 2013) extending most likely to long time scales. The climate scenarios for the next century predict shorter ice season and thinner ice cover in Arctic lakes (e.g. Brown and Duguay 2010), which raises the question how the physical and ecological processes in lakes are going to change. The ice records from Lake Kilpisjärvi have been used in long-term ice phenology studies in Finland and in Scandinavia (e.g. Blenckner et al. 2004, Korhonen 2006, Lei et al. 2012) but apart from them accurate observations on ice growth and melting have not been previously performed. This presentation gives results of recent research

on the heat budget, ice growth and melting, and ice climatology based on fieldwork in Lake Kilpisjärvi.

2. FIELD SITE AND OBSERVATIONS

Lake Kilpisjärvi is located in the northwestern corner of Finnish Lapland at 69°03'N 20°50'E, 473 m above sea level (Fig. 1). The distance to the shore of the northern North Atlantic Ocean is about 60 km. The lake is at the northeast end of a long valley, fells rising up to 1000 m elevation (500 m from the lake surface) on both sides, and the maximum fetch is 6.2 km. The surface area is 37.1 km^2, and the average and maximum depths are 19.5 m and 57 m, respectively. The inflow comes from small mountain brooks, and outflow is in the southeast corner to River Könkämäeno and further to the Baltic Sea. Kilpisjärvi Biological Station (KBS) of the University of Helsinki is located at the lakeshore. There are no industrial or agricultural activities in the drainage basin, apart from reindeer herding.

Ice records are available for Lake Kilpisjärvi since 1952, and a weather station was founded in 1962. Since mid-1960s, ice thickness has been measured at every 5–15 days, and in 1977 the snow depth on ice was added to the observation procedure (http://www.ymparisto.fi/). Snow-ice observations have been made in 1981–1990. The mean freezing and ice breakup dates were November 8 and June 18 in the period 1952–2010, the earliest freezing date was October 21 and the latest breakup date was July 1. The freezing date has delayed by 2.3 days per decade but the ice breakup date does not show a significant change (Lei et al. 2012). The average maximum annual ice thickness is 90 cm (the range is 75–115 cm), reached in April (Korhonen 2005). The annual mean air temperature is between –4ºC and –1ºC, with mean monthly air temperatures below 0ºC from October to April, and snow thickness on ground is on average 90 cm in March–April (http://www.helsinki.fi/kilpis/english/index.htm).

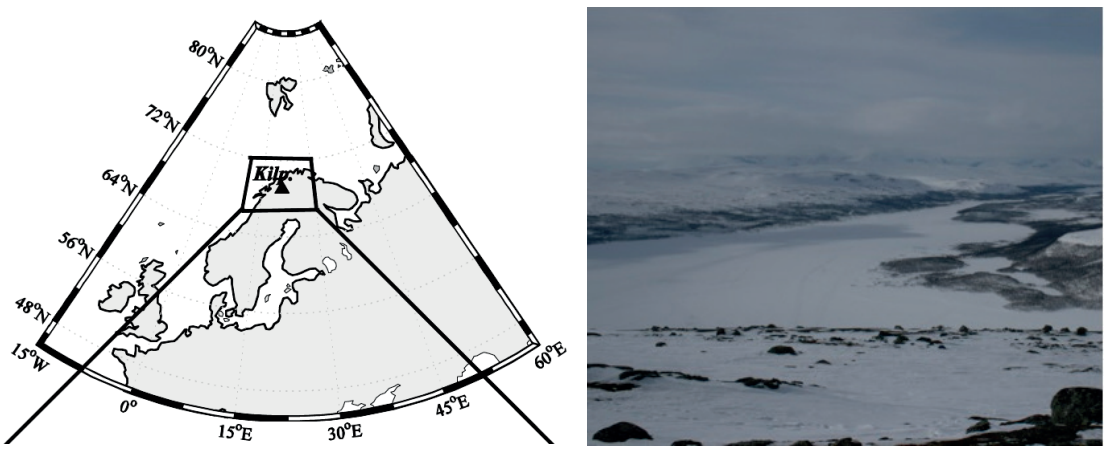

Figure 1. Lake Kilpisjärvi in tundra mountain area of Lapland at 69°03'N 20°50'E, 473 m above sea level. The photograph was taken on April 13, 2009 from Saana fell.

A joint Finnish-Japanese winter research programme was carried through in Lake Kilpisjärvi over two winters, 2007–2009 (Leppäranta et al. 2012). The work was based on an automatic ice station *Lotus*, manual measurements, and utilization of routine data. In 2012–2013 the field period was shorter and focused on the melting period, with much sounding data collected from the water body. Routine weather data were available throughout the year at KBS

Weather Station and at weather station Enontekiö Kilpisjärvi Kyläkeskus (EKK). At the northwest shore there is also a routine ice and snow monitoring station of the Finnish Environment Institute, where observations are made every ten days from November to May.

Due to safety issues field work during the melting period in all freezing lakes has been problematic, but the lack of data has been notified and spring time field campaigns to Lake Kilpisjärvi have also taken place twice, in 2013 and 2014. The analyses on observations of the ice structure, melting, light penetration through the ice cover and convective mixing is ongoing (see e.g. Graves et al. 2014, Kirillin et al. 2014), and will provide new insight into the physics during the melt season. This will add to the full ice season results presented here.

3. ALL-YEAR HEAT BUDGET

3.1 Ice growth and melting

Ice cover in Lake Kilpisjärvi consists of three principal layers: congelation ice, snow-ice and snow. Occasionally there may be slush sub-layers in the snow or snow-ice layer. In slush formation, snow is compacted so that the thickness of slush is less than the original snow thickness. The snow and snow-ice correspond to snow accumulation by about 75 cm, which is less than snow accumulation on ground (on average 90 cm), the difference largely due to drifting of snow from the lake.

Lake ice cover is a good sensor for the heat budget. The heat content in the ice cover is mainly latent heat and it can be determined from the thickness of ice layers. Define

$$S = \left[\rho_i(h_{ci} + h_{si}) + \rho_s h_s\right] L \tag{1}$$

where h_{ci}, h_{is} and h_s are the thicknesses of congelation ice, snow-ice and snow layers, ρ_i and ρ_s are ice and snow densities, and L is the latent heat of freezing. In the growth of ice cover, latent heat is released to form congelation ice but the latent heat of snow and for half of the snow-ice comes from solid precipitation. Thus the heat S is needed to melt the ice while the heat $S' = \rho_i(h_{ci} + ½\ h_{is})L$ is released in ice growth. Consequently, the mean rate of heat loss from the lake becomes 18.5 W m^{-2} during the 5-month growth season. Taking snow density as 400 kg m^{-3} (Järvinen and Leppäranta 2011), the additional latent heat ($S - S'$) due to snow accumulation is equivalent to the cooling rate of 3.9 W m^{-2} during the growth season. To melt the snow and ice in 50 days' time, the average net heat flux must be 75.2 W m^{-2}, which corresponds to 2.1 cm loss of ice per day. Melting takes place at the boundaries and in the interior, so that ice becomes porous and fragile, breaks due to its own weight into brash ice, and thereafter disappears very quickly.

Ice seasons 2007–2008 and 2008–2009 were close to normal for ice growth and snow accumulation. However, in 2008 there was much more snow-ice than normal but the opposite was observed a year later. Figure 2 shows the changes in thickness of the three layers at 10-day intervals in the latter season. Ice growth rate was on average 0.5 cm per day, while melting was very fast, at the rate of 1.5–3 cm per day.

3.2 Surface Heat Budget in Ice Season 2008–2009

The ice station started to work in September 9, 2008, two months before freezing. The surface water temperature was then 8.6ºC. A month later the surface temperature was 5.2ºC, and in October the surface temperature dropped from 6.3ºC to 3.3ºC. Thereafter, with the development of stable stratification, freezing took place on November 10. The mean cooling rate was thus 0.14ºC day^{-1} from September 9th until freeze-up. Assuming the mixed layer depth as 10 m, the mean cooling corresponded to heat loss by the rate of 68 W m^{-2}.

Net solar and terrestrial radiation were obtained directly from the measurements of incoming and outgoing solar radiation and total radiation balance. Turbulent heat fluxes were estimated with bulk formulae with constant transfer coefficients corresponding to neutral stratification (e.g., Leppäranta, 2009). Therefore the estimated autumn values may be somewhat biased down but that does not influence the main conclusions.

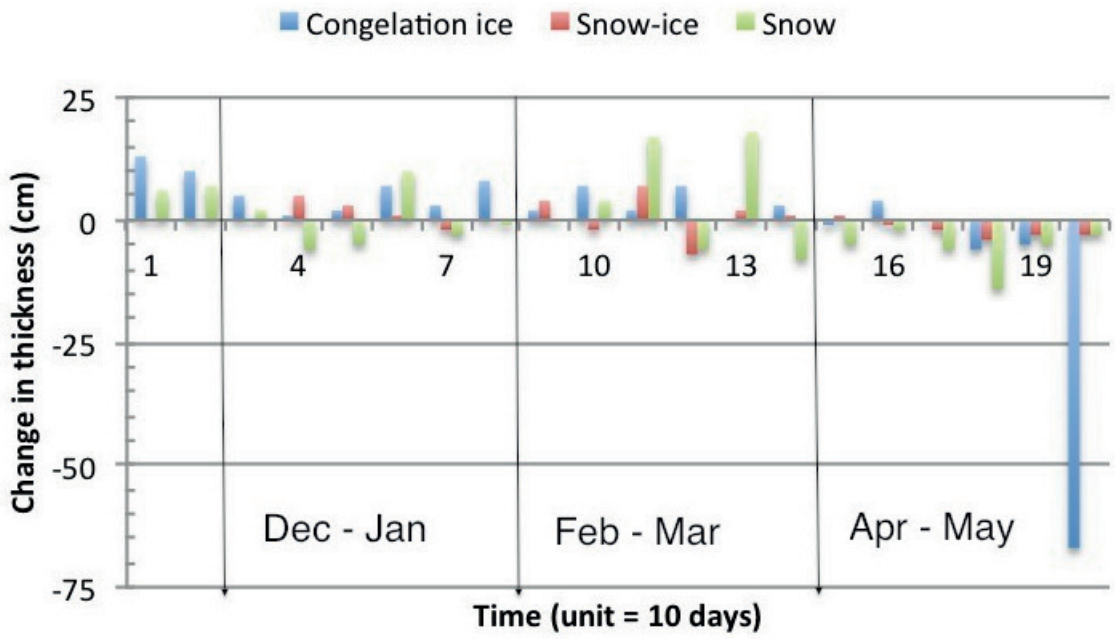

Figure 2. Thickness changes of congelation ice, snow-ice, and snow thickness in Lake Kilpisjärvi ice season 2008–2009, shown in 10-day intervals.

In September 2008, solar radiation was still strong and the net surface heat flux was positive until September 25th, on average at the rate of 20 W m^{-2} (Figure 3a). Net terrestrial radiation was between –60 and –30 W m^{-2} and turbulent fluxes were between –30 and –10 W m^{-2}, latent heat flux being lower. Until September 23 the surface temperature was stable and within 8.3–8.8ºC, and therefore convection distributed the heat gain deeper. Then, with the loss of solar power, the net surface flux turned strongly negative, daily values reaching –100 W m^{-2} at minimum, continuing to November 25. After freeze up the magnitude of turbulent fluxes became small but due to the radiative heat loss ice grew by 23 cm during November 10–30. The latent heat released in freezing corresponded well with the measured surface heat loss. In December the net surface flux was just slightly negative, and occasionally sensible heat flux reached 20 W m^{-2} due to warm air advection from the northern North Atlantic.

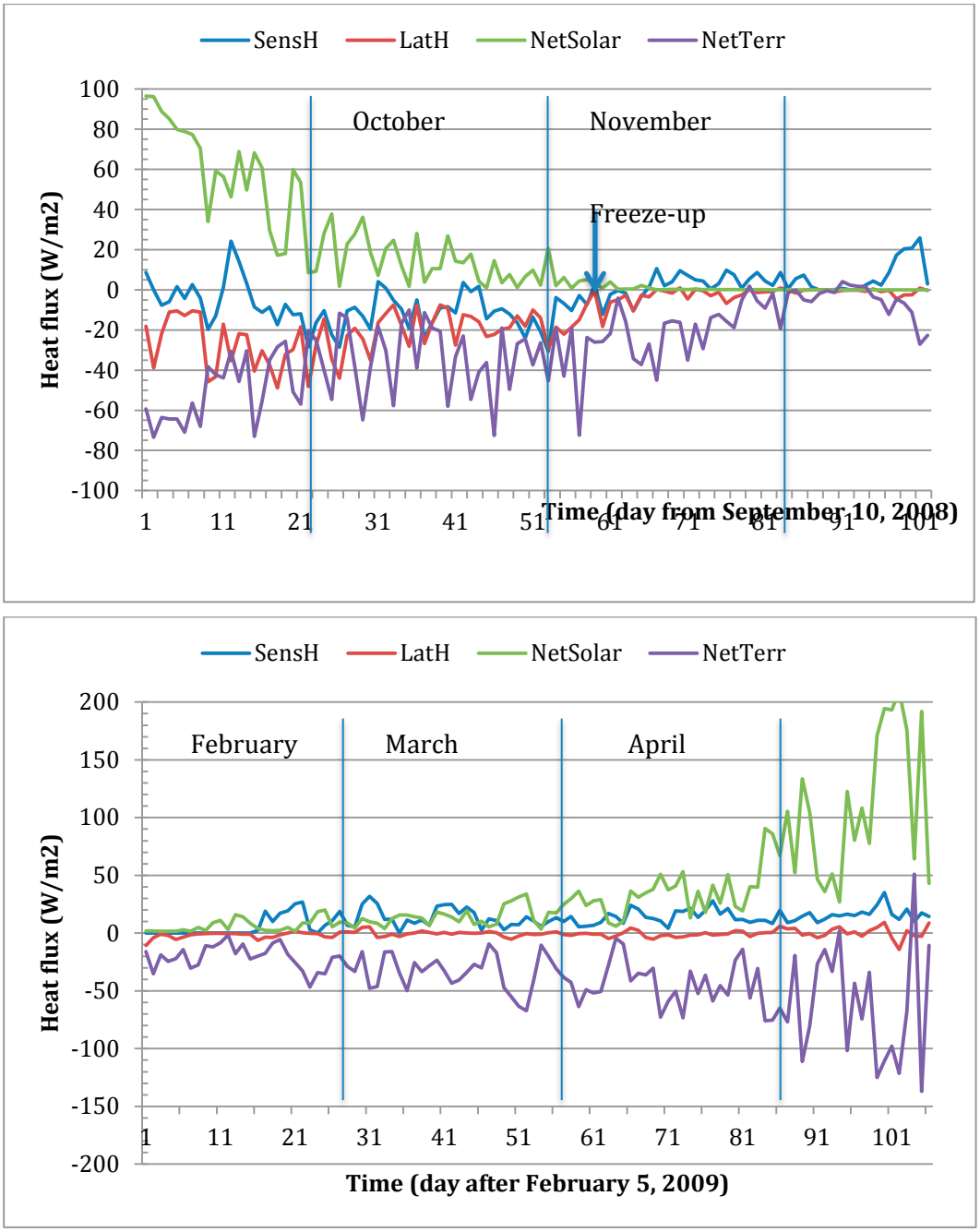

Figure 3. Surface heat balance of Lake Kilpisjärvi. (a) September 10 – December 20, 2008; (b) February 5 – May 20, 2008.

4. CONCLUSIONS

The ice season of Lake Kilpisjärvi in the northwestern Finnish Lapland has been examined based on field surveys. The mean freezing and breakup dates are November 8 and June 18, respectively. A two-year field study was performed there in 2007–2009 with data collected of ice, snow and weather conditions with an automatic weather station in the lake, and in 2012–2013 the focus was in the solar radiation budget and ice melting in May–June.

The heat budget was dominated by the radiation balance. Terrestrial radiation losses created the ice sheet, while solar radiation melted the ice. Growth rate was 0.5–1 cm and melt rate averaged to 2.1 cm per day. Turbulent fluxes were large during the cooling period of open water lake but in the ice season they were small, the magnitude was below 20 W m^{-2}. Occasionally sensible heat flux could be large but remained small on monthly average level. Latent heat flux was small during the whole ice season. The latent heat released due to ice growth and taken for ice melting agreed well with the observed surface heat balance. Further on ice – water body interaction, modelling, and climate sensitivity of the lake is ongoing.

Acknowledgments

Our field research was based in Kilpisjärvi Biological Station of the University of Helsinki. The station director, Professor Antero Järvinen and technician Mr. Oula Kalttapää are greatly acknowledged for use of station facilities and help. This work is a contribution of the Nordic Center of Excellence Cryosphere–atmosphere interactions in a changing Arctic climate (CRAICC), and has also been supported by the Academy of Finland (project #140939).

References

Blenckner, T., Järvinen, M. & Weyhenmeyer, G.A. 2004 Atmospheric circulation and its impacts on ice phenology in Scandinavia. *Boreal Environment Research* ***9,*** 371–380.

Brown, L. & Duguay, C. 2010 The response and role of ice cover in lake-climate interactions. *Progress in Physical Geography* **34**, 671–704.

Golosov, S., Maher, O.A., Schipunova, E., Terzhevik, A., Zdorovennova, G. & Kirillin, G. 2007 Physical background of the development of oxygen depletion in ice-covered lakes. *Oecologia* 151, 331–340.

Graves, K., Laval, B.-E., Forrest, A. & Kirillin, G. 2014 Under-ice circulation, modified by Earth's rotation, in an arctic lake. In *Proceedings of the 22nd IAHR International Symposium on Ice*.

Jakkila, J., Leppäranta, M., Kawamura, T., Shirasawa, K. & Salonen, K. 2009 Radiation transfer and heat budget during the melting season in Lake Pääjärvi. *Aquatic Ecology* **43**(3), 681–692.

Järvinen, O. & Leppäranta, M. 2011 Transmission of solar radiation through snow cover on floating ice. *Journal of Glaciology* **57**(205), 861–870.

Kirillin, G., Engelhardt, C., Forrest, A., Graves, K., Laval, B.-E., Leppäranta, M. & Rizk, W. 2014 Standing waves during ice breakup in a polar lake. In *Proceedings of the 22nd IAHR International Symposium on Ice*.

Kirillin, G., Leppäranta, M. Terzhevik, A., Bernhardt, J., Engelhardt, C., Granin, N., Golosov, S., Efremova, T., Palshin, N., Sherstyankin P., Zdorovennova, G. & Zdorovennov, R. 2012 Physics of seasonally ice-covered lakes: major drivers and temporal/spatial scales. *Aquatic Ecology* **74**: 659–682. DOI 10.1007/s00027-012-0279-y.

Korhonen, J. 2005 Ice conditions in lakes and rivers in Finland. *Suomen ympäristö* 751 (Available at http://www.ymparisto.fi/julkaisut). Finnish Environment Institute, Helsinki.

Korhonen, J. 2006 Long-term changes in lake ice cover in Finland. *Nordic Hydrology* **37**, 347–363.

Lei, R., Leppäranta, M., Cheng, B., Heil, P. & Li, Z. 2012 Changes in ice-season characteristics of a European Arctic lake from 1964 to 2008. *Climatic Change* **115**, 725–739. DOI 10.1007/s10584-012-0489-2

Leppäranta, M. 2015 *Freezing of lakes and the evolution of their ice cover*. 301 p. Springer-Praxis, Heidelberg, Germany.

Leppäranta, M., Shirawawa, K. & Takatsuka, T. 2012 Ice season in Lake Kilpisjärvi in Arctic tundra. *Proceedings of the 21st IAHR Ice Symposium*.

Magnuson J.J., Robertson, D.M., Benson, B.J., Wynne, R.H., Livingstone, D.M., Arai, T., Assel, R.A., Barry, R.G., Card, V., Kuusisto, E., Granin, N.G., Prowse, T.D., Stewart, K.M. and Vuglinski, V.V., 2000 Historical trends in lake and river ice cover in the Northern Hemisphere. Science 289, 1743–1746.

Salonen, K., Leppäranta, M., Viljanen, M. & Gulati, R. 2009 Perspectives in winter limnology: closing the annual cycle of freezing lakes. *Aquatic Ecology* **43**(3), 609–616.

Yang, Y., Cheng, B., Kourzeneva, E., Semmler, T., Rontu, L., Leppäranta, M., Shirasawa, K. & Li, Z. 2013 Modelling experiments on air-snow interactions over Kilpisärvi, a lake in northern Finland. *Boreal Environment Research* **18**, 341–358.

The value of hydrological information - real world examples from a consultant's perspective

Wolf-Dietrich Marchand*, Kjetil Arne Vaskinn, Samuel Vingerhagen

Sweco Norge AS, 7030 Trondheim, NORWAY
** wolf.marchand@sweco.no*

EXTENDED ABSTRACT

Hydrological information is needed for many purposes, both in research and for industrial applications by both the public and the private sector. While research often aims to improve the understanding and modelling of the underlying physical processes, industry is more interested in applying the models and the application of the results.

Nevertheless, both research and industry rely on good hydrological information in order to get the best possible results. Data such as time series of rainfall, runoff or temperature, for either model input or calibration must be of the best possible quality.

From a consultant's perspective, which involves work with real world projects the value of hydrological information becomes apparent in many different ways but most often the economical aspect is in focus.

In this presentation examples focusing on cases where the use of hydrological data plays a key role for the overall outcome are presented. The examples are taken from decision-making processes, such as investment decisions, and from the design process in connection to flood calculations and hydropower.

Methods for improving the hydrological information are presented, such as the hydraulic modelling of the rating curve for gauging stations to derive better flood estimates.

KEYWORDS

Stage hydrograph modelling; rating curve modelling; flood analysis; hydrological information; hydrological data; CO2 value of hydropower; normal lake water level; natural high water level; natural low water level

Case study Rullestad: rating curve and value of data quality

In connection to the early stage planning of a dam, in the outlet of an existing lake, there was a requirement that the water level should not rise significantly in a flood situation, in order to prevent damages to existing roads and other infrastructure. To create a basic design, the bathymetry of the outlet was measured by using ADCP. Based on the runoff series from a gauging station (VM 42.5.0 Rullestadvatn, Norwegian Water and Energy Directorate (NVE)), located close to the outlet, the values for flow and water level at the design flood were calculated. The values indicated a very large flood values with a moderate rise in water level. However, expert knowledge and information about the terrain characteristics of the site, from field work, led to doubt, that the estimated large flood could pass through the narrow passage at the respective stage. A brief verification of the rating curve of the gauging station strengthened the doubt. For flood situations, the curve showed only moderate rise for the stage with massive increase of the flow values. The rating curve was based on NVE measurements up to a flow of 22 m3/s, while the curve was extrapolated to 280 m3/s at water level 3.5 m. As a rule of thumb an extrapolation of 3 times the maximum value is acceptable, but in this case the extrapolation exceeded a factor of 12. It was decided to set up a 2D hydraulic model

(RiverFlow2D, Hydronia LCC, 2013) in order to verify or disprove the extrapolated rating curve. By combining bathymetry data with terrain data from GPS and Lidar measurements the geometry for the hydraulic model was developed. Roughness values were estimated from field observations and experience. Different roughness values were analysed with sensitivity analysis (up to ± 20 %) and it was concluded that for high flow values, the roughness had minor influence on the modelling results, compared to the terrain geometry. Hydraulic simulations were then performed for many different flows and a rating curve was established base on the results.

A plot of the modelled ration curve (Sweco) against the extrapolated rating curve (NVE) showed that there is a major difference between the two curves, see Figure 2.

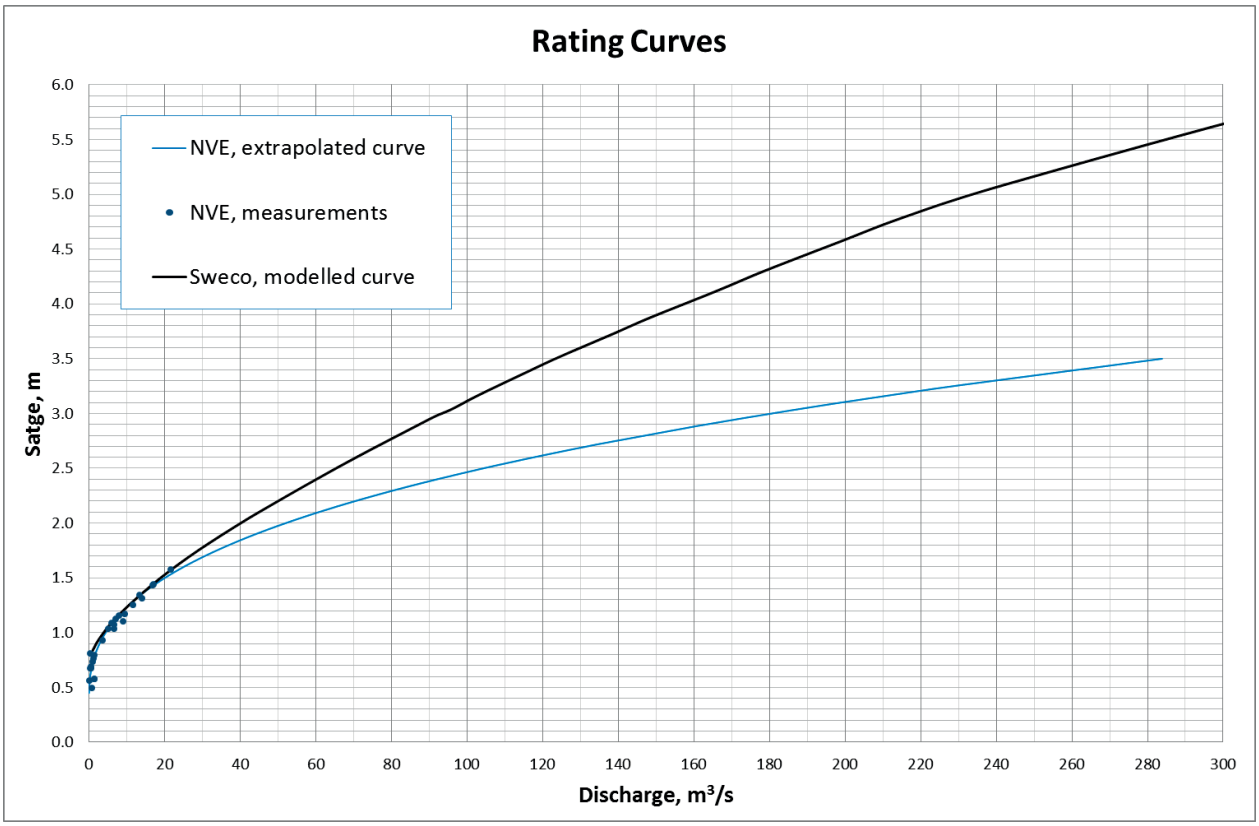

Figure 2 Comparison of rating curves

For the maximum measured hydrograph stage of 3.5 m the modelled curve shows a flow of 124 m^3/s, compared to 283 m^3/s from the extrapolated curve. That means that the extrapolated flow is more than double of the magnitude. Even if it cannot be claimed that the modelled rating curve is describing the real world situation exactly, it can be expected that it is much closer to reality than the extrapolated curve.

Based on the described findings and the modelled rating curve the time series for the discharge for VM Rullestad was recalculated and a new design flood was calculated. With the new design flood it will be possible to build a conventional dam with open flood spillway. Considering the flood value based on the extrapolated rating curve, which was around 2.3 times larger, it would have been necessary to build a dam with either a labyrinth spillway or a closed conduit/tunnel spillway. Both solutions would be more complicated and especially the tunnel spillway would be much more expensive than the traditional open spillway. The cost

could easily increase by the factor of 10. Further on, a closed spillway is in general not a preferred solution due to risk of blocking and the unfavorable capacity curve.

The described case shows the importance and value of a good quality time series and the advantageous possibility of improving extrapolated rating curves by hydraulic modelling.

Case study Øvre Forsland: Determination of natural variation of water level in lakes

When it comes to establishing new hydropower reservoirs, one important decision is whether the reservoir should be regulated or not. A regulated reservoir is favorable for buffering floods. This will reduce downstream flood damages, which means both increased safety and economic savings. Additionally, the avoided or reduced flood spill gives a higher power production, thus a better income for the power plant owner. However, a main drawback of a regulated reservoir is the increase of environmental conflicts and thus a higher threshold to get the permit for the establishment of the power plant.

For a small hydropower plant, especially one with a quick responding catchment, even a small buffer is often enough to avoid major flood spill, to make it possible to run the turbine at a better efficiency and thus produce more power. In many cases this can make the difference if the power plant is profitable or not. If the regulation of the reservoir is within the natural variation of the lake water level, the environmental impact is not that large and it is easier to get the permit, compared to a larger regulation. But what is the natural variation of the water level? Typically, many different opinions exist, depending on who is asked. Often it is relatively easy to find high water marks by studying vegetation or the color of rock surfaces, but to determine the natural low water level is much more difficult. This is where the importance of hydrological data comes in. If someone has a plan to develop a hydropower scheme it is very advisable to start the collection of hydrological data at an early stage. This is the case for discharge measurements, but also for measurement of natural variations of lake water surface. Since the focus of interest for the latter one is not on extreme values, but on moderate natural variations, it is typically enough to measure a few years to get data for typical variations.

The method for defining the natural water level variability and the normal water level is not defined very clearly in Norway, but in agreement with the NVE the following method has been used in many projects, to find the actual values from stage measurements.

Normal lake water level:	Median value of the measurements.
Natural high water level:	Remove the highest 5 % of the values. The largest remaining value is the normal high water level.
Natural low water level:	Remove the lowest 5 % of the values. The smallest remaining value is the normal low water level.

To visualize the variations within the natural low and high water level, connected to the time, the remaining 90 % can be plotted as a duration curve.

In the case of the hydropower project Øvre Forsland the described method has been used and the permit for 0.7 m regulation was obtained, while the possibility for regulation was doubted at first place. The introduced regulation gave an additional 10 % of planned production, increasing the total production from 30 to 33 GWh. This means an average additional profit of around 100 000 Euro, at an assumed a price of 34 Cent/kWh. Considering carbon dioxide (CO2) emission, the 3 GWh surplus production could reduce CO2 emission by 3600 tons annually, if it would replace power produced by an fossil fuel power station (brown coal).

If the lack of having hydrological data would lead to the reduction or disappearance of the reservoir and the additional power production, the practical emission implications could be large. With the power plant being unprofitable, and thus not build, it would cause annual emissions of around 40 000 tons of CO2, when being replaced by the production by energy from coal.

The case Øvre Forsland illustrates that proper hydrological data can have a great value in the decision making process and for the overall economic and environmental sustainability.

Arctic Snow Microstructure Experiment for comparison of snow emission models to produce more accurate remote sensing observations of SWE

William Maslanka[1], Leena Leppänen[2*]

[1] *Department of Meteorology, University of Reading, Reading, England, RG6 6AL, UK*
[2] *Arctic Research, Finnish Meteorological Institute, Sodankylä, 99600, FINLAND*
** leena.leppanen@fmi.fi*

ABSTRACT

Passive radiometers measure microwave emission (brightness temperature) of snow, which is directly related to its dielectric properties and therefore SWE. Snow emission models describe microwave radiation extinction within the snowpack. These models are used to invert SWE from observed brightness temperatures.

The Arctic Snow Microstructure Experiment (ASMEx) project made ground-based microwave radiometer measurements and manual reference measurements of snow structure from the homogenous snow slabs of natural snowpack in Sodankylä, Finland. Measurements were made during two winter seasons 2014-2015. Radiometer measurements were made with 18.7, 21.0, 37.5, 89.0 and 150.0 GHz frequencies. Manual measurements included measurements of snow hardness, microstructure, density and temperature; those measurements also studied homogeneity of the slab.

The aim of the study is to understand better microwave extinction in snow and develop modelling of passive microwave measurements for SWE remote sensing purposes. Simulations of two emission models, HUT snow model and MEMLS, are compared to radiometer observations to analyze accuracy of the models in different situations and then update the extinction coefficient to produce more accurate inversions of SWE. Preliminary results show that the two emission models produce brightness temperatures that are in agreement with those measured with the radiometers. Accuracy of HUT and MEMLS depends on measurement setup and used frequency. HUT performs better than MEMLS on absorbing base while performing worse than MEMLS on the reflecting plate.

Future work related to ASMEx measurements are needed to study modelling errors and improve extinction coefficient for more accurate SWE remote sensing observations.

KEYWORDS

Snow cover; Microwave radiometry; Brightness temperature; In situ measurements; Snow emission modelling

1. INTRODUCTION

Snow water equivalent (SWE) is an important parameter to describe amount of water within the snowpack, which is used for studies and research, such as climate change (e.g. Takala et al, 2011). Globally, SWE observations are made from remote sensing measurements (e.g. Chang et al. 1982; Pulliainen & Hallikainen, 2001), because extensive in situ observations are not possible in sparsely populated areas in the northern hemisphere. Instruments with certain microwave frequencies can estimate the amount of SWE from dry snowpack (Mätzler, 1994). Microwave instruments for SWE observations include radiometers SSM/I (Special Sensor Microwave Imager) and AMSR-E (Advanced Microwave Scanning Radiometer - Earth

Observing System) in DMSP (Defense Meteorological Satellite Program) and NASA (National Aeronautics and Space Administration) Aqua satellites. However, in addition to radiometer observations of the snow emission, functional models are needed to invert SWE from observations (e.g. Pulliainen & Hallikainen, 2001). Therefore, development and comparison of different snow emission models is important.

Remote sensing observations of SWE are made with passive microwave radiometers. A radiometer measures the emission of electromagnetic radiation from an object, in terms of brightness temperature. The brightness temperature is related to the object's dielectric properties, which describes electrical conductivity of the object. In snow observations, wetness and density, and therefore SWE, influence such dielectric properties (e.g. Dozier & Warren 1982). Wetness has large effect to the observed brightness temperatures by causing large bias, and therefore SWE observations are useful only from the dry snow periods. However, some models are developed to simulate emission of the wet snowpacks (Pan et al. 2014). Depending on the frequency, microwave radiometers observe microwave radiation that originates from the snowpack, and from the ground (which has been scattered by the snowpack). Therefore, an increase in SWE reduces the observed brightness temperature. At lower frequencies, the amount of scattering is small, thus allowing for a greater penetration depth into the snowpack. For the snow measurements, the most useful frequencies are between 10-90 GHz; with frequencies around 19 GHz and 36 GHz being the most used for historical reasons. Observed brightness temperature depends also on polarization. Additionally, snow microstructure and layering has an influence on the radiation transfer within the snowpack and therefore to the observed brightness temperatures (e.g. Wiesmann & Mätzler, 1999).

Ground-based observations are made for comparison of brightness temperatures to snow parameters without the effect of the atmosphere or vegetation. Observations are made with similar instruments to those found on satellites. Snow parameters, including SWE, can be measured manually from the same area as radiometer measurements, with a small time difference. That allows direct comparison between measured and modelled values.

The Arctic Snow Microstructure Experiment (ASMEx) project is a co-operation project by the Finnish Meteorological Institute, University of Reading, and WSL Institute of Snow and Avalanche Research SLF. During ASMEx, ground-based microwave radiometer measurements and manual reference measurements of snow structure were made in Sodankylä, northern Finland. Measurements were made from the homogenous snow slabs from the natural snowpack during two winter seasons 2014-2015. During both winters, a total of 14 snow slabs were measured, which represents different layers in the snowpack; 13 of those slabs were dry snow and 1 slab was measured at air temperature above 0 °C and it is considered to be wet. The slabs were taken out from the undisturbed snowpack and carried to radiometer tower for the measurements. Manual measurements were made after radiometer measurements from the same snow slab.

Microwave radiometer measurements were made with two tower-based radiometers, which have 18.7, 21.0, 36.5, 89.0 and 150.0 GHz frequency channels, at both horizontal and vertical polarizations (manufactured by Radiometer Physics GmbH, Germany). However, all frequencies were not available over whole measurement periods. Radiometer measurements were made from snow with metal plate base, from snow with absorber material base and from sky. Radiometers were also calibrated before and after measurements, and empty setup was measured to define noise related to the platform. Manual measurements included measurements of layers, snow microstructure, density and temperature. Those measurements also studied homogeneity of the slab.

The snow emission models describe microwave radiation extinction within the snowpack, and models are used to invert snow parameters from brightness temperature observations, or to simulate brightness temperatures if snow parameters are measured manually. The semi-empirical HUT (Helsinki University of Technology) snow emission model is used at FMI to invert SWE from radiometer observations (Pulliainen et al. 1999; Lemmetyinen et al. 2010). A single layer version of the semi-empirical HUT snow emission model is used to simulate the brightness temperatures from the manual in-situ observations. The main assumption of the model is that the radiation is concentrated in the forward direction and only one directional radiation is modelled. The influence of grain size, density, different layers, soil surface, forest canopy and atmosphere is also modeled. Measurements were made within the setup described above, thus allowing the soil and vegetation parameters to be modeled accurately, and atmospheric correction is not needed for ground-based measurements. Another important model is MEMLS (Microwave Emission Model for Layered Snowpacks, Wiesmann & Mätzler, 1999), which model both up and down welling radiation in a multilayer snowpack by using six-flux theory and taking grain size, type, wetness and density into account. Simulations of brightness temperatures from manual measurements are compared to radiometer measurements in all cases. Accuracy of both models in different situations is studied.

Similar experiment has been made before for Alpine snow (Wiesmann et al. 1998) to define extinction coefficients of MEMLS. The experiment was repeated because new developed technique allows more accurate measurements, and arctic snow has also different microstructure than alpine snow.

The aim of the study is to better understand microwave extinction in snow and develop modelling of passive microwave measurements by updating extinction coefficients for SWE remote sensing purposes.

2. METHODS AND MODELS

2.1 Snow slabs

Snow slabs were taken from the natural snowpack in Sodankylä, Finland. In total, 14 slabs were measured. The aim was to measure snow slabs with different grain sizes present, covering a range of snow types and sizes. Each snow slab was selected from a homogeneous layer; to best model microwave extinction. Therefore, snowpack layers were manually defined, before slab extraction and different homogenous layers were chosen for observation. However, layer definition was only made on one edge of the slab; therefore the homogeneity of the whole slab was analyzed manually after radiometer measurements.

The slab was extracted from the snowpack with a metal plate, surrounded by a plastic sheet to prevent freezing to the plate. A plastic frame was used to surround the edges of the slab sample, as shown in Figure 1. The slab dimensions were 80x60 cm, with a variable height (most commonly 15cm). The surface of the completed slab was artificially smoothened, with a metal plate. The snow slab was carried carefully up the radiometer tower for measurements.

After the first set of radiometer measurements, the metal plate was removed from underneath the slab. The slab was very sensitive to cracking during that process. However, the radiometer footprint was located in the middle of the slab, and cracks around the edge of the sample had no effect on measurements.

Figure 1. Snow sample was taken from snowpack with a metal bottom plate and a plastic frame

2.2 Radiometer measurements

Microwave measurements were made with two tower-based radiometers. The snow slab was placed on the experimental setup, which was made up of a rising trolley, absorber material and Styrofoam. The slab needs to be positioned close to the radiometer, to avoid external interference, and to allow the footprint to be centered in the snow slab. Therefore, the trolley was adjusted so that the bottom of the slab was at the same height. Absorber material was used to block emissions from below the snow. Low-density Styrofoam was a good construction material for these frequencies as it is transparent at microwave frequencies. The plastic frame had a very small influence on the microwave measurements. The scheme of setup is presented in Figure 2.

Observation frequencies varied during the measurement period. Table 1 lists the used frequencies in the measurement period. Measurements were made with at an inclination angle of 50°. Equivalent sky measurements were made to record the downwelling emission of microwaves. Slab measurements were first made with a metal plate base, and then with an absorbing base under the snow. The metal plate acts as a perfect reflector and reflects all downwelling sky. The absorbing base acts as a blackbody, and absorbs radiation at all frequencies, thus resulting in no reflection. Those two setups are used to define the real emission from the snow. Physical temperature of snow, air and absorbing material was also recorded for modeling purposes.

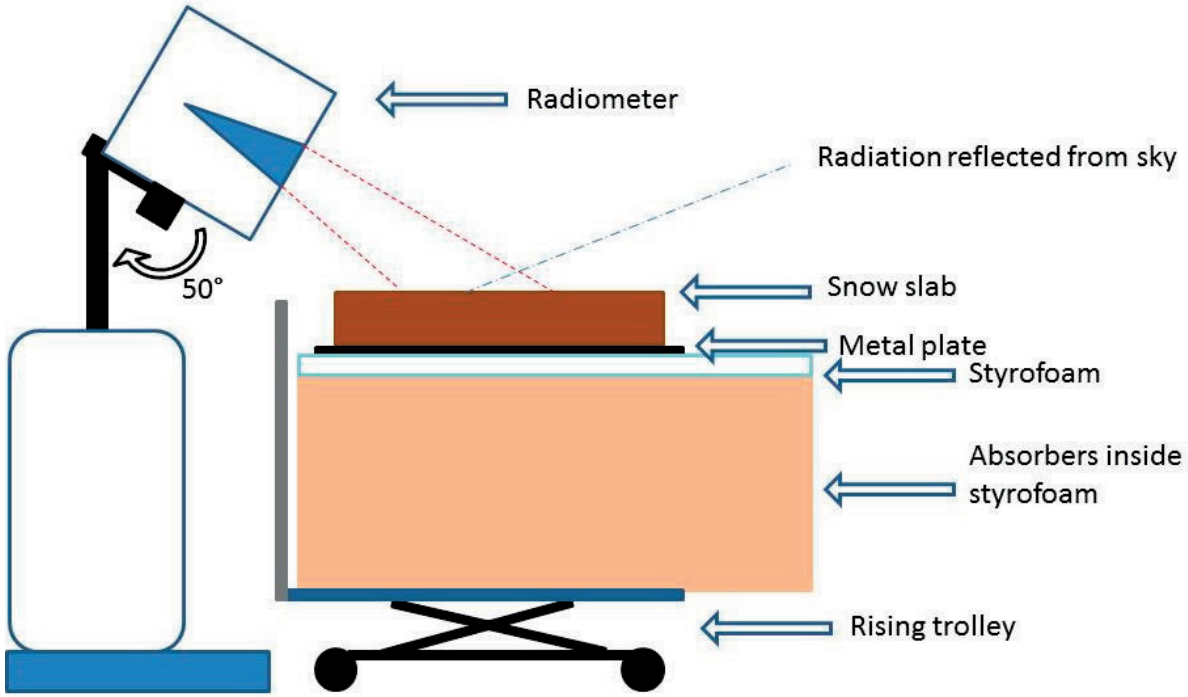

Figure 2. Setup for radiometer measurements with 50° inclination angle

Table 1. Measured radiometric data and manual in-situ data.

Radiometric data (GHz)	18.7	x		x	x	x	x	x	x	x	x	x	x	x	x
	21.0	x	x	x	x	x	x	x	x	x	x	x	x	x	x
	36.5	x	x						x	x	x	x	x	x	x
	89.0					x	x	x					x	x	x
	150.0					x	x	x					x	x	x
In-situ data	Temp.	x	x	x	x	x	x	x	x	x	x	x	x	x	x
	Density	x	x	x	x	x	x	x	x	x	x	x	x	x	x
	Gr. Size	x	x	x	x	x	x	x	x	x	x	x	x	x	x
	SMP	x	x	x	x	x	x	x	x	x	x	x	x	x	x
	IceCube	x	x	x	x				x	x	x	x	x	x	x
	Micro-CT	x	x	x	x	x	x	x	x	x	x	x	x	x	x

2.3 In-situ measurements

Manual in-situ measurements were performed upon completion of the radiometer measurements, including measurements of penetration force with Snow MicroPen (SMP) instrument (Schneebeli & Johnson 1998; Schneebeli et al. 1999), temperature, density, specific surface area (SSA) with IceCube instrument (Gallet et al. 2009) and grain size from

macrophotography (Leppänen et al. 2015), as well as micro computed tomography (micro-CT) sampling (Coléou et al. 2001; Flin et al. 2004; Schneebeli & Sokratov 2004). In-situ measurements for each slab are listed in Table 1 and summary of the measurements are presented in Table 2.

Table 2. Summary of manual in-situ measurement data. All values are averaged across the slab.

13/01/14	**A01**	-13.1	138	0.5	24.0	17.8	Yes
14/01/14	**A02**	-22.2	269	0.7	41.8	15.6	No
11/02/14	**A03**	-0.3	228	0.6	34.0	16.6	Yes (Wet)
13/02/14	**A04**	-0.5	226	0.9	33.9	18.0	No
03/03/14	**A05**	-0.8	287	0.9	44.7	15.6	No
18/03/14	**A06**	-7.6	280	0.8	41.5	14.8	Yes
20/03/14	**A07**	-5.1	285	0.9	42.0	14.8	No
02/0215	**B01**	-13.2	140	0.5	19.0	14.8	Yes
05/02/15	**B02**	-10.9	160	0.5	23.9	13.9	Yes
19/02/15	**B03**	-2.6	234	0.6	32.6	14.9	Yes
11/03/15	**B04**	-5.4	268	1.1	43.5	16.2	Yes
12/0315	**B05**	-3.2	337	1.9	18.1	5.4	Yes
24/03/15	**B06**	-5.4	317	1.3	45.7	14.5	Yes
25/03/15	**B07**	-3.7	283	2.0	43.0	15.2	No

Twelve SMP profiles were measured across the slab to access slab homogeneity. Finally, 9 slabs were totally homogenous. From the SMP measurements, it is possible to derive layers, density profile and correlation length profile of snow (Proksch et al 2015). The SMP measurements are based on a very sensitive tip at the head of penetrating rod, which detects changes in penetration force at a high resolution. After SMP measurements, snow depths of the penetration holes were measured. Other manual measurements were made from the edge of the sample. SSA is the ratio between the surface area and the mass of the snow. The SSA can be used as a snow microstructure parameter. A new optical method for measuring SSA is the commercially available IceCube instrument, which uses a 1310 nm infrared laser to measure hemispherical reflectance from the sample. Calibration data and radiative transfer modelling is used to convert reflectance to SSA. SSA was measured at 3cm intervals. Grain size macro-photographs were taken from every SSA sample. Measurement errors of the SSA and grain size macro-photography are discussed in Leppänen et al. (2015). Density and temperature profiles were measured every 5 cm from bottom to top of the slab. Micro-CT samples were taken from middle of the slab directly inside of the radiometer footprints. The samples will be analyzed in autumn 2015, with three-dimensional x-ray tomography in SLF, Switzerland, producing a three dimensional computer model of the snow. From this model, it is possible to define many important microstructural parameters, such as grain size, grain type, orientation of grains and bonding of grains (e.g. Lundy et al. 2002). Locations of the manual measurements in the slab are presented in Figure 3, with measurement method photographs being presented in Figure 4.

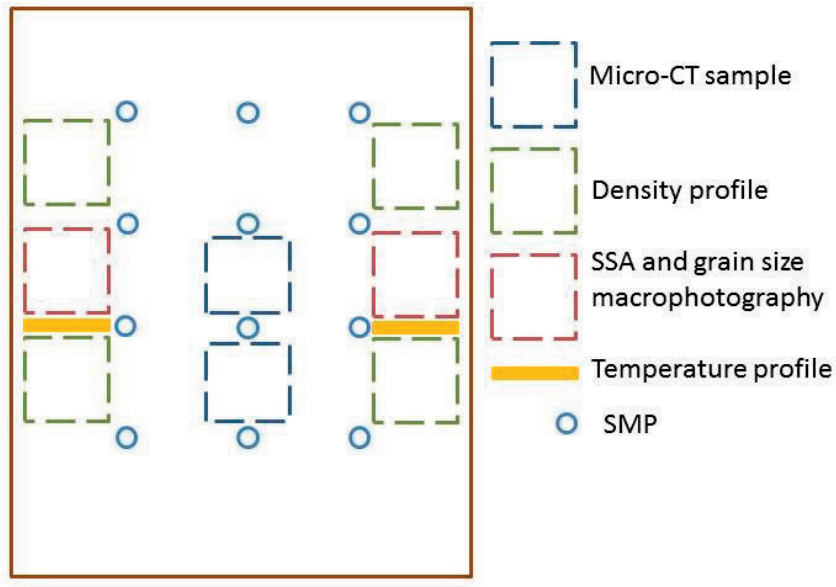

Figure 3. Approximate location of the in-situ measurements in the snow slab

3. RESULTS

3.1 Comparison of snow emission models HUT and MEMLS

Measurements of physical parameters (Table 2) were used in both the single layer HUT snow emission model and MEMLS, to produce brightness temperature simulations of all 13 dry slabs, upon absorbing and reflecting bases. The simulations were compared to the observed brightness temperature, and the RMSE was calculated at both horizontal and vertical polarization, on both the absorbing and reflective bases (Figure 5).

Upon the absorbing base, HUT performs equal to or better than MEMLS at 18.7, 21.0, and 36.5 GHz, while performing equal to or worse than MEMLS on the reflecting plate at the same frequencies. At the higher frequencies (89.0 and 150.0 GHz), with the exception of the horizontal absorbing case, HUT is routinely less accurate than MEMLS. These large errors in HUT may be explained due to the extinction coefficient used only being valid between 18-60 GHz (Pulliainen et al., 1999). The scattering coefficients used in MEMLS are valid between 5-100 GHz (Wiesmann & Mätzler, 1998), thus explaining why the RMSE values are consistent across the four situations shown in Figure 5.

Figure 4. a) SMP measurements, b) In situ density measurement, c) IceCube instrument for SSA measurement, d) In situ temperature measurement

4. CONCLUSION

The brightness temperature of homogeneous snow slabs extracted from the natural snowpack during ASMEx has been simulated with both the HUT snow emission model, and MEMLS. The HUT simulations had a lower RMSE value than MEMLS for the three lower frequencies measured; on top of the absorbing base. MEMLS simulations had lower errors associated with them for the reflective base cases. Errors at the two higher frequencies can begin to be explained by being outside the operational frequency range of the two models.

The errors in the lower three frequencies exist due to unaccounted internal scattering within the snow. These errors will be reduced in the future, via an improved understanding of internal scattering, and a revised extinction coefficient model. This revised extinction model will be calculated from microstructure information (from both modern and traditional methods) as well as radiometric data collected during ASMEx. The revised model for extinction will be implemented in the HUT snow emission model, and will aim to improve the current SWE estimations from model inversions with satellite observations.

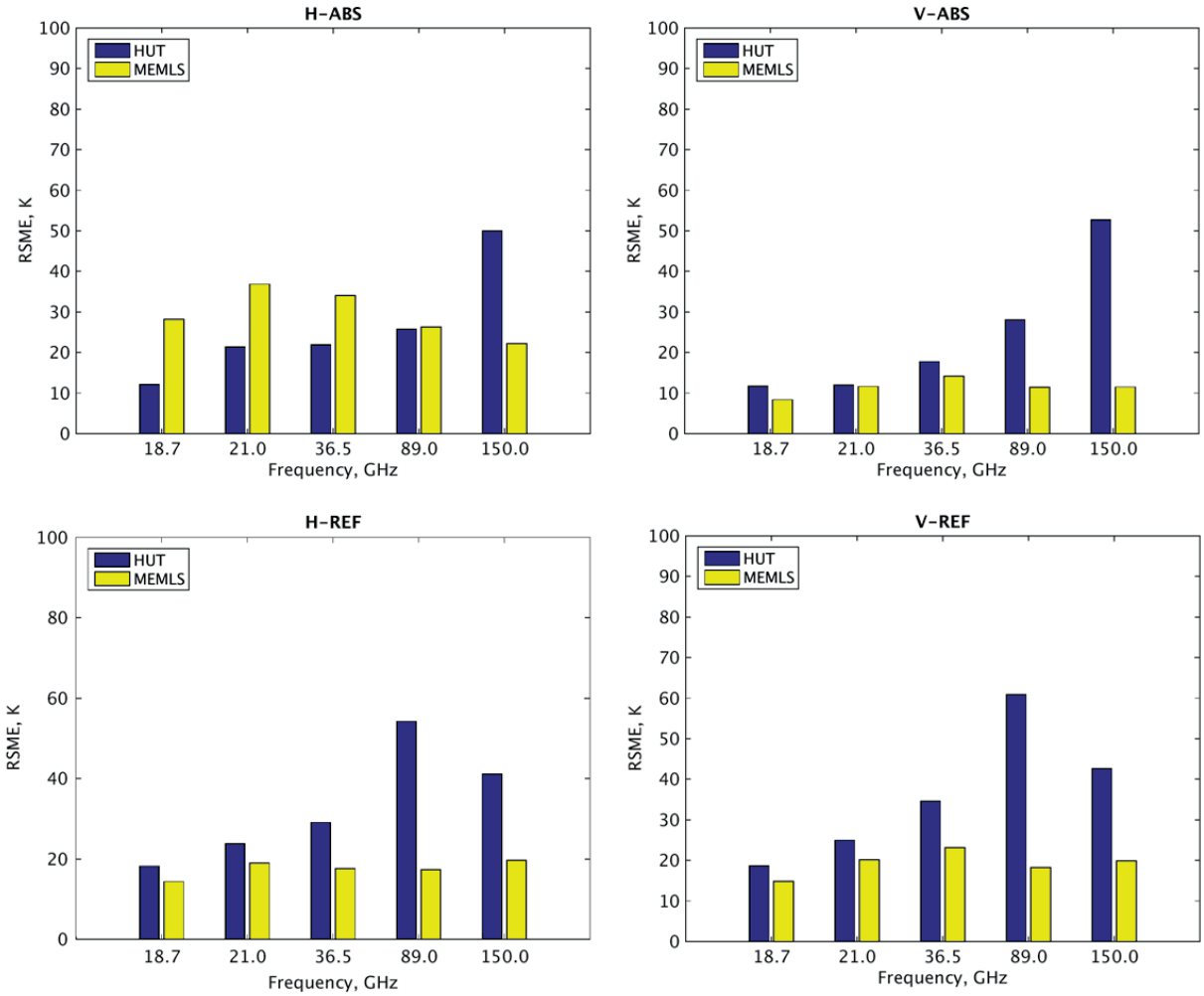

Figure 5. Brightness temperature RMSE at H and V polarizations for absorber material base (ABS) and reflective metal plate base (REF) for HUT model and MEMLS simulations.

AKNOWLEDGEMENT

We thank the staff of FMI Arctic Research Centre in Sodankylä for performing the ground-based radiometer measurements and in situ measurements. We also thank the staff of WSL Institute of Snow and Avalanche Research SLF from SMP instrument and becoming micro-CT analyses of snow samples. We thank especially Dr. Juha Lemmetyinen, Dr. Mel Sandells and Dr. Martin Schneebeli of planning and fulfillment the project.

REFERENCES

Chang A.T.C., Foster J.L., Hall D.K., Rango A. and Hartline B.K. 1982 Snow water equivalent estimation by microwave radiometry. *Cold Reg. Sci. Technol*. 5(3), 259–267.

Coléou C., Lesaffre, B., Brzoska, J.-B., Ludwig, W., and Boller, E. 2001 Three-dimensional snow images by X-ray microtomography. *Ann. Glaciol.* 32, 75–81.

Dozier J., & Warren, S. G. 1982 Effect of viewing angle on the infrared brightness temperature of snow. *Water Resources Research*. *18*(5), 1424-1434.

Flin F., Brzoska, J.-B., Lesaffre, B., Coléou, C., and Pieritz, R. A. 2004 Three-dimensional geometric measurements of snow microstructural evolution under isothermal conditions. *Ann. Glacio.* 38, 39–44.

Gallet J.C., F. Dominé, C. S. Zender, and G. Picard 2009 Measurement of the specific surface area of snow using infrared reflectance in an integrating sphere at 1310 and 1550 nm. *The Cryosphere.* vol. 3, 167-182.

Lemmetyinen J., J. Pulliainen, A. Rees, A. Kontu, Y. Qiu, and C. Derksen 2010 Multiple-layer adaptation of HUT snow emission model: comparison with experimental data. *IEEE Transactions on Geoscience and Remote Sensing*. vol. 48, no. 7, 2781-2794.

Leppänen L., Kontu, A., Vehviläinen, J., Lemmetyinen, J., & Pulliainen, J. 2015 Comparison of traditional and optical grain-size field measurements with SNOWPACK simulations in a taiga snowpack. *Journal of Glaciology*. *61*(225), 151.

Lundy C. C., Edens, M. Q., & Brown, R. L. 2002 Measurement of snow density and microstructure using computed tomography. *Journal of Glaciology*. *48*(161), 312-316.

Mätzler C. 1994 Passive microwave signatures of landscapes in winter. *Meteorology and Atmospheric Physics* 54 (1-4), 241-260.

Pan, J., Jiang L. and Zhang L. 2014 Comparison of the multi-layer HUT snow emission model with observations of wet snowpacks. *Hydrological Processes*. *28*(3), 1071-1083.

Proksch, M. H Löwe, and M Schneebeli 2015 Density, specific surface area, and correlation length of snow measured by high-resolution penetrometry. *J Geophys Res Earth Surf. 120*, 346-362

Pulliainen J., and M. Hallikainen 2001 Retrieval of regional snow water equivalent from space-borne passive microwave observations. *Remote sensing of environment* 75.1, 76-85.

Pulliainen J. T., J. Grandell, and M. T. Hallikainen 1999 HUT snow emission model and its applicability to snow water equivalent retrieval. *IEEE Transactions on Geoscience and Remote Sensing*. vol. 37, no. 3, 1378-1390.

Schneebeli M., Johnson, J.B. 1998 A constant-speed penetrometer for high-resolution snow stratigraphy. *Ann. Glaciol.* 26, 107–111

Schneebeli M., Pielmeier, C., Johnson, J.B. 1999 Measuring snow microstructure and hardness using a high resolution penetrometer. *Cold Reg. Sci. Technol*. 30, 101–114.

Schneebeli M. and S. A. Sokratov 2004 Tomography of temperature gradient metamorphism of snow and associated changes in heat conductivity. *Hydrol. Process.* 18, 3655– 3665.

Takala M., K. Luojus, J. Pulliainen, C. Derksen, J. Lemmetyinen, J-P Kärnä, J. Koskinen, and B. Bojkov 2011 Estimating northern hemisphere snow water equivalent for climate research through assimilation of space-borne radiometer data and ground-based measurements. *Remote Sensing of Environment*. vol. 115, 3517-3529.

Wiesmann A., C. Mätzler, and T. Weise 1998 Radiometric and structural measurements of snow samples. *Radio Science.* 33.2, 273-289.

Wiesmann A. and C. Mätzler 1999 Microwave emission model of layered snowpacks. *Remote Sensing of Environment.* vol. 70, no. 3, 307-316.

Measurement of snowmelt in a subarctic site using low cost temperature loggers

[1]Leo-Juhani Meriö*, [1]Pertti Ala-aho, [1]Hannu Marttila, [1]Bjørn Kløve, [2]Pekka Hänninen, [2]Jarkko Okkonen, [2]Raimo Sutinen

[1]Water Resources and Environmental Engineering Research Group, University of Oulu, FINLAND
[2]Geological Survey of Finland, FINLAND
**jmerio@student.oulu.fi*

KEYWORDS
Snowmelt, snow measurements, spatial variability, degree-day model, low-cost temperature loggers

1. INTRODUCTION
The snowpack properties typically have large spatial variability depending on the catchment and climate conditions. The measurements are usually discontinuous and the network is often very sparse due to high resource needs. The spatial and temporal accuracy of the results depend of the variability of the snowpack properties and the representativeness of the measurements points. Inexpensive temperature loggers can provide a cost efficient method to get more accurate spatial coverage of the snowpack including its variability in real time. In this study, the low-cost temperature loggers were tested, calibrated and utilized to measure the local and microscale variability of the snowmelt in subarctic fell at Pallastunturi region (Figure 1).

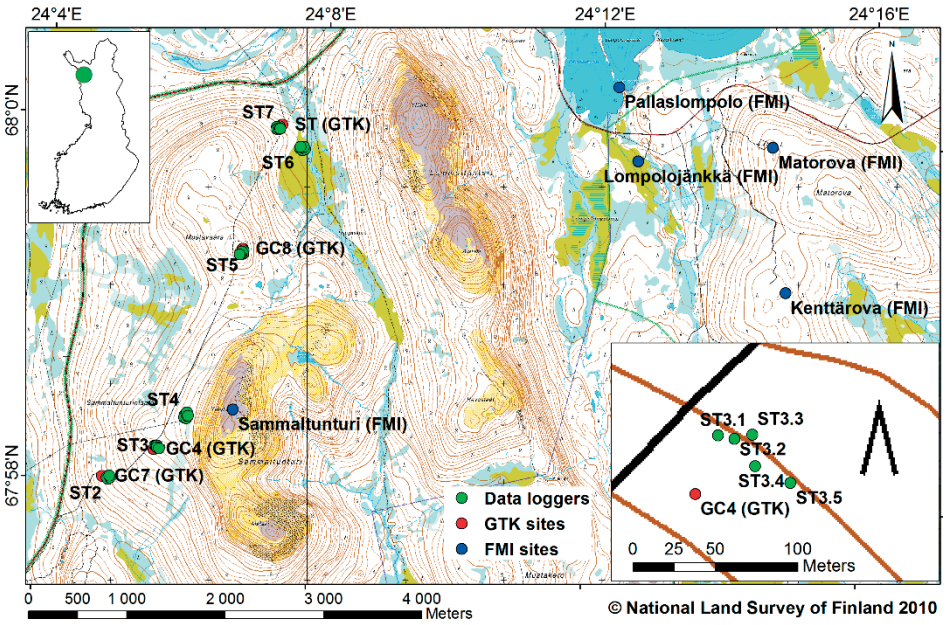

Figure 1. Experiment area and test plot locations. One test plot zoomed at the bottom right.

2. METHODS

The loggers were installed on the ground and on fixed height 30 cm above ground in six locations with different terrain type, topography and vegetation (Figure 1). Daily standard deviation of the logger temperatures (Figure 2) were used to determine the melting processes and rates. Snow depth data from adjacent measurement stations equipped with acoustic snow height sensors were used to verify the results.

Air temperature and precipitation data and melt rates determined using the temperature loggers were used in an empirical degree-day model (DeWalle & Rango 2008, 279-281) to study the validity of the results. Snowpack measurements on 16/17th of April 2014 were used to calibrate the model. The goodness of the model was evaluated using root mean squared error (RMSE) between the modelled and measured dates for the ending of the permanent snow cover.

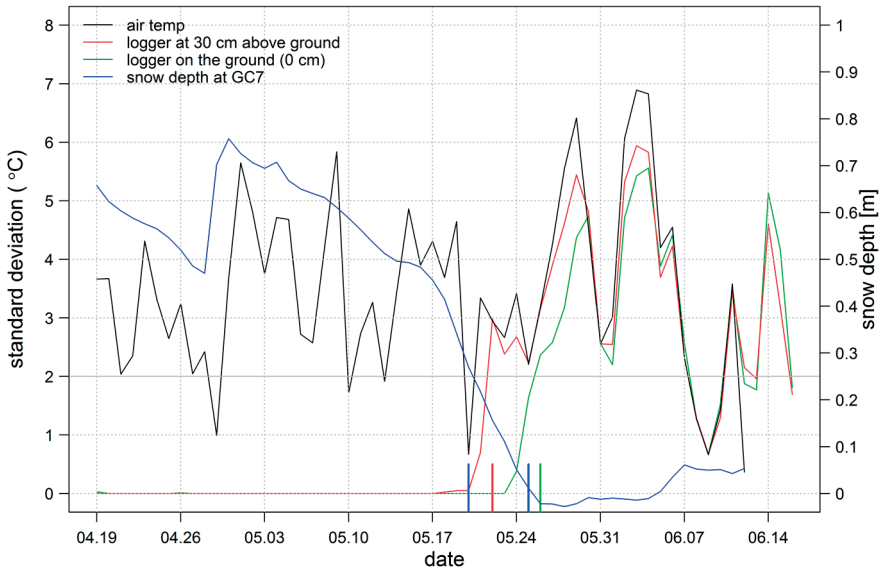

Figure 2. Daily standard deviation of the air and logger temperatures. Snow depth at the adjacent reference measurement site. The vertical lines on the x-axis show the dates when snow depth is 30 cm (red) and 0 cm (green) determined using the loggers and measured at reference site (blue).

3. RESULTS AND DISCUSSION

The results revealed difference in the timing and variability of the snowmelt (Figure 3). The variability was highest in plots with forest cover (ST2, ST3 and ST7) and lowest in the plot located on an open mire (ST6). The melt timing was earlier in open areas than in forest. Delay in melt timing at the northern slope (ST7) was also observed. The timing agreed reasonable well with the acoustic measurement data and gives additional information about the spatial variability of snowmelt.

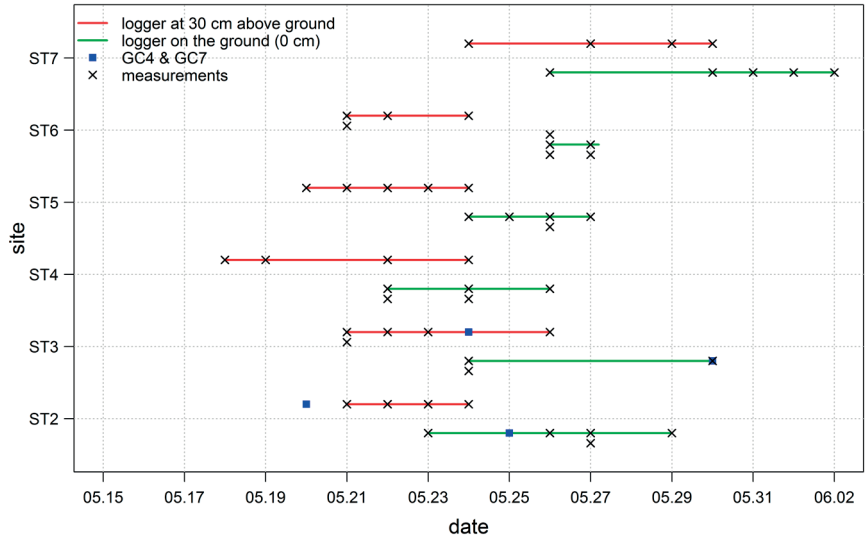

Figure 3. Determined spatial variability of snow melt timing at snowpack height of 30 cm and 0 cm. GTK reference measurements adjacent to ST2 and ST3 are marked in blue.

The modelled variability of snow water equivalent (SWE) on experiment winter is shown in Figure 4. The difference between modelled and measured date for the end of permanent snow cover is presented in Table 1. The RMSE at the end of permanent snow cover was 3.74 days. Smallest error was found on the open mire. In areas with more complex topography and forest the error was larger. Model was also run with median degree-day factors determined from the five test points at each test plot. The RMSE improved to 3.19 days. The error at the open mire was increased whereas in most of the other sites it was decreased.

Table 1. Difference between the modelled and measured date for the end of permanent snow cover in days. Overall mean and median: -0.29 & -1 days. Overall SD and IQR: 3.8 & 6 days.

	ST2	**ST3**	**ST4**	**ST5**	**ST6**	**ST7**
1	-2	-1	4	-5	1	-5
2	-2	NA	-2	4	1	-2
3	-5	4	-5	-1	-1	3
4	NA	5	5	2	NA	NA
5	-5	NA	NA	5	2	-7
Mean / SD	-3.5 / 1.73	2.66 / 3.21	0.5 /4.80	1 / 4.06	0.75 / 1.26	-2.75 / 4.35
Median / IQR	-3.5 / 3	4 / 3	1 / 7	2 / 5	1 / 0.75	-3.5 / 4.75

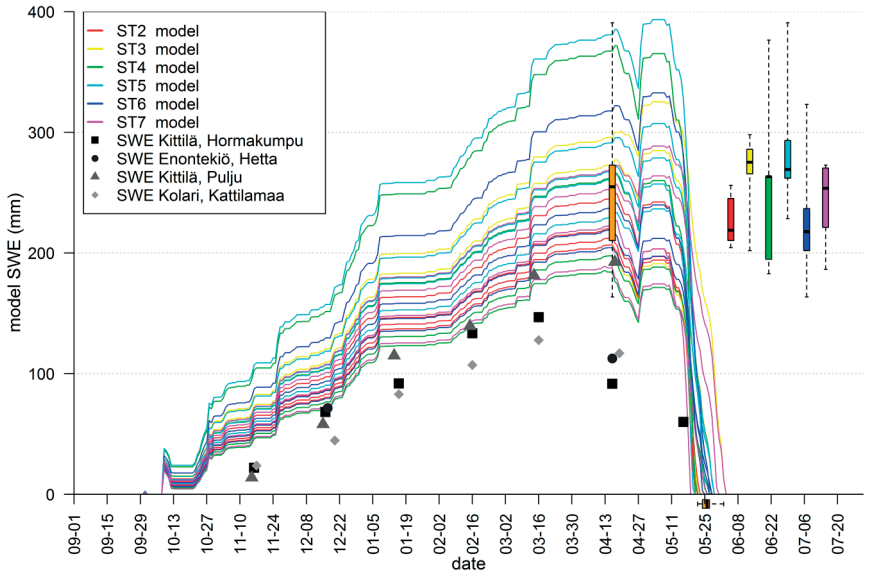

Figure 4. Modelled snow water equivalent using melt rates determined from each temperature logger pair. Box plots of measured snow water equivalents (orange) and end of permanent snow cover (horizontally in the x-axis). Boxplots on the right show the measured variability of SWE in each test plot. SWE measurements from snow courses provided by Finnish Environment Institute are shown in greyscale.

Natural variation of solar radiation absorbed by the temperature loggers and consequent heat emission increasing melt rate in the proximity of the logger is assumed to be the largest individual source of uncertainty for the method. Unknown snow properties during the melt were also expected to cause inaccuracy in melt rate determination. Possible displacement of the sensors due to snow pack metamorphosis during the melt can cause additional uncertainty.

4. CONCLUSIONS

The melt rates determined using the low-cost temperature loggers were found to be reasonable accurate on open, flat and relatively homogenous terrain conditions, such as open mire. In more complex topography and forested areas the microscale accuracy decreased, thus usage of median determined melt rates improved the accuracy in test plot (mesoscale) level. The timing of the snow melt agreed reasonably well with the reference measurement sites. Overall, the usage of inexpensive temperature loggers for snow melt measurements was observed to be reasonably accurate method to gain information about spatial variability of the snow melt timing and rates. The method could especially be suitable for areas where available regional snow measurements are not representative and in remote ungauged basins. Using wireless connections with logger's measurement method could be utilised also in real time operational use.

5. REFERENCES

DeWalle, D. R., & Rango, A. 2008 *Principles of snow hydrology*. Cambridge University Press.

Comparison of snow water equivalent derived from passive microwave radiometer with in-situ snow course observations in Finland

Mikko Moisander[1], Sari Metsämäki[2], Heidi Sjöblom[2], Johanna Korhonen[2*], Kristin Böttcher[2], Hannu Sirviö[2]

[1] Finnish Meteorological Institute (FMI), P.O. Box 503, 00101 Helsinki, FINLAND
[2]Finnish Environment Institute (SYKE), P.O. Box 140, 00251 Helsinki, FINLAND
**johanna.korhonen@ymparisto.fi*

ABSTRACT

Information on snow water equivalent (SWE) is needed e.g. for climate research and flood forecasts. Finnish Environment Institute (SYKE) monitors snow water equivalent with network of 150 snow courses with monthly observations within different terrains. For improvement of flood forecasting more frequent observations are needed. Satellite based microwave radiometers enable daily observations on SWE at good spatial coverage. Suitability of radiometer data for improvement of snow water equivalent monitoring was investigated by comparing radiometer data with in-situ snow course measurements done in the field for winters 2011-2013. Study shows some differences between radiometer and in-situ measurements and improving radiometer algorithms is still needed to fulfill desired accuracy of satellite measurements.

KEYWORDS

Snow water equivalent; in-situ observations; passive microwave radiometer data; Finland

1. INTRODUCTION

Snow plays an important role in the water cycle and energy balance in the northern latitudes as it is producing main runoff peaks during the spring time. Approximately half of annual precipitation in Finland falls as snow. Snow water equivalent (SWE) is needed e.g. for climate research, modelling of river systems, flood forecasting and for regulating the water level for hydropower.

Traditionally snow water equivalent information has been obtained from in-situ manual observations and by spatially and temporally interpolating data from weather stations and other gauging networks. Interpolations from weather data for this purpose tend not be precise enough and gauging networks are usually limited and have rather sparse. Information on SWE on daily basis and globally can also be obtained from satellite microwave radiometer observations (eg. Chang et al 1982). In this study, suitability of radiometer data for improvement of snow water equivalent monitoring was investigated by comparing radiometer data with in-situ snow course measurements done in the field different parts of Finland. This paper is based on Master's Thesis by Moisander (2014). Earlier Pulliainen and Hallikainen (2001) have studied suitability of radiometer measurements in Kemijoki river basin area.

2. DATA AND METHODS

2.1 Snow line measurements

Snow water equivalent (SWE) defines how much water (mm=kg/m^2) is contained within snowpack. Finnish Environment Institute (SYKE) governs a network of ~150 snow courses with monthly observations within different terrains. A snow line is a 2 to 4 km long route containing examples of all terrain types found within surrounding region. Eight weight measurements are done to determine density of snow together with 80 depth measurements. These measurements are used to estimate average SWEs for each terrain type and for whole line. There are six different terrain types observed on snow lines operated by SYKE: open areas, forest openings, bogs and forests dominated either by pine, spruce or deciduous leaved species. In this study, 21 of SYKE's snow lines located different parts of the country were included.

2.2 SYKE snow model

For each snow course daily SWE values are estimated using temperature and precipitation data from nearby weather stations. These daily values are then interpolated to 10 km by 10 km grid and corrected with topological factors to produce maps on SWE.

Estimated values are then corrected to values observed in situ using least square fitting and by changing snow accumulation and melting parameters. Degree day model is used to estimate snow melt.

Figure 1 depicts modelling result given by SYKE snow model using precipitation and air temperature data of near-by weather stations. Modelled accumulation of SWE is marked with black and blue lines, where black line is results based on modelling only and blue line shows results corrected to in situ observations (red asterisks).

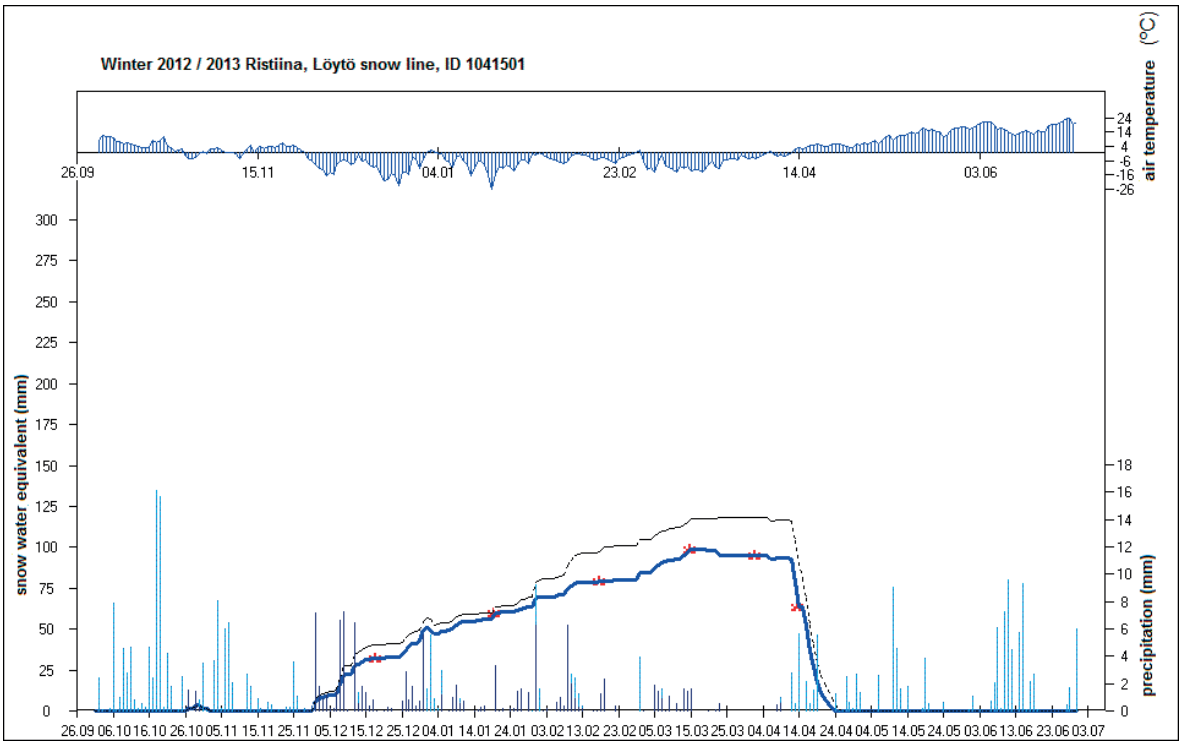

Figure 1. Simulation of SWE with SYKE snow model.

2.3 Radiometer observations

Using satellite based microwave radiometers it is possible to acquire daily observations on SWE over vast areas, with global coverage achieved every two or three days. Additionally observations can be done both day and night and in all weather conditions.

Method is based on detecting natural energy emitted by frozen ground. Two different frequencies are used, one penetrating the snow, while the other is dampened depending on thickness, density and other properties of the snow cover. SWE can be estimated from observed intensity difference between frequencies.

Same energy readings can be achieved with many different combinations of snow slab thickness, snow density, vegetation cover and local atmospheric properties (see Figure 2). As result standalone microwave observations can be somewhat imprecise. In addition instrument's coarse spatial resolution (5 – 25 km) and sensitivity to liquid water limits number of potential uses. Most commonly used channel difference is between 37 and 19 GHz and works only on snow depths between 5 cm and 1 m. For thinner snow difference between frequencies is too small and on greater snow depths the radiation no longer penetrates the snow cover. Using lower frequencies applicable snow depth can be increased, but with cost of worsened spatial resolution.

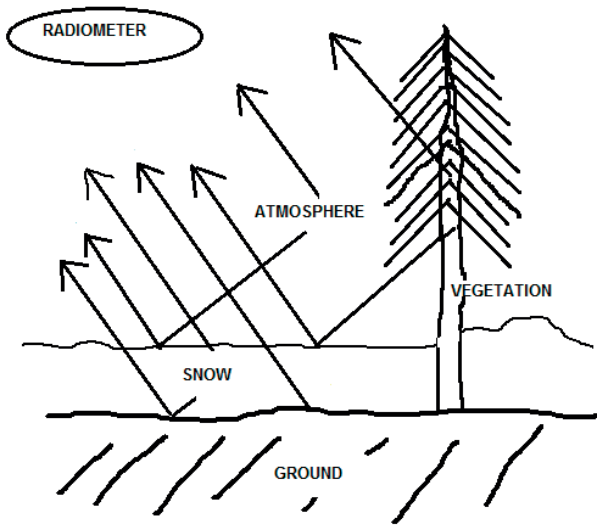

Figure 2. Energy signature observed by radiometer comes from multiple sources.

Using vegetation cover maps and atmospheric models together with data assimilation (Pulliainen 2006) to solve background snow depth, variations in SWE estimates can be bound to more acceptable levels. If additional knowledge on snow properties is available, results can be further improved.

2.4 SWE-maps

SWE-maps were produced with observation from Special Sensor Microwave Imager (SSM/I) and Advanced Microwave Scanning Radiometer for EOS (AMSR-E) sensors, using Helsinki University of Technology (HUT) snow emission model (Pulliainen et al. 1999), and corrected with FMI's synoptic weather station snow depth data, using assimilation method (Pulliainen 2006). Maps on SWE produced this way were compared with in situ observations from SYKE's snowlines and with areal snow water equivalents calculated thereof.

Maps of daily values and seasonal averages were compared visually and root mean squared error (RMSE) rates were calculated. To take account effects of different scales between data sources; SWE on snow lines was recalculated using land cover class distributions data from Corine 2006 for radiometer pixels containing snow lines.

3. RESULTS AND DISCUSSION

A strong seasonally changing bias was discovered. Microwave radiometer-based technique tends to overestimate SWE during early- and mid-winter accumulation period and severely underestimate it once spring melt has started. We also identified several sites, where difference between radiometer and in-situ observations remains high and consistently biased throughout the seasons and between years. First type of bias can be mostly tracked to spatially and temporally changing attributes of snow cover. Latter cases point to presence of some systematic error source such as sparseness of gauging network, quick changes in elevation or wrongly interpreted terrain type. Figure 3 shows evolution of differences between satellite and in-situ based products during the spring 2011.

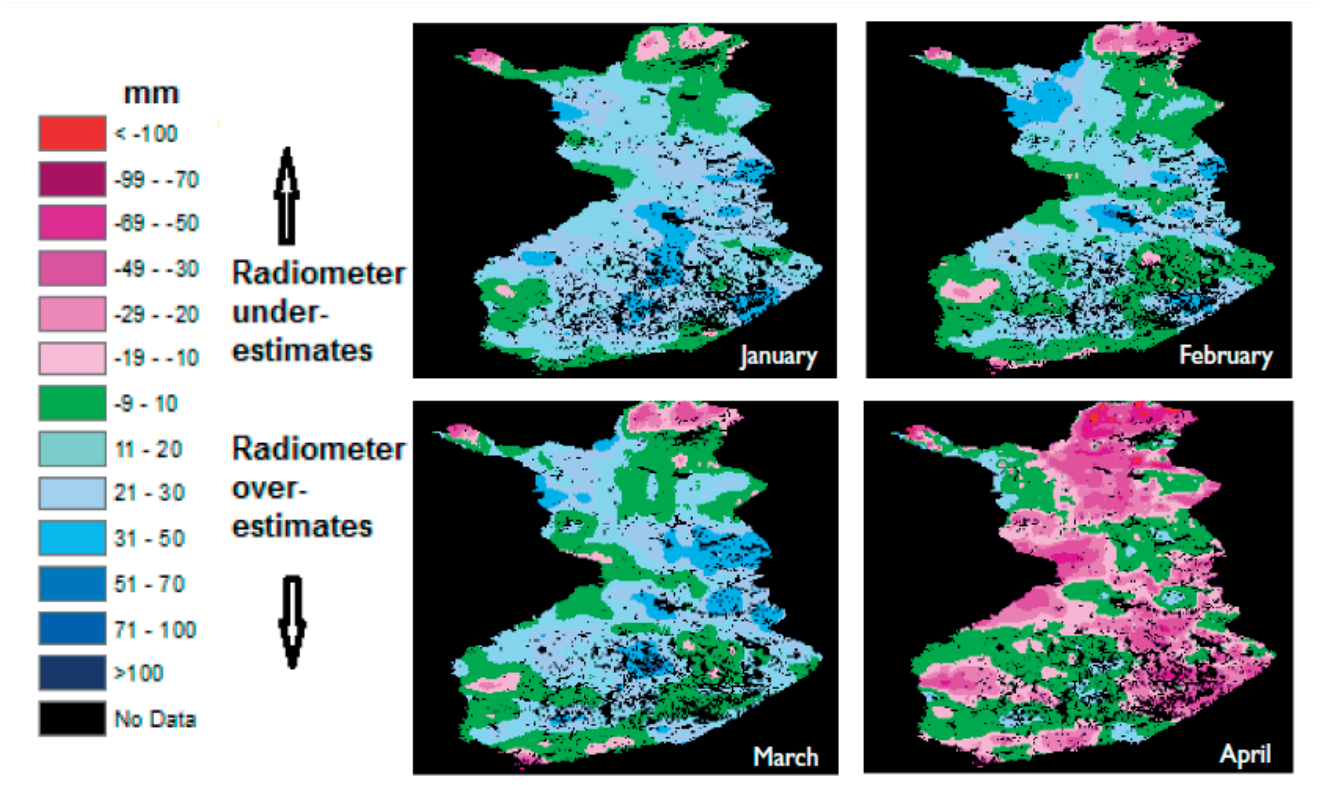

Figure 3. Evolution of differences between satellite and in-situ based products during the spring 2011.

Snow density and depth, and how they evolve over time, can vary greatly between different terrain types. Weather stations are mostly located on open and relatively flat areas and interpolating snow depth values over terrain with varying elevation and vegetation cover can lead to errors in background maps of snow depth. These errors can be reduced by using in situ (e.g. snow line) information on how snow depth varies between different terrain types, especially between open and densely vegetated areas.

Currently there are no daily observations available on how snow density evolves over time. Interpreting SWE from satellite images has to rely on using constant values or use functions fitted to time series in order to describe how snow's density changes. Both methods disregard quick changes in snow density caused by rapid melting or heavy snow falls. In addition, when interpreting SWE over larger areas such as whole country problem raises that start and end dates of winter and thus snow's density can and usually will vary significantly over different parts of the area observed. This means that using single constant or function to whole area will cause errors.

Correcting SWE values with local values of snow density and depth was investigated. Results were promising with RMSE rates considerably reduced. More research on how to best include this data to the assimilation process itself is needed. One possibility is that data from snow lines could be used to improve snow depth maps used in assimilation of radiometer observations.

Significant part of the seasonal bias is caused by using same density function for whole country. Winter usually starts earlier and last longer in Northern Finland than in the south. Also in the south melting and refreezing occurs often during a winter. Therefore density of the snow varies greatly between different parts of the country. Country was divided in two at the latitude 63.5° and new regional density functions were calculated. RMSE rate for northern subset dropped from 28 mm to 20 mm. Southern subset was more heterogeneous and the new density function did not improve results. RMSE values were reduced only at 40% of sites with overall RMSE rising from 31 mm to 33 mm (see figure 4 for effects of using regional density functions).

New versions of the algorithm used to interpret the microwave signal take into account better such things as layered structure of snow and effects of frozen water bodies in instruments field of view. These improvements increase the accuracy of the method and reduce the need for auxiliary data but do not remove it completely.

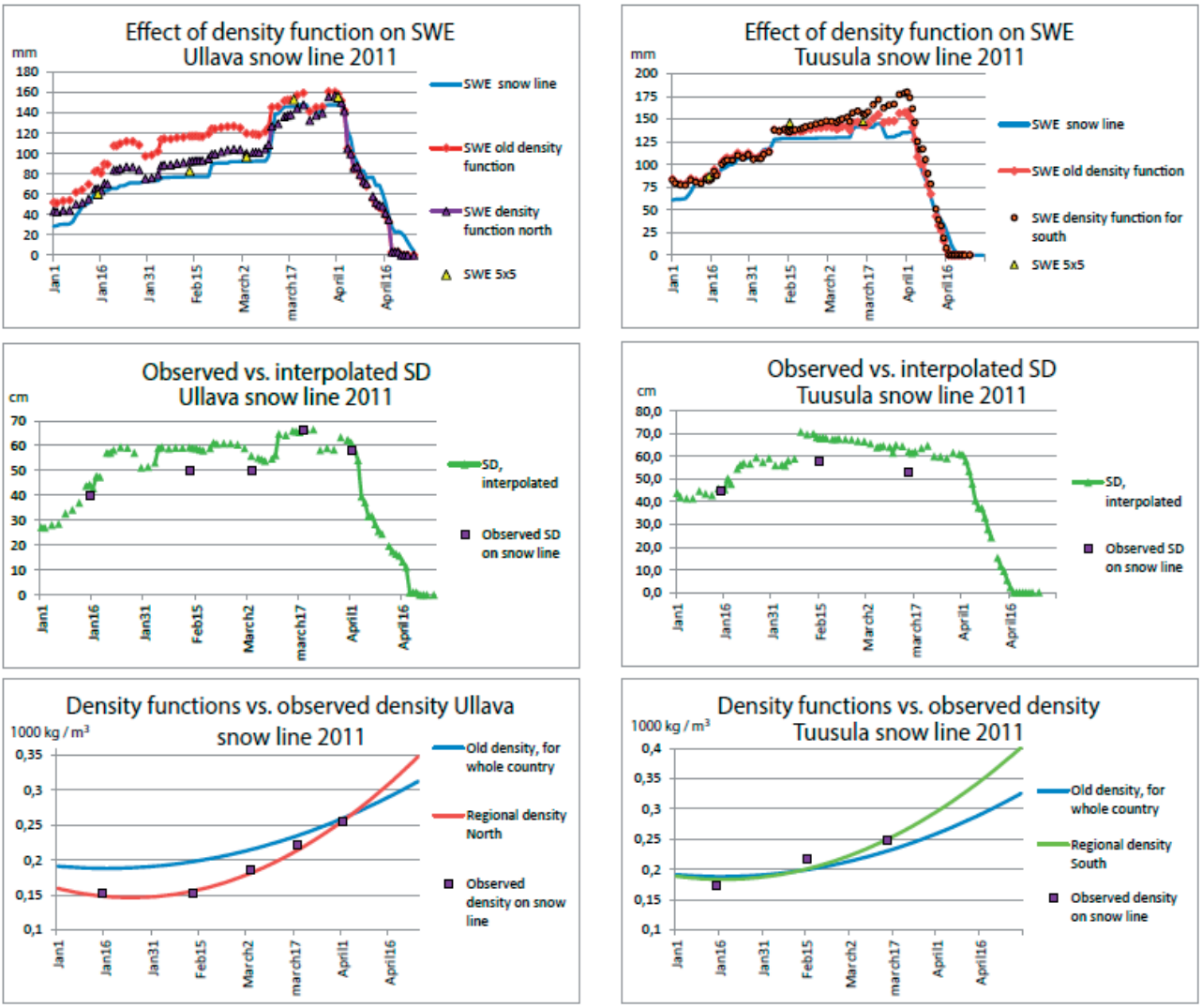

Figure 4. Effects of using regional density functions for two different snow lines Ullava and Tuusula 2011.

4. CONCLUSIONS

Satellite based microwave radiometer observations provide daily information on SWE over large areas. Comparison of in-situ observations and satellite SWE products showed seasonal bias, which was highest during the snow melt period. To improve method's accuracy to requirements of operational observations, challenges caused by temporally and spatially changing snow attributes need to be first solved. Radiometer measurements need ground truth information on snow density and snow depth to give more accurate results. For purposes of operational observations work, best way to use satellite products is to combine them with the snow course observations data.

5. REFERENCES

Chang A.T.C., Foster J.L., Hall D.K., Rango A. & Hartline B.K. 1982 Snow water equivalent estimation by microwave radiometry. *Cold Reg. Sci. Technol*. 5(3), 259–267.

Moisander, M. 2014 *Supporting operational observations of snow water equivalent with remote sensing data.* Master's Thesis, Aalto University. 75 p. (in Finnish)

Pulliainen J. 2006 Mapping of snow water equivalent and snow depth in boreal and sub-arctic zones by assimilating space-borne microwave radiometer data and ground-based observations. *Remote Sensing of Environment issue* 101:257-269.

Pulliainen J., Grandell J. & Hallikainen M. 1999 HUT Snow Emission Model and its Applicability to Snow Water Equivalent Retrieval. *IEEE Transactions on Geoscience and Remote sensing* Vol. 37. No 5.

Pulliainen, J. & Hallikainen, M. 2001 Retrieval of Regional Snow Water Equivalent from Space-Borne Passive Microwave Observations. *Remote Sens. Environ.* 75:76–85.

Experiences and recommendations on automated groundwater monitoring

Risto Mäkinen[1]*, Mirjam Orvomaa[1]

[1]*Freshwater Centre, Finnish Environment Institute, Helsinki, 00100, FINLAND*
** risto.p.makinen@ymparisto.fi*

ABSTRACT

Automation of groundwater monitoring has increased vastly during the past decade. However, there is little written data on impartial recommendations based on actual monitoring experiences which can serve as a guide. As automation leads to expanded valuable information on groundwater behaviour as well as a possible saving in resources (in the long run) it is important to initialize automation correctly. This study discusses key issues based on actual experiences in automation at some of SYKEs monitoring sites. The recommendations listed should be taken into consideration to obtain accurate reliable long-term data from groundwater formations in automated monitoring.

KEYWORDS

groundwater; automation; monitoring

1. INTRODUCTION

Manual on site measurements have been the sole mean of measuring groundwater table from observation tubes for the past decades. Measurements have been done twice a month at approximately 80 nationwide groundwater monitoring stations of which over half have been functioning since the late 70's (Soveri et al. 2001). To acquire more valuable information on groundwater behavior, automated monitoring has been included increasingly during the past ten years. The network now has around 80 automated observation tubes that monitor groundwater table, and of these 40 tubes have sensors that enable temperature monitoring. Factual results are crucial for e.g. understanding which groundwater changes are plausible effects of climate change and the ones that subsume as natural variation.

The recommendations are based on experiences gained through data from several monitoring sites where for e.g. changes in water tables and temperatures reveal incorrect results that can lead to wrong interpretations. As an example of these erroneous factors are noticeable irregular gushes of warmer or colder water and changes in groundwater tables immediately after rain showers or during spring thaw.

The benefits of automation are immense but to ensure factual monitoring results there are several key issues that must be considered: 1) the importance of properly installed and sealed observation tubes, 2) the necessary background information of prior manual measurements to determine at which height to set the monitoring sensor (the scale of water table changes and possible different groundwater layers), 3) geological and geographical information, 4) the proper trial period with automatic measuring devices to determine whether the changes can be determined as reliable and representative in the long run, and 5) the ideal amount of automated measuring devices per observation site.

2. METHODS

The groundwater monitoring stations SYKE observes generally have ten installed groundwater tubes, from which an average groundwater table is calculated. The stations are located nation widely and the examples presented are all from different monitoring stations.

2.1 Planning automation of groundwater table measurements

Background information of the range of water table variation in the monitoring tube is essential when planning the automation of groundwater table measurements. The first key measure is the distance between the top of the monitoring tube and the mean groundwater table (Figure 1a). If the highest water (HW) groundwater table (Figure 1b), and the lowest water table (LW) (Figure 1c) are not known the estimation should rather be excessive to rule out the possibility of water levels dropping below the pressure sensors depth as pointed out in Figure 2. Many sensors are vulnerable and may break down if subjected above water level. The measuring scale of the logger is selected according to the range of variation in water levels. The generally used variation range in Finland is five meters although the average range for groundwater table is 1,5-2 meters (Salonen et al. 2002 and Soveri et al. 2001). It is important that the measuring range is not exceeded as pressure sensors have a certain pressure resistance, after which they may be damaged. The pressure sensor should be installed at a sufficient distance from the bottom of the monitoring tube to prevent contact with sludge (Figure 1d).

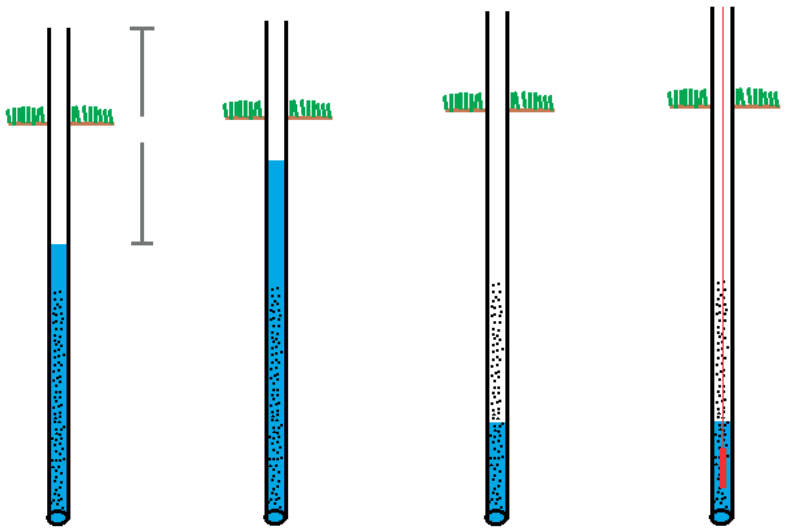

Figure 1a, 1b, 1c, and 1d. The distance between the top of the monitoring tube and the mean groundwater table, the highest water groundwater, the lowest water table, and the correct depth to install above sludge.

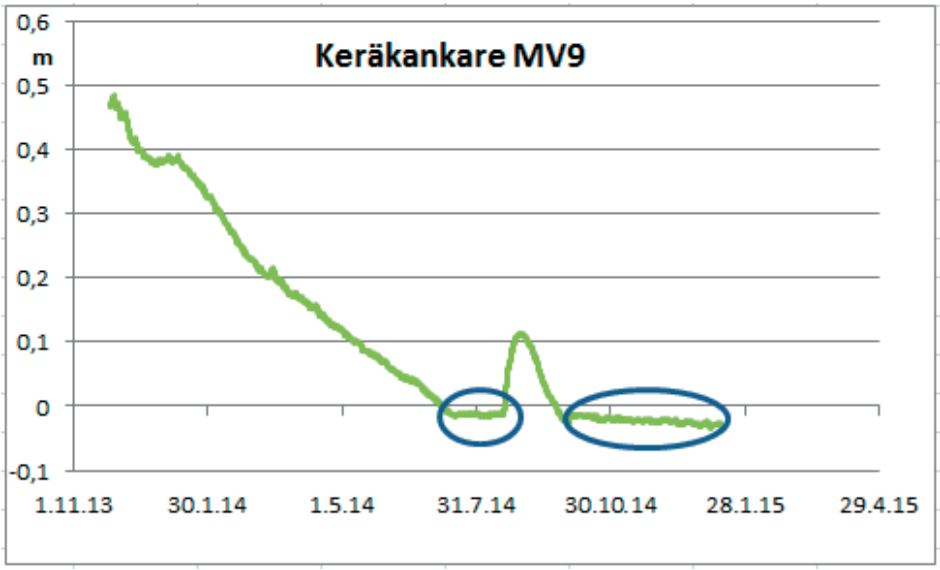

Figure 2. The water table has dropped below the pressure sensors depth.

The automation of groundwater table measurements of the Finnish Environment Institute (hereafter abbreviated as SYKE) uses mainly vented loggers where barometric pressure is compensated with a ventilation cable directly from atmospheric pressure. As groundwater mainly occurs in shallow formations in Finland (generally less than 30 m) (Salonen et al. 2002), there is usually no issue with the cord lengths, which must always be considered in for e.g. Central Europe's karst formations. The effect of air pressure must be compensated when using non-vented sensors with separate barometric instruments. SYKE has experienced problems with separate barometric instruments during winter time as the instruments have frozen. The use of vented sensors is more secure but moisture must be prevented from infiltrating the ventilation cable. The required cable length is calculated with adding the lowest water table + one meter to the difference of between the top of the monitoring tube and the mean groundwater table + two meters. The extra two meters is needed for installing the device to a separate pole next to the monitoring tube. The loggers have a memory capacity for measurements for more than a years time span. Data transfer is mainly through GSM-connections every 1-3 days. The equipment uses solar energy and batteries as power supply. The battery is needed to ensure year-round power especially during the winter months. The pressure sensor is installed at the top of the monitoring tube with a mechanism that can be re-installed precisely at the same height. Accurate re-installment is necessary after maintenance or procedures for water sampling. Validation measurements are mainly done twice a month at manned monitoring stations but infrequently at unmanned stations. Preferably the validation should be done at a minimum of twice a year.

2.2 Measuring groundwater temperature

It is important to case-specifically consider the proper measurement interval. In some cases only one measurement is necessary whereas in others several measurements average is needed to require the needed accuracy. Some digital sensors measure the average of a couple of measurements and save only the average into the data log. When using analogic sensors several measurements should be done and afterwards calculate the average to eliminate ripple effect (Figure 3) and obtain accuracy. All loggers used at SYKE are year-round in daylight saving time (UTC + 2 in Finland) to avoid confusions.

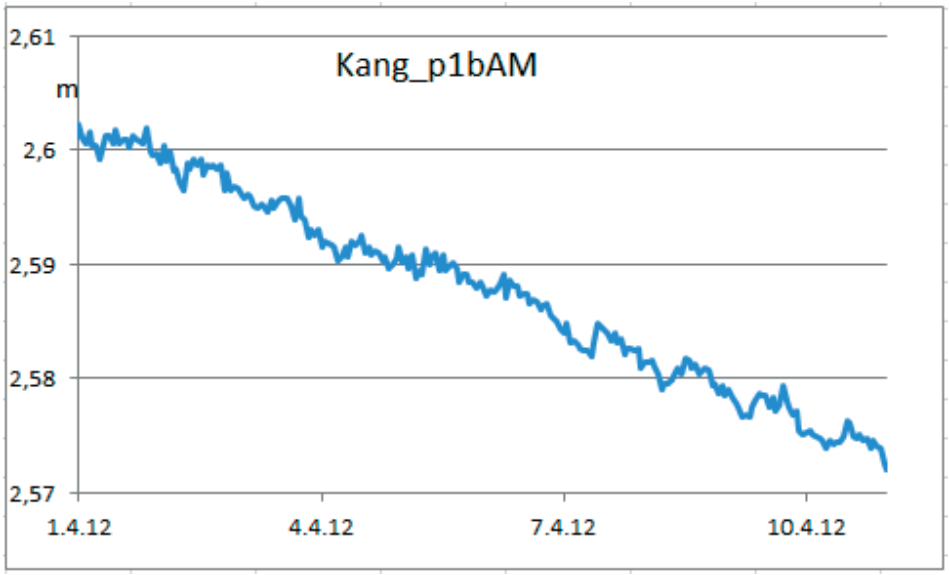

Figure 3. Ripples from separate measurements (analogic sensor).

The temperature of the groundwater is measured either with a water table sensor that has an integrated temperature sensor or with separate temperature sensor. The temperature sensor should be installed at a level between the sieve's range to measure the actual inflowing waters temperature. The installment depth affects the measured temperature of groundwater, the deeper is, the smaller the variation range. The temperature of groundwater can vary in the same monitoring tube as groundwater inflow may occur in several different layers. The hydrogeological cycle of groundwater in Finland is short and the temperatures are highest during winter and coldest during summer (Backman et al. 1999). Some phase transfer also occurs (POVET-database). Sudden changes in groundwater temperature indicate poor installation or lack of proper seal with for e.g. bentonite clay after installment. Spring meltwaters lower and fall or winter downpours raise the temperatures in the monitoring tube as seen in Figure 4 when surface water infiltrates directly by the sides of the tube via the sieve into the monitoring tube. To obtain the temperature profile and the flow of groundwater in the formation it is recommended to measure at several different layers.

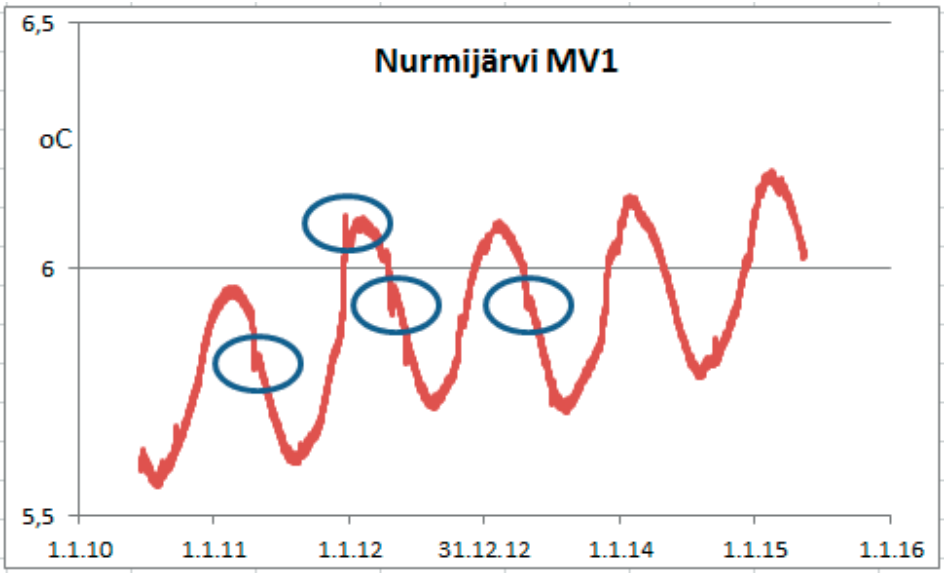

Figure 4. Direct inflow of surface water by the sides of the tube via the sieve into the monitoring tube.

2.3 Experiences of proper trial periods

Automation has been ongoing at some of SYKEs sites for almost a decade but the majority has had them for 2-5 years. Based on these trial periods there is no overall rule that can be given yet. At some sites even five years has not been enough when at others two years has been sufficient. It is important to prolong the trial period until it can be determined if the changes are reliable and representative in the long run.

2.4 Adequate automation at monitoring sites

The groundwater monitoring stations SYKE observes generally have ten installed groundwater tubes, from which an average is calculated. As it is not possible to automate all monitoring tubes different variations have been tried out to case specifically to understand the amount of monitoring devices needed to generate the same average result as manual observations from all ten monitoring tubes. Overall rules cannot be applied and the sufficient trial periods will determine which tubes should be the ones which will be followed in the long-run. In SYKEs experience the basis is generally 3-5 devices to start with and 2-3 "permanently".

2.5 Terrain inventories

Inventories of changes in the terrain at monitoring sites should be updated regularly. Changes in terrain conditions, such as for e.g. tree felling or digging of drainage dikes, affects both groundwater table behavior and causes change in water quality. If trend changes in temperature occur, the inventories aid in investigating if the changes are caused by the terrain modifications or if the effects of climate change is the plausible explanation.

3. RESULTS AND DISCUSSION

Valuable new information on groundwater behavior and characteristics is obtained with continuous measurement of groundwater table and temperature. There are great challenges in collecting any kind of long term data and in maintaining the comparability. Groundwater table measurements are amongst the simplest ones and as presented also has its difficulties. Validation measurements must be done at proper intervals to eliminate the "wandering" of sensor (Figure 5). In some cases, as presented in Figure 6, the pressure sensor is stable but the manual validation measurement is incorrect. As all pressure sensors behave somewhat individually combined with groundwater table quirks, a proper monitoring period must be implemented before determining the correct validation interval.

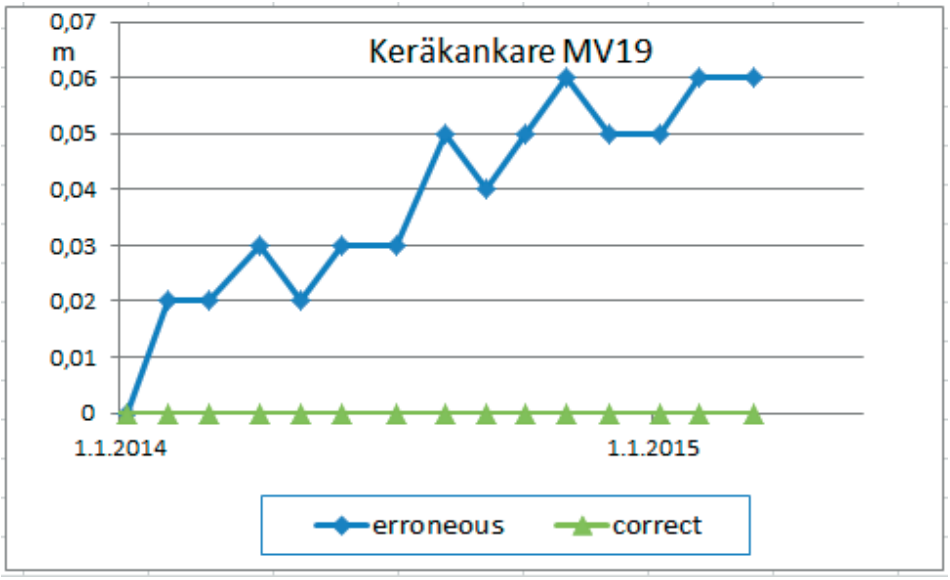

Figure 5. The "wandering" movement of the pressure sensor.

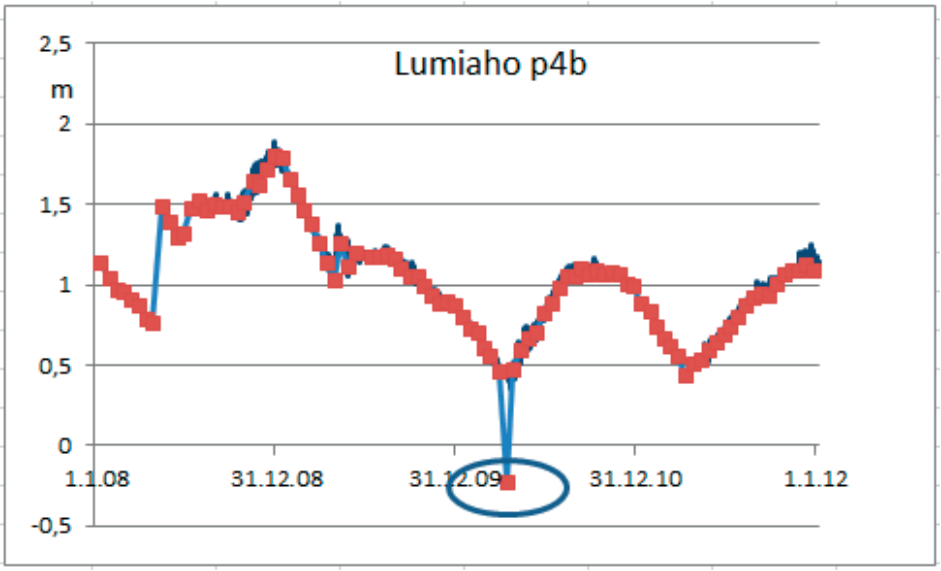

Figure 6. Comparing automated results and manual validation measurements. Here the manual validation value is incorrect.

Temperature sensors that are installed at different depths give a different range of temperature variation. Even the mean temperature may differ in these cases as presented in Figure 7 where the temperature at Kinkelinkangas monitoring tube (Kink_p2) varies in two different behavioral patterns between 4-5 ^{o}C and at a more stagnant 4,5-4,7 ^{o}C . Therefore it is recommended to install two temperature sensors in one monitoring tube.

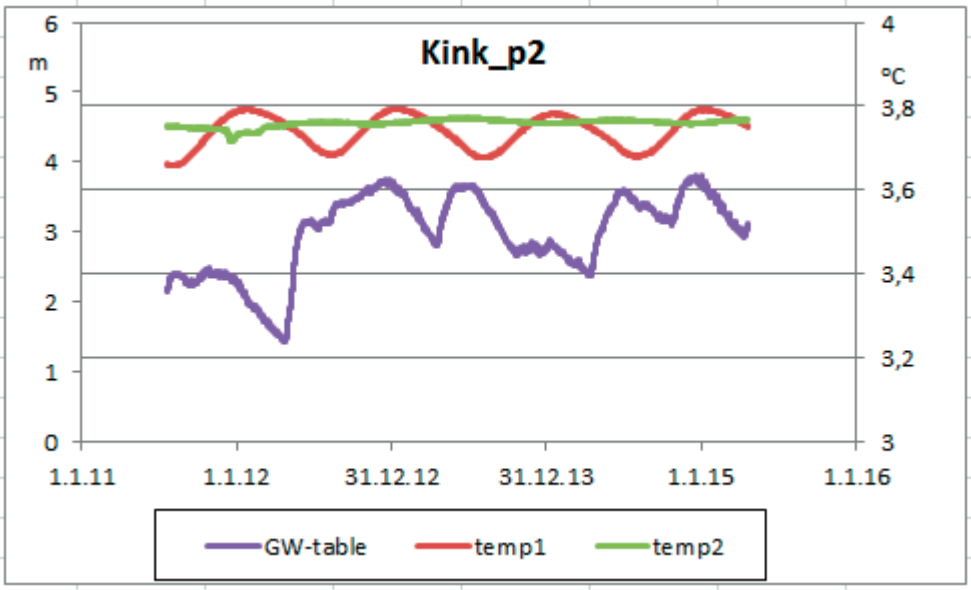

Figure 7. A monitoring tube at Kinkelinkangas (Kink_p2) which is infiltrated with groundwater from two different depths with differing temperatures.

The fall time behavior of water temperature is generally quite symmetrical in short cycled groundwater formations and temperatures are highest in late fall, as seen in the water temperature cycle at the Lehtimäki monitoring site (Figure 8). However, in larger formations with longer hydrogeological cycles, water temperatures are highest in late winter onto early spring (Figure 9).

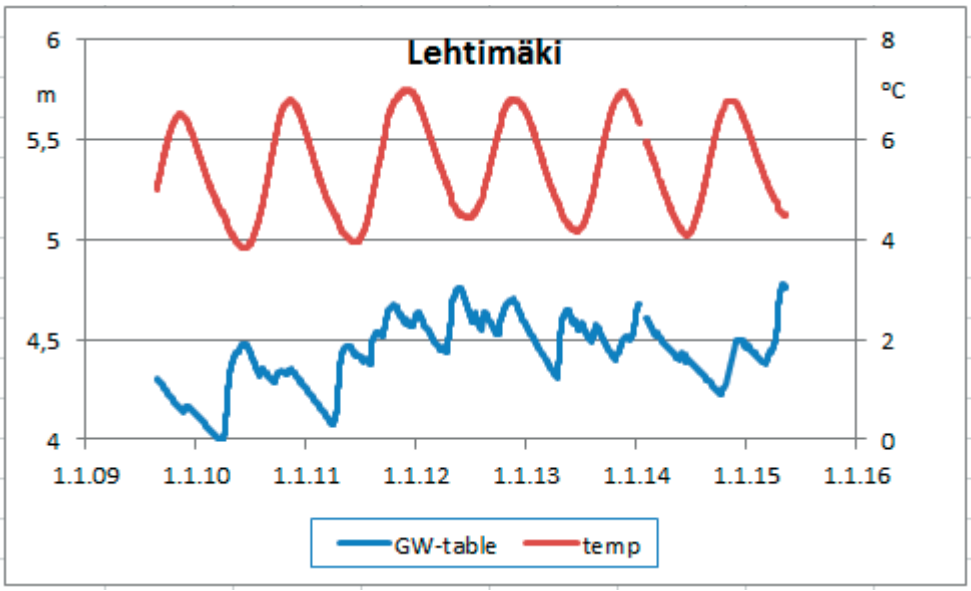

Figure 8. The symmetrical fall time behavior with temperature peaks in a short cycled groundwater formation.

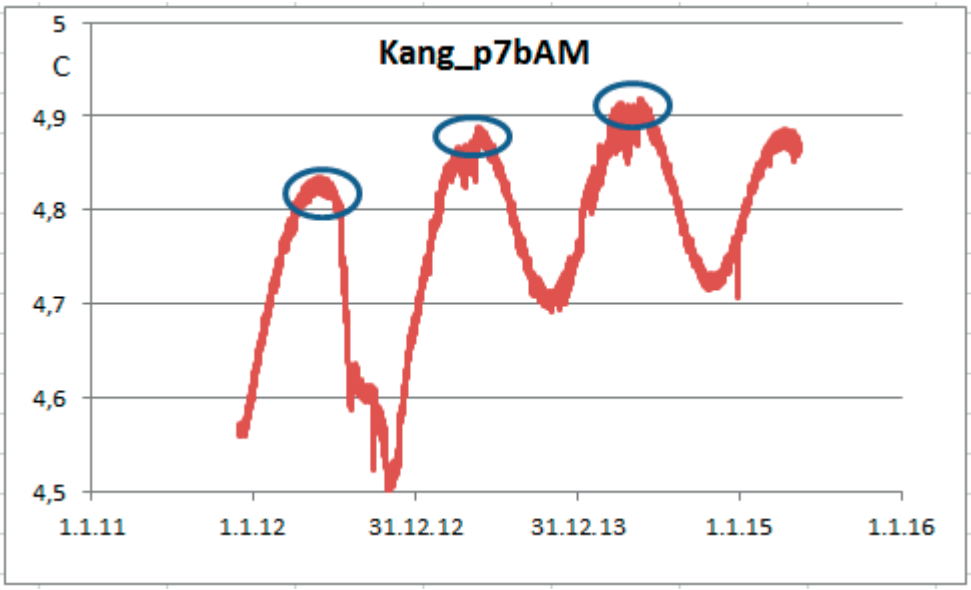

Figure 9. In groundwater formations that have longer hydrogeological cycles, the water temperatures are highest during springtime.

The hydrogeological cycle of groundwater at different depths may have differing temperatures (Figure 7). During warm summers, the solar warming effect in shallow and short cycled groundwater formations is noticeable as the infiltrating warm water raises the water temperature inside the monitoring tube (Figure 10). This natural phenomenon is visible as a gradual linear change in the graph in comparison to the abrupt temperature changes caused by surface water intrusion in poorly installed monitoring tubes presented earlier in Figure 4.

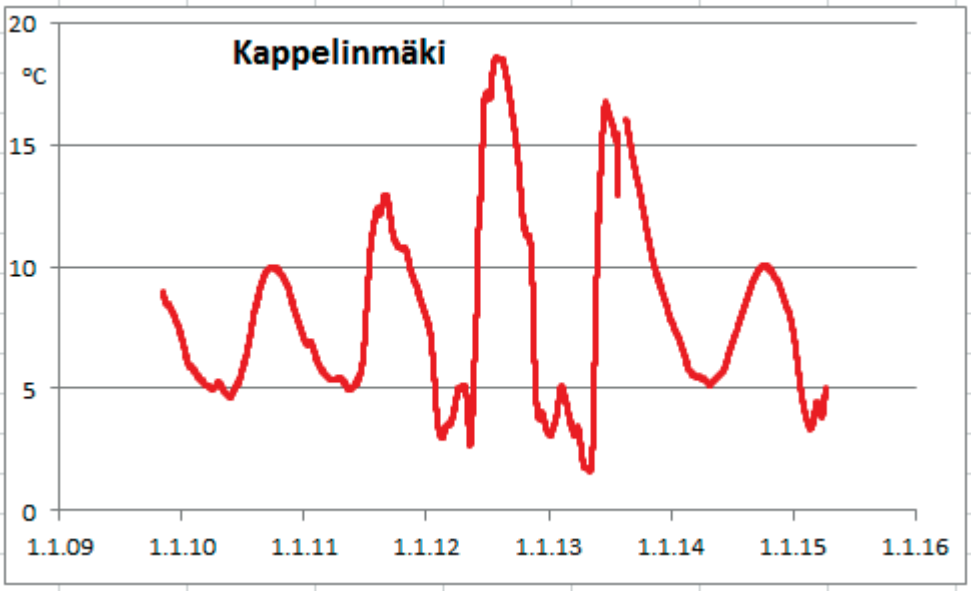

Figure 10. Summertime infiltration of warm water raises the water temperature inside the monitoring tube.

As the climatic conditions vary greatly in the northern and southern parts of Finland it is also visible in groundwater temperatures. The priorly presented figures have all been from Southern or Central Finland where temperatures have generally varied between 4-8 °C. Up north the average temperatures are lower and sink the more northwards you measure. In Figure 11 from Salla, which is located in Northeastern Finland, the annual temperatures during the period of May 2013 to May 2015 varied between 2,5-4,5°C.

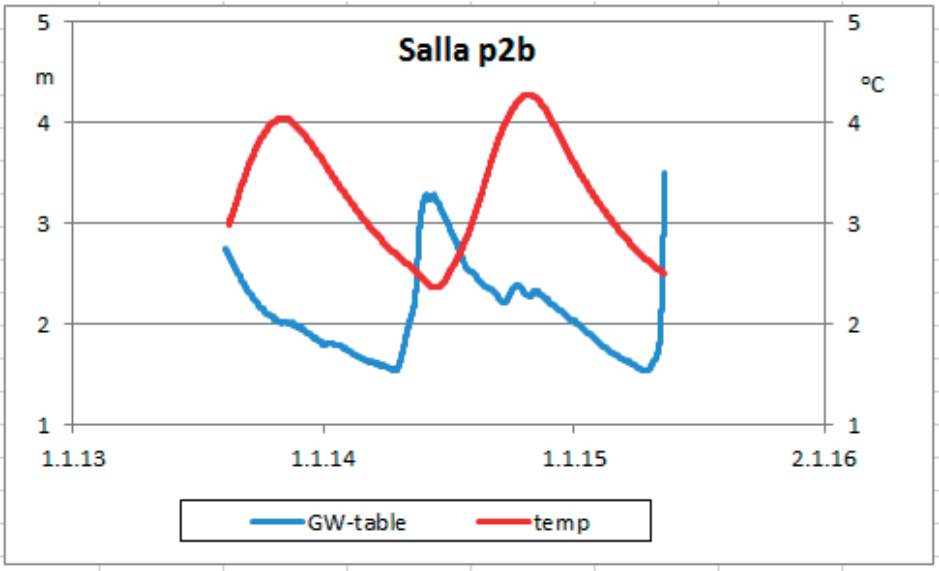

Figure 11. Groundwater table and temperature behavior in Salla in Northeastern Finland where seasonal change and the northern influence is visible.

In many cases, as shown earlier in Figure 4, infiltration of spring meltwater can momentarily lower the temperature of groundwater. As water is most dense (heaviest) at 4 °C (Boehrer and Schultze 2008), change in temperature to near 4°C causes turnover in the monitoring tube (Figure 12).

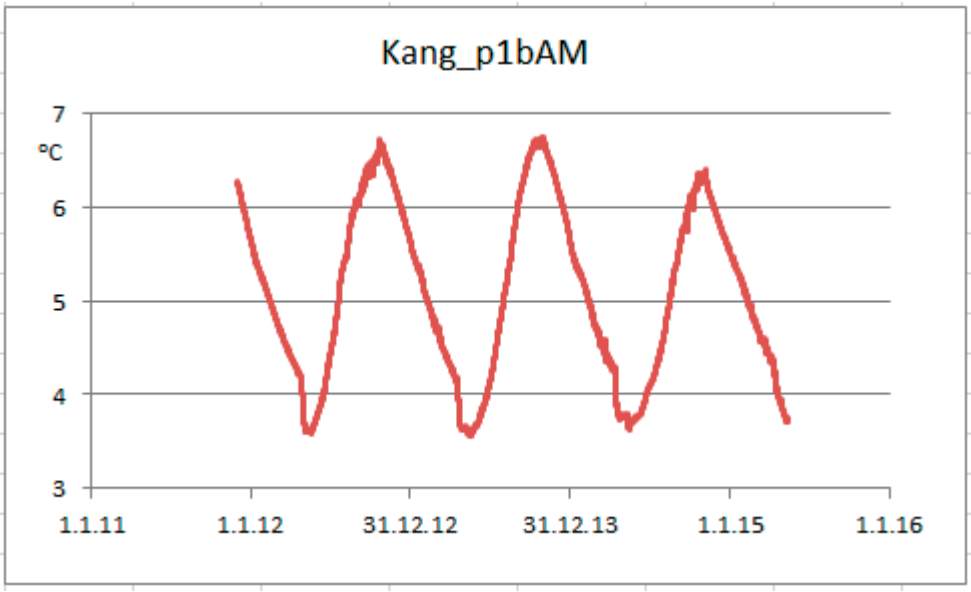

Figure 12. As water is most dense at 4 °C, change in temperature causes turnover in the monitoring tube.

4. CONCLUSIONS

To obtain accurate reliable long-term data in shallow groundwater formations is to use ventilated pressure sensors as they do not require atmospheric calculations. Real-time data transfers every 1-3 days enables the controlling the quality of data and data can directly be saved into data systems (in comparison to manual data feed. Validating measurements must be done with sufficient intervals. Pressure sensors must be installed at the correct level (below LW) to avoid erroneous results and the malfunction or possible break down of the sensor. Proper instalment of the groundwater monitoring tube is crucial to avoid infiltration of water via the sides of the tube.

Temperature measurements are recommended to be monitored at several depths (at least two) to explain the effect of the measurement depth in comparison to water temperatures in the monitoring tube. Inventories of changes in the terrain at monitoring sites should be updated regularly so that the side effects of terrain change can be ruled out when investigating the effects of climate change in for e.g. temperature change trends at the monitoring sites.

5. REFERENCES

Backman, B., Lahermo, P., Väisänen, U., Paukola, T., Juntunen, R., Karhu, J., Pullinen, A., Raino, H. and Tanskanen, H. 1999 *Geologian ja ihmisen toiminnan vaikutus pohjaveteen – Seurantatutkimuksen tulokset vuosilta 1969 – 1996*. Geologian tutkimuskeskus, Espoo.

Boehrer, B. and Schultze, M. 2008 Stratification of lakes. *Reviews of Geophysics.* 46(2).

Soveri, J., Mäkinen, R. and Peltonen, K. 2001 *Pohjaveden korkeuden ja laadun vaihteluista Suomessa 1975 – 1999.* Tummavuoren kirjapaino Oy, Helsinki.

Salonen, V-P., Eronen, M. and Saarnisto, M. 2002 *Käytännön maaperägeologia.* Kirja-Aurora, Turku.

Causes and implications of extreme freeze- and break-up of freshwater ice in Canada

Newton, B.W.* and Prowse, T.D.

Water and Climate Impacts Research Centre, University of Victoria, Victoria BC, V8W 3R4, CANADA
**bwnewton@uvic.ca*

ABSTRACT

Extreme hydroclimatic events are infrequent, high-magnitude phenomena that can have severe geophysical, biological, and socioeconomic impacts. Although extreme weather events are often thought of as discrete incidents, a number of extreme hydroclimatic events are preceded by antecedent conditions that increase the likelihood and/or magnitude of the event. This research evaluates the conditions leading to the generation of two such extreme events in Canada: lake-effect snowfall and river ice jam flooding. Lake-effect snowfall occurs when a cold, dry air mass passes over a sufficiently warm body of water, enhancing evaporation, and producing localized snowfall downwind of the lake. Extreme ice jam flooding can occur during a premature break-up when a pulse of water travels to colder downstream regions with a strong intact ice cover. In the case of lake-effect snowfall, extremely early break-up of ice cover can amplify conditions conducive to the production of lake-effect snowfall by increasing the duration that solar radiation is absorbed, and, thus, the amount of heat that is stored and released during autumn and winter. The antecedent environment conducive to river ice jam flooding includes high freeze-up stage and/or mid-winter break-up. Therefore, autumn and winter climatic and hydrologic conditions influence spring break-up severity. As antecedent conditions strongly influence the generation of cold-regions hydrologic extremes, understanding the temporal sequencing of climatic and hydrologic conditions is fundamental to diagnosing and forecasting extreme events.

KEYWORDS

Cold regions; hydro-climatic extremes; antecedent conditions; freshwater ice

1. INTRODUCTION

Ice and snow are vital components of the hydrologic cycle in cold regions. The properties of frozen and liquid water, including albedo, heat capacity, and latent heat fluxes, are important for terrestrial and aquatic environments, and influence regional to global climate (Callaghan et al., 2011a; Prowse et al., 2011a). Similarly, freshwater ice dynamics are essential to aquatic ecosystems, affecting water temperature, primary productivity, and biogeochemical cycles (Wrona et al., 2005; Lind et al., 2014). Additionally, frozen water storage and release provide a significant contribution to seasonal water resource availability, particularly in mountainous watersheds (Barnett et al., 2005).

A large percentage of Northern Hemisphere land mass is subject to temperatures sufficiently cold to produce substantial freshwater ice and snow cover. Bates and Bilello (1966) and Brooks et al. (2013) used the January 0°C isotherm to delineate Northern Hemisphere cold regions and found that the majority of the land mass north of 40°N is below freezing for a portion of the year. Bennett and Prowse (2010) defined three areas based on the January, winter (Oct-Mar), and annual 0°C isotherms, corresponding to 0.5, 3, and 6 month periods of freezing temperatures, and consequently, the duration and extent of ice covered rivers. They

determined that the majority of Canada is below freezing at least 6 months of the year except for southern regions which are below freezing for 3-6 months.

Extreme hydroclimatic events are, by definition, infrequent, high-magnitude occurrences that can have severe geophysical, biological, and socioeconomic impacts (IPCC, 2012; Coumou and Rahmstorf, 2012). Extreme weather events are often thought of as discrete occurrences, such as anomalously hot or cold air temperatures or high-intensity precipitation (Rahmstorf and Coumou, 2011; Donat et al., 2013). Discrete hydroclimatic extremes occur in cold regions; however, the temporal sequencing of hydroclimatic events, often beginning with the initial crossing of the 0°C isotherm, can provide the antecedent conditions necessary to generate extreme events even when the trigger itself is not extreme. This paper will focus on two such cold-regions hydrologic extremes: lake-effect snowfall and river ice break-up.

2. LAKE EFFECT SNOWFALL

There is a strong interaction between the thermal regime and seasonal ice cover of mid- and high-latitude lakes and the local-regional climate (Rouse et al., 2008a; Brown and Duguay, 2010). However, given the differences in heat capacities between air, water, and land surfaces, there is a considerable lag, depending on the size of the lake, between seasonal changes in air and water temperature. Lake-effect snowfall can cause considerable snow accumulation downwind of a medium-large lake in a relatively short period of time (Niziol et al., 1995; Kunkel et al., 2002; Liu and Moore, 2004), and can have profound socioeconomic and hydrologic impacts including transportation, recreation, infrastructure damage (Kunkel et al., 2000), and high soil moisture leading to flooding during snowmelt (Burnett et al., 2003). A number of conditions are necessary to produce lake-effect snowfall, and much of our current knowledge results from extensive studies of lake-effect snowfall in the Laurentian Great Lakes region.

The fundamental requirement for the production of lake-effect precipitation is a sufficient temperature gradient between the surface water and overlying air mass (Lavoie, 1972; Niziol et al., 1995), and when the boundary layer air temperature below 0°C precipitation is solid (Miner and Fritsch 1997). Atmospheric circulation typically associated with sufficiently cold air masses to produce lake-effect snow is characterized by meridional flow of cold, dry Arctic air (Kunkel et al. 2002). The temperature gradient between the warm lake and cold, dry air mass enhances evaporation, which rises and condenses, then falls as snow, often heavy and dense, as it travels over the relatively cold land surface downwind of the lake (Blanken et al., 2000; Blanken et al., 2008). Several studies have quantified minimum air temperature gradients; however, these values appear to be site or situation specific. For example, a minimum air temperature gradient of 13°C was found for the Laurentian Great Lakes (Holroyd, 1971; Niziol, 1987), except when the ambient air temperature was between -10°C and 0°C, in which case a gradient of 7°C was sufficient (Kunkel et al. 2002). Similarly, Alcott et al. (2012) reported a minimum temperature difference of 12.4°C was necessary to produce lake-effect snow over Great Salt Lake, with most events occurring with a 16°C temperature difference. Temperature gradient thresholds are unknown for other cold regions including Northern Canada.

To pick up enough moisture to produce a lake-effect snowstorm, the water body must have a long fetch (Niziol et al., 1995). Therefore, for narrow lakes the wind must be parallel or nearly parallel to the long axis (Laird et al., 2003a; Holroyd, 1971). Conversely, large lakes with a broad length and width or irregular shape have sufficient fetch in nearly any direction to produce lake-effect snow. Additionally, the presence of multiple water bodies, or upwind

lakes, enhances the volume of atmospheric moisture (Vavrus et al., 2013). The intensity and location of lake-effect snow is also influenced by wind speed (Laird et al. 2003b), shoreline topography (Wright et al., 2013), and terrestrial topographic gradient (Lavoie, 1972; Niziol 1987; Hjelmfelt 1992). Water evaporated from lakes surrounded by extensive regions of low relief, such as Great Slave Lake, may travel a fair distance before precipitation occurs (Szeto, 2002).

The ice-free period of a lake can be divided into two thermally- and atmospherically-driven phases: the period between initial break-up of lake ice and peak lake heat storage, and between peak heat storage and freeze-up of lake ice. During the first phase, available energy is used to warm the lake and the overlying atmosphere is warmer than the lake, leading to stable atmospheric conditions (Rouse et al., 2003; Rouse et al., 2008b). Conversely, during the second phase, the lake acts as a heat source (Rouse et al., 2008b), evaporation is high (Blanken et al., 2003), and the overlying atmosphere is cooler than the lake, resulting in unstable conditions (Miner and Fritsch, 1997). This produces an environment conducive to lake-effect precipitation, particularly just prior to freeze-up when evaporation peaks (Blanken et al., 2003).

The spring ablation of lake ice cover is largely controlled by air temperature (Rouse et al., 2008b). Given the north-south temperature gradient, break-up timing is also strongly related to latitude (Weyhenmeyer et al., 2011). The amount of heat absorbed is dependent upon the lake depth (Oswald and Rouse, 2004; Korhonen, 2006) and angle of solar incidence (Brown and Duguay, 2010). Furthermore, the length of time it takes a lake to heat up is proportional to the size of the lake (Rouse et al., 2005). Freeze-up is a function of heat absorption and storage during the open water season (Brown and Duguay, 2010); therefore, freeze-up is correlated with the timing of break-up, particularly for high-latitude lakes (Blanken et al., 2003; Rouse et al., 2008b). The presence of ice on the lake reduces the overwater fetch and heat flux is dramatically decreased when ice concentration exceeds 70% (Gerbush et al., 2008). However, partial or fractured ice cover can provide sufficient heat flux from the water surface to the atmosphere to generate a lake-effect snowstorm (Niziol, 1987; Kunkel et al., 2002; Wright et al., 2013).

Large, deep lakes absorb more energy, retain heat longer, and freeze-up later than smaller lakes (Oswald and Rouse, 2004; Rouse et al., 2005). For example, the average ice free period on Great Slave Lake is between mid-June and late-November, and lake shifts from being a heat sink to a heat source at the end of August (Rouse et al., 2008a). A small, shallow lake in the same region has an ice-free period of early-June through late-September with no distinct shift between warming and cooling as it responds very rapidly to changes in ambient air temperature (Rouse et al., 2008a). Additionally, the length and interannual variability of the ice-free season decrease with increasing latitude (Rouse et al., 2008a; Weyhenmeyer et al., 2011). Lakes at lower latitudes, including the Laurentian Great Lakes, reach maximum ice extend in February-March; however, they typically do not become fully ice covered, and ice covered area exhibits considerable interannual variability (Wang et al., 2012).

Concern has been raised over changing ice regimes of mid- and high-latitude lakes, with implications for increased autumn-winter evaporation and lake-effect snowfall (Prowse et al., 2011b). Trend analysis has indicated an increase in the frequency of lake-effect snowfalls in the Laurentian Great Lakes region (Ellis and Johnson, 2004; Norton and Bolsegna, 1993) associated with increasing water surface temperature and decreasing ice cover extent (Assel et al., 2003). Additionally, Kunkel et al. (2009) found that an increase in atmospheric circulation patterns conducive to cold air outbreaks also contributed to the positive trend. Wright et al. (2013) modelled ice cover over the Laurentian Great Lakes and found that

removing the ice cover and increasing the lake temperature increased the frequency and magnitude of lake-effect snow as well as the overall snowfall in the region surrounding the lakes. Decreasing trends in high-latitude lake ice duration (Duguay et al., 2006; Latifovic and Pouliot, 2007) may have implications for energy flux and lake-effect snowfall.

3. RIVER ICE BREAK-UP

Ice jams are responsible for some of the most extreme flooding in cold regions (Beltaos and Prowse, 2001; Prowse and Beltaos, 2002), can cause extensive erosion and redistribution of sediment (Prowse and Culp, 2003; Beltaos 2008b), affecting ecosystem structure and function (Prowse 2001). Additionally, ice jams and flooding damage infrastructure (Van Der Vinne et al. 1991) and affect the generation of hydroelectricity (Timalsina et al. 2015). These events are often sudden; with a rapid rise in stage behind the ice jam and a surge of water and ice following ice jam release (Beltaos and Prowse, 2001). Unlike open-water flooding, ice jam-induced increases in stage occur without a proportional increase in discharge (Gray and Prowse, 1993; de Rham et al. 2008). Additionally, the flood levels associated with ice jams have a lower recurrence interval than open water floods (Beltaos and Prowse, 2001; Prowse and Beltaos, 2002). Therefore, river ice is one of the most important factors in cold regions hydrologic extremes.

River ice formation and break-up are highly correlated with air temperature (Prowse and Beltaos, 2002). Rivers located in regions where the temperature is below freezing for 6 months of the year are known for lengthy ice covered seasons and some of the most dramatic break-up events (Prowse, 1986; Kowalczyk Hutchison and Hicks, 2007; de Rham et al., 2008; Beltaos, 2008a,b). During the freeze-up process a portion of river flow is abstracted and held in frozen or hydraulic storage, which contributes to flow during the melt period (Prowse and Carter, 2002; Beltaos and Prowse, 2009). Additionally, during the cold season, snow accumulation increases the volume of water held in frozen storage until the spring melt season.

The break-up of river ice can be classified as thermal or mechanical; however, break-up is typically the product of both thermodynamic and hydrodynamic processes (Beltaos and Prowse, 2001; Beltaos, 2003). Over time, the driving forces increase and the resisting forces decrease until the break-up occurs. In a purely thermal (overmature) break-up, thermodynamic processes dominate and resisting forces diminish without a substantial increase in driving forces (Beltaos, 2008a), and the process is similar to that of lake ice break-up (Gray and Prowse, 1993). Conversely, a purely mechanical break-up occurs when driving forces increase to the point where they exceed maximum resisting forces (Beltaos, 2008a), often resulting in high flood stage (Beltaos, 2008b; de Rham et al., 2008). Furthermore, the ice cover on a river can break up sequentially, progressively breaking up downstream, or non-sequentially, with long sections of open water between areas of intact ice cover (Prowse, 1986; Prowse and Marsh, 1989).

During spring as the temperatures rise and the angle of solar declination increases, river ice cover begins to deteriorate (Prowse and Marsh, 1989). Initially, radiation is used to raise the temperature of the ice cover. Once it becomes 0°C isothermal, the ice cover begins to melt (Prowse et al., 1990a; Gray and Prowse, 1993). During these processes the strength of the ice cover decreases (Prowse et al., 1990b); however, the thickness of the ice sheet can be unaffected (Gerard, 1990). As the strength of the ice cover decreases, the ability of the spring flood wave to easily pass through without jamming increases (Prowse and Demuth, 1993). Deterioration can also occur on the underside of the ice sheet when heat from the moving

water induces melt (Gray and Prowse, 1993). This can be an important process in non-sequential break-ups with long stretches of open water, leading to considerable differences in water temperature between the open water and edge of the ice cover (Parkinson, 1982; Marsh and Prowse, 1987). Thermal break-up often occurs when spring temperatures are mild and the combination of slow snowmelt and little or no rainfall produce low runoff (Gray and Prowse, 1993; Beltaos, 2003).

Mechanical break-up is often associated with a large, rapid spring pulse onset driven by high-intensity snowmelt, and in some cases heavy rainfall (Gray and Prowse, 1993). When the spring freshet is anomalously early, the river ice cover lacks thermal deterioration (Beltaos, 2003). The spring flood wave reaches an area with a hydraulically strong, intact ice cover that may still be attached to the bed and banks (Prowse et al., 1990a). Water backs up behind the jam, often spilling over the banks and flooding the surrounding area. Water held in hydraulic storage is released once the jam breaks, creating a surge of water commonly referred to as a "jave" (Beltaos, 2007; Jasek and Beltaos, 2008) causing a rapid increase in stage and amplification of hydrodynamic forces downstream of the jam release (Beltaos and Prowse, 2001). The surge of floodwater, ice fragments, and ice sheets travel downstream until it is obstructed by a strong intact ice cover where the ice can be incorporated into a new jam (Jasek, 2003). However, the powerful force of the jave can trigger downstream ice jam releases (Beltaos, 2007).

Extreme flooding is associated with high backwater storage and the release of a hydraulically strong ice jam. For example, ice jam release waves of up to 4.3m have been reported on the lower Athabasca River, an area of frequent ice-jam flooding (Kowalczyk Hutchison and Hicks, 2007). However, measurements of ice jam surges are difficult to record (Hicks and Beltaos, 2008; Hicks, 2009). During a sequential break-up, the ice jams and releases multiple times in a relatively short succession, and can cause serious flooding in numerous areas along the river (Marsh and Prowse, 1987). For non-sequential breakups, the ice run can travel a long distance downstream until it is impeded (Jasek, 2003; Jasek and Beltaos, 2008).

Numerous factors influence the timing and magnitude of break-up that occurs at various points along a river. The degree of hydraulic strength of an ice cover, and thus the amount of backwater storage, is a function of the river bed and ice cover roughness and thickness (Prowse and Beltaos, 2002; Beltaos, 2008b). White ice, produced by the agglomeration of frazil ice or by slushing on the ice surface, are rougher and more resistant to thermal decay than black ice (Gerard, 1990). Although ice jams can occur at any point along the river, certain areas are more susceptible due to changes in flow velocity, such as changes in slope or width, bends or curves, or at the confluence with a tributary (Gray and Prowse, 1993; Beltaos, 2003; Beltaos, 2008a). Additionally, temperature gradient along the length of the river is an important factor in mechanical break-up and ice jam formation. The most severe break-up events tend to be driven by high-intensity snowmelt in a relatively warm upstream area producing a flood wave that travels to colder downstream areas (Prowse and Marsh, 1989; Beltaos, 2008a).

Although the type of break-up and the location and severity of ice jam flooding is unpredictable, antecedent conditions during autumn-winter freeze-up can contribute to spring break-up processes. In particular, freeze-up discharge and stage can increase or decrease the probability of the frequency and severity of an ice jam. For example, low stage and discharge during freeze-up coupled with a low-moderate spring runoff can lead to a mechanical break-up of moderate severity (Beltaos and Prowse, 2001; Beltaos, 2008a). Conversely, high stage and discharge during freeze-up coupled with a low-moderate spring runoff leads to a thermal break-up (Beltaos and Prowse, 2001; Beltaos, 2008a). The most severe, damaging, and highly

dangerous mechanical break-up and associated flooding is produced when high freeze-up stage is coupled with high spring runoff (Beltaos and Prowse, 2001). In this case, backwater storage is high, and the ice jam release surge is high. Therefore, high precipitation during the autumn-winter freeze-up period and high winter snow accumulation and/or high-intensity spring snowmelt in a relatively warm upstream region can produce the most severe ice jam flooding.

Thus far, this review has focused on spring break-up; however, in temperate and Maritime regions, winter temperatures rising above freezing and/or rain-on-snow events can trigger a mid-winter break-up (Prowse et al., 1990b; Beltaos, 2002; Beltaos and Prowse, 2001). Mid-winter break-ups lack the thermal decay processes that occur during spring; therefore, the ice cover is typically strong and intact and the resulting break-up is mechanical (Beltaos, 2002; Beltaos, 2003). Mid-winter thaws can trigger a break-up and increase stage. The fragmented ice refreezes, resulting in an ice cover that is thicker and rougher, and increasing the hydraulic strength of the ice cover (Beltaos, 2002). However, if the mid-winter melt is large enough to reduce the magnitude of the surrounding snowpack, the potential for high hydrodynamic forces during the spring melt is decreased (Beltaos, 2008c).

4. SUMMARY

Often the greatest impact to geophysical, biological, and socioeconomic systems occur during extreme hydroclimatic events. Although extreme events can be short-term discrete occurrences, the cumulative effects of a number of weather events and interactions between solid and liquid water and the surrounding environment can result in the generation of hydroclimatic extremes, even when the event trigger itself is not considered extreme. The extreme events described in this paper occur or are amplified by the temporal sequencing of events that provide the antecedent conditions necessary to produce an extreme event.

Freshwater ice is an integral component of the local to regional climate and hydrology. Air temperature plays a strong role in seasonal ice cover freeze- and break-up, and concern has been raised over increasing mid- and high-latitude temperatures and decreasing ice cover duration (Magnuson et al., 2000; Duguay et al., 2006; Latifovic and Pouliot, 2007; von de Wall, 2011). Decreased lake ice cover duration and, consequently, increased open water season, has implications for regional energy and moisture balance (Rouse et al., 2008a; Brown and Duguay, 2010), and the generation of lake-effect snowfall (Assel et al., 2003; Prowse et al., 2011b). Increasing spring temperatures, particularly when strong regional variability exists, increases the risk of premature mechanical break-up (Beltaos and Prowse, 2001; Beltaos, 2008b). Furthermore, winter warming events leading to mid-winter break-ups can amplify the risk of a severe spring break-up (Beltaos, 2002; Beltaos, 2003).

This review has provided evidence for the importance of antecedent conditions and the temporal sequencing of hydro-climatic events that generate two cold regions hydrologic extremes, lake-effect snowfall and river ice break-up. Evidence suggests the frequency of discrete extreme events may be increasing (Rahmstorf Coumou, 2011; Donat et al., 2013), and it is essential to determine what role these discrete events play in the generation of cold regions hydrologic extremes. Future research needs includes evaluating discrete extremes within the realm of temporal sequencing, to assess whether they increase/decrease the risk of lake-effect snowfall and extreme river ice break-up.

5. REFERENCES

Alcott, T.I., Steenburgh, W.J., & Laird, N.F. 2012 Great Salt Lake-effect precipitation: Observed frequency, characteristics, and associated environmental factors. *Weather Forecast* 27, 954-971

Assel R.A., Cronk K., & Norton D. 2003 Recent trends in Laurentian Great Lakes ice cover. *Climatic Change* 57,185–204.

Barnett, T.P., Adam, J.C., & Lettenmaier, D.P. 2005 Potential impacts of a warming climate on water availability in snow-dominated regions. *Nature* 438(7066), 303-309.

Bates, R.E. & Bilello, M.A. 1966 Defining the cold regions of the Northern Hemisphere. USA CRREL Technical Report 178, 11p

Beltaos S. 2003 Threshold between mechanical and thermal breakup of river ice cover. *Cold Reg Sci Technol* 37, 1-13

Beltaos, S. & Prowse, T.D. 2001 Climate impacts on extreme ice-jam events in Canadian rivers, *Hydrolog Sci J* 46(1), 157-181

Beltaos, S. 2002 Effects of climate on mid-winter ice jams. *Hydrol Process* 16, 789-804.

Beltaos, S. & Burrell, B.C. 2005 Field measurements of ice-jam-release surges. *Can J Civil Eng* 32(4), 699-711.

Beltaos, S. 2007 The role of waves in ice-jam flooding of the Peace-Athabasca Delta. *Hydrol Process*, 21(19), 2548-2559.

Beltaos, S. 2008a Onset of breakup. In River ice breakup, ed. Beltaos,S., 167–206. Highlands Ranch: Water Resources Publications.

Beltaos, S. 2008b Ice jams. In River ice breakup, ed. Beltaos,S., 207–246. Highlands Ranch: Water Resources Publications.

Beltaos, S. 2008c Progress in the study and management of river ice jams. *Cold Reg Sci Technol* 51(1), 2-19.

Beltaos, S., Ismail, S., & Burrell, B.C. 2003. Midwinter breakup and jamming on the upper Saint John River: a case study. *Can J Civil Eng* 30(1), 77-88.

Beltaos, S., & Prowse, T. 2009 River-ice hydrology in a shrinking cryosphere. *Hydrol Process*, *23*(1), 122-144.

Bennett K.E. & Prowse T.D. 2010 Northern Hemisphere geography of ice-covered rivers. *Hydrol Process* 24: 235-240

Blanken, P.D., Rouse, W.R., Culf, A.D., Spence, C., Boudreau, L.D., Jasper, J.N.,…Verseghy, D. 2000 Eddy covariance measurements of evaporation from Great Slave Lake, Northwest Territories, Canada. *Water Resour Res* 36(4), 1069-1077

Blanken, P.D., Rouse, W.R., and Schertzer, W.M. 2003 Enhancement of evaporation from a large Northern lake by entrainment of warm, dry air. *J Hydrometeorol* 4, 680-693.

Blanken, P., Rouse, W.R., & Schertzer, W. 2008 The time scales of evaporation from Great Slave Lake. In *Cold region atmospheric and hydrologic studies. The Mackenzie GEWEX experience Volume 2: Hydrologic Processes* (pp. 181-196). Springer Berlin Heidelberg

Brooks, R.N., Prowse, T.D., & O'Connell, I.J., 2013 Quantifying Northern Hemisphere freshwater ice. *Geophys Res Lett* 40,1128-1131

Brown, L.C. & Duguay, C.R. 2010 The response and role of ice cover in lake-climate interactions. *Prog Phys Geog* 34(5) 671-704

Burnett, A.W., Kirby, M.E., Mullins, H.T., & Patterson, W.P. 2003 Increasing Great Lake-Effect snowfall during the twentieth century: A regional response to global warming? *J Climate* 16, 3535-3542

Callaghan, T.V., Johansson, M., Key, J., Prowse, T., Ananicheva, M., & Klepikov, A. 2011a Feedbacks and interactions: From the arctic cryosphere to the climate system. *Ambio* 40(1), 75-86

Cordeira, J.M. & Laird, N.F. 2008 The influence of ice cover on two lake-effect snow events over Lake Erie. *Mon Weather Rev* 136, 2747-2763

Coumou, D., & Rahmstorf, S. 2012 A decade of weather extremes. *Nature Climate Change*, *2*(7), 491-496.

de Rham LP, Prowse TD, Beltaos S, & Lacroix MP. 2008 Assessment of annual high-water events for the Mackenzie River basin, Canada. *Hydrol Process* 22, 3864-3880.

Donat, M.G., Alexander, L.V., Yang, H., Durre, I., Vose, R., Dunn, R.J.H.,… Kitching, S. 2013 Updated analyses of temperature and precipitation extreme indices since the beginning of the twentieth century: The HadEX2 dataset. *J Geophys Res-Atmos* 118(5), 2098-2118

Duguay C.R., Prowse T.D., Bonsal B.R., Brown R.D., Lacroix M.P., & Menard P. 2006 Recent trends in Canadian lake ice cover. *Hydrol Process* 20,781-801

Ellis A.W. & Johnson J.J. 2004 Hydroclimatic analysis of snowfall trends associated with the North American Great Lakes. *J Hydrometeorol* 5,471–486

Gerard R. 1990 Hydrology of floating ice. In Northern Hydrology, Canadian Perspectives, Prowse T.D., Ommanney C.S.L. (eds). NHRI Science Report No. 1, National Hydrology Research Institute, Environment Canada: Saskatoon; 103–134

Gerbush, M.R., Kristovich, D.A.R., & Laird, N.F. 2008 Mesoscale boundary layer and heat flux variations over pack ice-covered Lake Erie. *J Appl Meteorol Clim* 47, 668-682

Gray, D.M., Prowse, T.D., 1993 Snow and floating ice. In: Maidment, D. (Ed.), Handbook of Hydrology. McGraw-Hill, New York, pp. 7.1–7.58

Hicks, F., & Beltaos, S. 2008 River ice. In *Cold Region Atmospheric and Hydrologic Studies. The Mackenzie GEWEX Experience* (pp. 281-305). Springer Berlin Heidelberg.

Hicks, F. 2009 An overview of river ice problems: CRIPE07 guest editorial. *Cold Reg Sci Technol*, 55(2), 175-185.

Hjelmfelt, M.R. 1992 Orographic effects in simulated lake-effect snowstorms over Lake Michigan. *Mon Weather Rev* 120, 373-377

Holroyd III, E.W. 1971 Lake-effect cloud bands as seen from weather satellites. *J Atmos Sci* 28(7), 1165-1170.

IPCC 2012 Summary for Policymakers. In: Managing the Risks of Extreme Events and Disasters to Advance Climate Change Adaptation [Field, C.B., Barros, V., Stocker, T.F., Qin, D., Dokken, D.J., Ebi, K.L.,… Midgley, P.M. (eds.)]. A Special Report of Working Groups I and II of the Intergovernmental Panel on Climate Change. Cambridge University Press, Cambridge, UK, and New York, NY, USA, pp. 3-21

Jasek, M. 2003 Ice jam release surges, ice runs, and breaking fronts: field measurements, physical descriptions, and research needs. *Can J Civil Eng* 30(1), 113-127.

Jasek, M. & Beltaos, S. 2008 Ice-jam release: Javes, ice runs and breaking fronts. In River ice breakup, ed. Beltaos,S., 247–303. Highlands Ranch: Water Resources Publications.

Korhonen, J. 2006 Long-term changes in lake ice cover in Finland. *Nord Hydrol* 37(4-5), 347-363

Kowalczyk Hutchison, T., & Hicks, F.E. 2007 Observations of ice jam release waves on the Athabasca River near Fort McMurray, Alberta. *Can J Civil Eng* 34(4), 473-484.

Kunkel K.E., Ensor L., Palecki M., Easterling D., Robinson D., Hubbard K.G., & Redmond, K. 2009 A new look at lake- effect snowfall trends in the Laurentian Great Lakes using a temporally homogeneous data set. *J Great Lakes Res* 35, 23–29.

Kunkel, K.E., Westcott, N.E., & Kristovich, D.A.R. 2002 Assessment of Potential Effects of Climate Change on Heavy Lake-Effect Snowstorms Near Lake Erie. *J Great Lakes Res* 28(4), 521-536

Kunkel, K.E., Wescott, N.E., & Kristovich, D.A. 2000 Climate change and lake-effect snow. *Preparing for a Changing Climate: The Potential Consequences of Climate Variability and Change*, 25-28.

Laird, N.F., Walsh, J.E., & Kristovich, D.A.R. 2003a Model simulations examining the relationship of lake-effect morphology to lake shape, wind direction, and wind speed. *Mon Weather Rev* 131, 2102–2111.

Laird, N.F., Kristovich, D.A.R., & Walsh, J.E. 2003b Idealized model simulations examining the mesoscale structure of winter lake-effect circulations. *Mon Weather Rev* 131, 206–221.

Laird, N.F. & Kristovich, D.A.R. 2004 Comparison of observations with idealized model results for a method to resolve winter lake-effect mesoscale morphology. *Mon Weather Rev* 132, 1093–1103.

Latifovic, R. & Pouliot, D. 2007 Analysis of climate change impacts on lake ice phenology in Canada using the historical satellite data record. *Remote Sens Environ* 106, 492-507

Lavoie, R.L. 1972 A mesoscale numerical mode of lake-effect storms. *J Atmos Sci* 29, 1025-1040

Lind, L., Nilsson, C., Polvi, L.E. & Weber, C. 2014 The role of ice dynamics in shaping vegetation in flowing waters. *Biol Rev* 89,791–804

Liu, A.Q. & Moore, G.W.K. 2004 Lake-effect snowstorms over southern Ontario, Canada, and their associated synoptic-scale environment. *Mon Weather Rev* 132, 2595-2609

Magnuson, J.J., Robertson, D.M., Benson, B.J., Wynne, R.H., Livingstone, D.M., Arai, T., ... & Vuglinski, V.S. 2000 Historical trends in lake and river ice cover in the Northern Hemisphere. *Science*, *289*(5485), 1743-1746.

Marsh, P. & Prowse, T.D. 1987 Water temperature and heat flux at the base of river ice covers. *Cold Reg Sci Technol* 14, 33-50

Miner, T.J. & Fritsch, J.M. 1997 Lake-effect rain events. *Mon Weather Rev* 125, 3231-3248

Niziol, T.A. 1987 Operational forecasting of lake-effect snowfall in western and central New York. *Weather Forecast* 2,310–321

Niziol, T.A., Snyder, W.R., & Waldstreicher, J.S. 1995 Winter weather forecasting throughout the Eastern United States. Part IV: Lake effect snow. *Weather Forecast* 10, 61-77

Norton D.C. & Bolsegna S.J. 1993 Spatiotemporal trends in lake effect and continental snowfall in the Laurentian Great Lakes, 1951–1980. *J Climate* 6, 1943–1956

Oswald, C.J. & Rouse, W.R. 2004 Thermal characteristics and energy balance of various-size Canadian Shield lakes in the Mackenzie River Basin. *J Hydrometeorol* 5, 129-144

Parkinson, F.E. 1982 Water temperature observations during break-up on the Liard-Mackenzie river system. Proc. Workshop on hydraulics of ice covered rivers, NRCC, Edmonton, Alberta, 261-295

Prowse T.D. & Culp J.M. 2003 Ice breakup: a neglected factor in river ecology. *Can J Civil Eng* 30, 128–144.

Prowse T.D. & Beltaos S. 2002 Climatic control of river-ice hydrology: A review. *Hydrol Process* 16, 805-822.

Prowse T.D. & Carter T. 2002 Significance of ice-induced storage to spring runoff: A case study of the Mackenzie River. *Hydrol Process* 16(4), 779–788.

Prowse, T.D. 1986 Ice jam characteristics, Liard-Mackenzie rivers confluence. *Can J Civil Eng* 13(6), 653-665.

Prowse, T.D. 2001 River-ice ecology. II: Biological aspects. *J Cold Reg Eng* 15(1), 17-33.

Prowse, T., Alfredsen, K., Beltaos, S., Bonsal, B., Duguay, C., Korhola, A.,… Weyhenmeyer, G.A. 2011a Arctic freshwater ice and its climatic role. *Ambio*, *40*(1), 46-52.

Prowse, T., Alfredsen, K., Beltaos, S., Bonsal, B., Duguay, C., Korhola, A.,… Weyhenmeyer, G. 2011b Changing lake and river ice regimes: Trends, effects and implications. In *Snow, Water, Ice and Permafrost in the Arctic (SWIPA)*, Arctic Monitoring and Assessment Programme (AMAP), Oslo

Prowse, T.D., Chew, H.A.M., & Demuth, M.N. 1990b The deterioration of freshwater ice due to radiation decay. *J Hydraul Res* 28(6), 685-697

Prowse, T.D., Demuth, M.N., & Chew, H.A.M. 1990a Changes in the flexural strength of ice under radiation decay. *Nord Hydrol* 21(4-5), 341-354.

Prowse, T.D. & Demuth, M.N. 1993 Strength variability of major river-ice types. *Nord Hydrol* 24 169-182

Prowse, T.D., Furgal, C., Chouinard, R., Melling, H., Milburn, D., & Smith, S.L. 2009 Implications of climate change for economic development in Northern Canada: Energy, resource, and transportation sectors. *Ambio* 38(5), 272-281

Prowse, T.D., & Marsh, P. 1989 Thermal budget of river ice covers during breakup. *Can J Civil Eng* 16, 62-71

Rahmstorf, S., & Coumou, D. 2011 Increase of extreme events in a warming world. *PNAS* 108(44), 17905-17909

Rouse W.R., Oswald C.J., Binyamin J., Blanken P.D., Schertzer W.M., & Spence C. 2003 Interannual and seasonal variability of the surface energy balance and temperature of central Great Slave Lake. *J Hydrometeorol* 4,720-730

Rouse, W.R., Oswald, C.J., Binyamin, J., Spence, C., Schertzer, W.M., Blanken, P.D.,... Duguay, C. R. 2005 The role of northern lakes in a regional energy balance. *Journal of Hydrometeorol 6*(3), 291-305.

Rouse, W.R., Blanken, P.D., Duguay, C.R., Oswald, C.J., & Schertzer, W.M. 2008a Climate-lake interactions. In *Cold region atmospheric and hydrologic studies. The Mackenzie GEWEX experience* (pp. 139-160). Springer Berlin Heidelberg.

Rouse, W.R., Blanken, P.D., Bussières, N., Oswald, C.J., Schertzer, W.M., Spence, C., & Walker, A.E. 2008b An investigation of the thermal and energy balance regimes of Great Slave and Great Bear Lakes. *J Hydrometeorol* 9, 1318-1333

Szeto, K.K. 2002 Moisture recycling over the Mackenzie basin. Atmos Ocean 40,181-197

Timalsina, N.P., Alfredsen, K., & Killingtveit, Å. 2015 Impact of climate change on ice regime in a river regulated for hydropower. *Can J Civil Eng* 42, 1-11

Van der Vinne G., Prowse T.D., Andres D. 1991 Economic impact of river ice jams in Canada. In Northern Hydrology, Selected Perspectives, Prowse T.D., Ommanney C.S.L. (eds). NHRI Symposium No. 6, National Hydrology Research Institute, Environment Canada: Saskatoon; 333–352

Vavrus, S., Notaro, M., & Zarrin, A. 2013 The role of ice cover in heavy lake-effect snowstorms over the Great Lakes Basin as simulated by RegCM4. *Mon Weather Rev* 141, 148-165

Von de Wall, S.J. 2011 An assessment of the river ice break-up season in Canada. Master's Thesis. University of Victoria

Wang, J., Bai, X., Hu., H., Clites, A., Colton, M., & Lofgren, B. 2012 Temporal and Spatial Variability of Great Lakes Ice Cover, 1973-2010. *J Climate*, 25(4), 1318-1329

Weyhenmeyer, G.A., Livingstone, D.M., Meilis, M., Jensen, O., Benson, B., & Magnuson, J.J. 2011 Large geographical differences in the sensitivity of ice-covered lakes and

rivers in the Northern Hemisphere to temperature changes. *Global Change Biol* 17, 268-275

Wright, D.M., Posselt, D.J., & Steiner, A.L. 2013 Sensitivity of lake-effect snowfall to lake ice cover and temperature in the Great Lakes Region. *Mon Weather Rev* 141, 670-689

Wrona, F.J., Prowse, T.D., Reist, J.D., Beamish, R., Gibson, J.J., Hobbie, J.,…Vincent, W. 2005 Freshwater ecosystems and fisheries. In: Arctic climate impact assessment. Cambridge University Press, New York, pp 353-452

The use of standard hydrological data and process-based modelling to study possible transformation of permafrost landscapes after fire

Semenova O.[1,2*], Lebedeva L.[3], Nesterova N.[2]

[1]*Gidrotehproekt Ltd., St. Petersburg, 194223, RUSSIA*
[2]*St. Petersburg State University, St. Petersburg, 199178, RUSSIA*
[3] *Melnikov Permafrost Institute, Yakutsk, 677010, RUSSIA*
**omakarieva@gmail.com*

Though northern basins are the subject to regular forest fires, often little information is available about fire impact in remote regions except their timing and areal distribution. Observed changes of hydrological response at burnt watersheds may serve as the only indirect quantitative evidence of soil, vegetation and permafrost transformation due to fire. In this study the analysis of hydrological data and process scenario modelling is used to reveal possible changes of landscape properties.

Large territories of the Transbaikal region of Russia (the headwaters of the Lena and Amur Rivers) were severely burnt by forest fires in 2003. Based on remote sensing data analysis several basins with available long-term runoff observations (not less than 30 years including year of fire) with the area of fire impact from 13 to 78 % were detected.The studied watersheds are situated in mountainous area to the east of the Baikal Lake. This remote region is characterized by very low density of hydrometeorological network which considerably complicates the study.

The analysis of long-term hydrological data allowed detecting apparent hydrological response to fire at several basins. Semenova et al. (2015a, 2015b) revealed short-term increase of summer flow following the fire event at two watersheds of the Amalat and Vitimkan Rivers. Confirming the speculations by Moody et al. (2013), Semenova et al. (2015a, 2015b) have shown that the detection of fire impact was possible only at the watersheds with reliable meteorological information and during extreme precipitation events.

For the watersheds of the Amalat (2100 km^2) and Vitimkan Rivers (969 km^2) different scenarios of soil and vegetation transformation were developed based on remote sensing data analysis and literature review. Different factors such as the removal of organic layer, albedo and evapotranspiration changes, intensification of soil thaw, reduction of infiltration rate, increase of upper subsurface flow fraction in summer flood events following the fire and others were implied.

The hydrological model Hydrograph (Vinogradov et al., 2011; Semenova et al., 2013) was applied to conduct simulation experiments aiming to reveal which landscape changes scenarios were more plausible. The advantages of chosen hydrological model for this study are 1) that it takes into consideration thermal processes in soils which in case of permafrost and seasonal soil freezing presence can play leading role in runoff formation (Semenova et al., 2014) and 2) that observable vegetation and soil properties are used as its parameters allowing minimal resort to calibration (Lebedeva et al., 2014). The model can use dynamic set of parameters performing pre-assigned abrupt and/or gradual changes of landscape characteristics (Semenova et al., 2015b).

The modelling experiments were conducted in two stages. Initially, continuous runoff simulation with "pre-fire" parameters was performed for 1966-2012 period (including fire year 2003) for studied watersheds with daily time step. Its results allowed assuming that up to 40 and 130 mm of observed flow depth (35 – 40 %) in August 2003 can be attributed to flow increase due to fire impact at the Amalat and the Vitimkan Rivers respectively. Next step of the research was the application of the model parameters developed for post-fire environment suggesting the intensification of soil thaw due to change of surface energy balance (Jiang et al., 2015) and reduction of infiltration rate and evapotranspiration which in general lead to the increase of surface and preferential flow in soil horizons destroyed by fire (Koch et al., 2014) during summer flood events.

Hydrological models are regularly applied to look into the processes of flow changes due to landscape transformation (ex., Seibert et al., 2010). Though future projections of flow characteristics based on calibrated models are generally questionable (Semenova and Beven, 2015). The dynamic-parameter modelling approach based on *a priori* assessment of the model parameters used here is promising and has the potential for application in modelling studies in changing environment.

ACKNOWLEDGMENT

The reported study was funded by Russian Foundation for Basic Research according to the research projects №14-05-00665 and 14-05-31194.

REFERENCES

Jiang, Y., Rocha, A. V., O'Donnell, J. A., Drysdale, J. A., Rastetter, E. B., Shaver, G. R., & Zhuang, Q. 2015 Contrasting soil thermal responses to fire in Alaskan tundra and boreal forest. *J. Geophys. Res. Earth Surf.* 120 (2), 363–378 doi:10.1002/2014JF003180

Koch, J. C., Kikuchi, C. P., Wickland, K. P. & Schuster, P. 2014 Runoff sources and flow paths in a partially burned, upland boreal catchment underlain by permafrost. *Water Resour. Res.* 50, 8141–8158 doi:10.1002/2014WR015586

Lebedeva, L., Semenova, O. & Vinogradova, T. 2014 Simulation of Active Layer Dynamics, Upper Kolyma, Russia, using the Hydrograph Hydrological Model. *Permafrost and Periglac.Process.* 25 (4), 270–280 doi: 10.1002/ppp.1821

Moody, J.A., Shakesby, R.F., Robichaud, P.R., Cannon, S.H. & Martin, D.A. 2013 Current research issues related to post-wildfire runoff and erosion processes. *Earth-Science Reviews* 122, 10–37.

Seibert, J., McDonnell, J. J. & Woodsmith, R. D. 2010 Effects of wildfire on catchment runoff response: a modelling approach to detect changes in snow-dominated forested catchments. *Hydrol. Res.* 41, 378–390. doi:10.2166/Nh.2010.036

Semenova, O. & Beven, K. 2015 Barriers to progress in distributed hydrological modeling. *Hydrol. Process.* 29, 2074–2078 doi: 10.1002/hyp.10434

Semenova, O., Lebedeva, L. & Vinogradov, Yu. (2013) Simulation of subsurface heat and water dynamics, and runoff generation in mountainous permafrost conditions, in the Upper Kolyma River basin, Russia. *Hydrogeology Journal* 21 (1), 107-119 DOI:10.1007/s10040-012-0936-1

Semenova, O., Lebedeva, L., Volkova, N., Korenev, I., Forkel, M., Eberle J. & Urban, M. 2015a Detecting immediate wildfire impact on runoff in a poorly-gauged mountainous permafrost basin. *Hydrological Sciences Journal*, DOI: 10.1080/02626667.2014.959960

Semenova, O., Vinogradov, Y., Vinogradova, T. & Lebedeva, L. 2014 Simulation of soil profile heat dynamics and integration into hydrologic modelling in the permafrost zone. *Permafrost and Periglac.Process.* 25 (4), 257–269 doi: 10.1002/ppp.1820.

Semenova, O. M., Lebedeva, L. S., Nesterova, N. V., & Vinogradova, T. A. 2015b Evaluation of short-term changes of hydrological response in mountainous basins of the Vitim Plateau (Russia) after forest fires based on data analysis and hydrological modeling. *Proc. IAHS* 371, 157-162 doi:10.5194/piahs-371-157-2015

Vinogradov, Y. B., Semenova, O. M. & Vinogradova, T. A. 2011 An approach to the scaling problem in hydrological modelling: the deterministic modelling hydrological system. *Hydrol. Process.* 25: 1055–1073 doi: 10.1002/hyp.7901

Observation and simulation study of atmosphere stability over the high-latitude Ngoring lake in the Tibetan Plateau

Lijuan Wen*, Shihua Lv, Zhaoguo Li, Lin Zhao

Cold and Arid Regions Environmental and Engineering Research Institute, Chinese Academy of Sciences, Lanzhou, Gansu,73000, CHINA

**wlj@lzb.ac.cn; gamevictory@gmail.com*

ABSTRACT

The Tibetan Plateau harbors thousands of lakes; however few studies focus on characteristics of energy/water cycle and their impacts on local climate in the region. To investigate the corresponding characteristics of Ngoring Lake in the study, field experiments and numerical simulations are performed over the biggest lake in the Yellow River source region in the Tibetan Plateau. The air temperature difference between lake and land in the period with ice varied with snow over lake and was mostly positive without snow. Almost persistent unstable atmosphere existed over ice-free Ngoring lake from 2011-2013, contrasting with the stabel atmosphere over temporate lakes in the same period. Offline simulations with CLM4.5 show that the low air temperature owing to the high altitude and the lake freezing contribute a lot to the unstable atmosphere.

KEYWORDS

Ngoring lake; Tibetan Plateau; unstable atmosphere; CLM4.5; cold air temperature

1. INTRODUCTION

An army of researchers and scientists accept the observation and the outputs from simulations showing that lakes affect local climate significantly and the effects vary spatially and temporally (Hostetler et al., 1993; Lauwaet et al., 2012; MacKay et al., 2009; Mishra et al., 2011; Ricko et al., 2011; Samuelsson et al., 2010; Steiger et al., 2009; Stepanenko et al., 2010). For example, the surface temperature was 4 °C less over the Great Slave Lake and the Great Bear Lake in Canada as compared to land in vicinity during July (Long et al., 2007). While the simulation shows that the lake temperature is usually higher than that of land in southern Finland during all seasons (Samuelsson et al., 2010). Two large lakes on South-Central Baffin Island in Canada, delay the seasonal cooling in fall and early winter for the interior lowlands under the influence of strong positive sensible heat fluxes (Jacobs and Grondin, 1988). Temperature response to the lakes varies. Characteristics of energy budget over the lake surface are different. For example, research study from Lake Tanganyika in East Africa illustrates the annual mean heat loss increase by 13% and 18% by latent and sensible heat fluxes, resulting from the unstable atmosphere (Verburg and Antenucci, 2010). Contrastingly, the atmosphere during summer is usually stable for the North American Great Lakes (Verburg and Antenucci, 2010). The above references elucidate the lake effect is although apparent in different regions worldwide, the characteristics and exact nature differ from lake to lake and depend on many factors, including lake size and depth, as well as regional climate conditions, require more measurements in different regions over a wide range of weather and climate conditions.

The Tibetan Plateau harbors thousands of lakes on the highest altitude worldwide. The lake network covers nearly 44,993.3 km2 including more than 1091 lakes with individual areas greater than 1.0 km2, and covers about 49.4% of the total lake area in China (Jiang and Huang, 2004). However, among the world areas with large amount of lakes, like Fennoscandia and Northern Canada, the Tibetian Plateau is a less investigated and a more extraordinary lake system due to strong seasonal and synoptic variations.

In recent years, a few scholars have performed research on the lake-atmosphere interaction in the Tibetan Plateau (Haginoya et al., 2009; Li et al., 2014; Li et al., 2015; Yang et al., 2015). In the study, the observed unstable atmosphere in ice-free Ngorling lake is shown and the effecting factors have been anaylyzed using CLM4.5 (Community Land model version 4.5) model.

2. STUDY AREA, OBSERVATIONS AND MODEL

Ngoring Lake is the biggest lake in the Yellow River source region with 610 km^2 surface area and lies in the eastern Tibetan Plateau with 4274 m lake surface altitude. The mean depth of the lake is 17 m and the maximum depth is 32 m. The lake is a fresh lake with few fish. Only in the riparian area, do aquatic plants grow. With a small seasonal variation of vegetation height (about 5 cm), alpine meadow grows over the ground and low hills around the lake. The measured conductivity of lake water is 0.36–0.42 ms cm^{-1} and the PH value is 8.49. The Ngoring lake basin is mainly dominated with the cold and semi-arid continetal climate. According to 1953-2012 data from Maduo meterological station (98.2 °E, 34.9 °N) belong to CMA (China Meteorological Administration), the mean monthly temperature is −3.7 °C with the mininum −16.2 °C in January and the maximum 7.7 °C in July ; the average annual precipitation is 321.4 mm with 90% falling from May to Sepetembeter. The lake completely froze from early December to early April (Li et al., 2015).

Except using the data from Maduo meterological station and Modis surface temperature data in the study, we also use the observations from LS (Lake station, 97º38′58.70″E、35º01′28.77″N) during ice-free period in 2011, 2012,2013 and LBS (Lake border station, 97º33.25′E, 35º54.75′N) since 2012 October, including radiation, enrgy flux and meteological data. There is another longest observation station TS (the tower station, 35º54.75′N, 97º33.25′E) with uo to 18 m height 5-layer meteological observation. Because it was difficult to instal instruments in deep water in the centre of the lake, our LS observation platform had to be built on a submerged rock (about 1.0 m below the water surface) near the shore. The platform stood in the northwest region of Ngoring Lake, located 200 m to the northwest lakeshore and 50 m to the southwest island (Fig. 1). The lakewater within 200m around the platformwas about 3–5 m in average depth. To the southeast side of the platform there was the centre of the lake, and the water depth could exceed 15 m at a distance of 1 km to the platform (Li et al., 2015). LBS was instablled in the southwest lakeshore of Ngorling lake. TS is very close to LBS, only a few meters far.

The CLM4.5 model is employed to study the interaction between the atmosphere and the lake surface in the study (Subin et al., 2012). In the model, lake processes and lake-atmosphere interactions are dynamically simulated using a 1-D mass and energy balance lake scheme with 10 lake water layers (Oleson et al., 2004). The calculation of surface fluxes of lake is close to that of non-vegetated surfaces, which is used to calculate LSST. The calculation of each layer lake temperature is depended on the Crank-Nicholson thermal diffusion solution (Oleson et al., 2004).

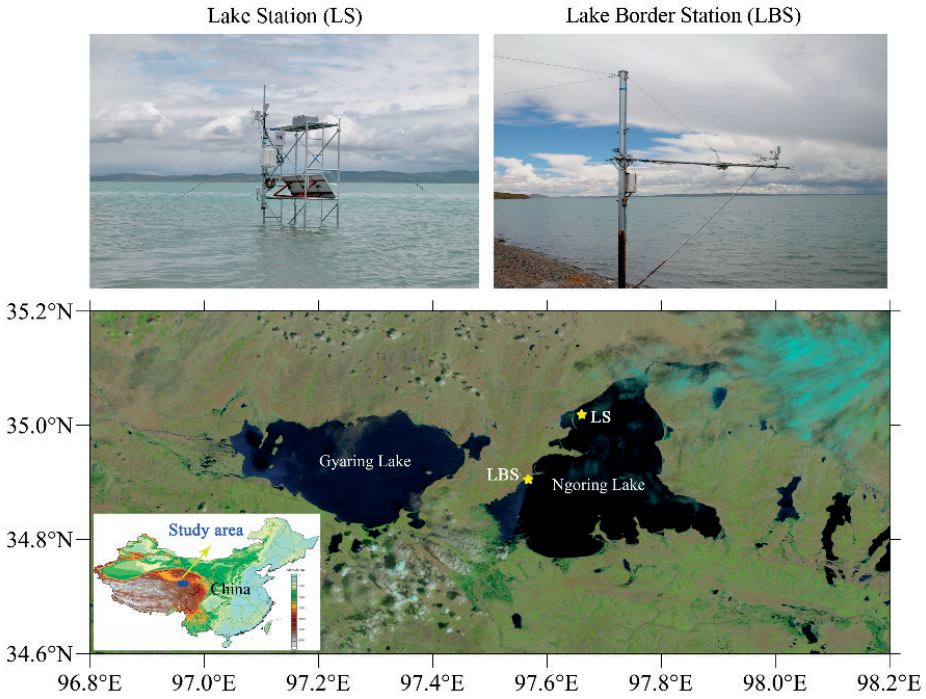

Figure 1 Study area and observation stations

3. RESULTS AND DISCUSSION

3.1 FROZEN LAKE EFFECT AND SNOW

The winter precipitation that should be snow owing to the low air temperature is more than the average from 2011 to 2012 and less from 2012 to 2013 (Fig. 2). There was very few precipitation in the winter from 2012 to 2013 and snow barely cover the lake. Compared to the multi-year (1953-2012) average and winter from 2012 to 2013, there was more snow over the lake. With snow, the air over lake is colder than that over land. With very less snow, the lake has warm effect from December 2012 to March 2013.

MODIS data (Fig. 3) show that there is no surface temperature difference between lake and land in the winter day and night with snowcover; without snow, the winter lake is obviously warmer than surrounded land at night and colder in the day.

2-day observations over frozen lake (Fig. 4) show that the the observed albedo over frozen lake was low, about 0.15 at noon. Much downward radiation went into the lake. The temperature of lake ice was higher than the air over the frozen lake. And there is no obvious air temperature difference between 0.3 and 1.5 m high over the lake.

(a) Monthly precipitation anomalies of Maduo station (%)

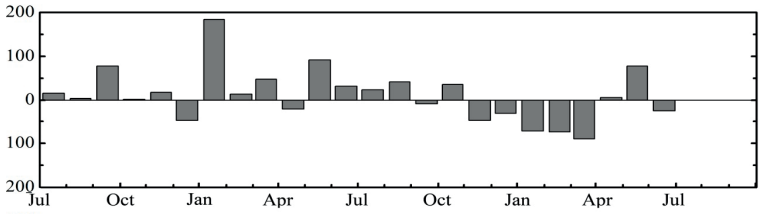

(b) Monthly precipitation (mm)

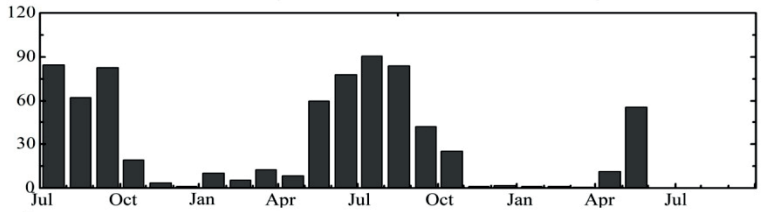

(c) Monthly air temperature difference between Maduo and TS(^{0}C)

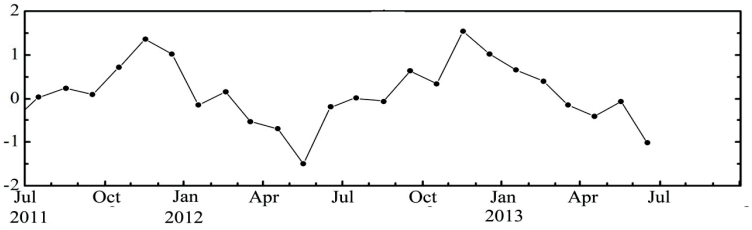

Fig. 2 Monthly precipitation and temperature

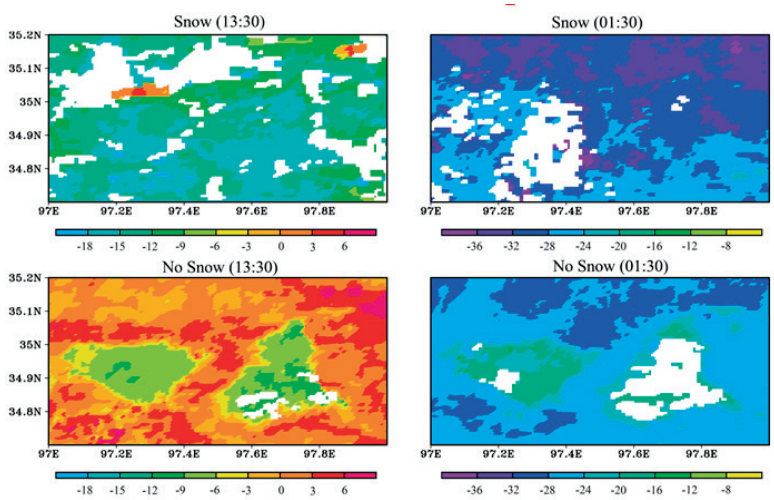

Fig. 3 MODIS surface temperature in winter

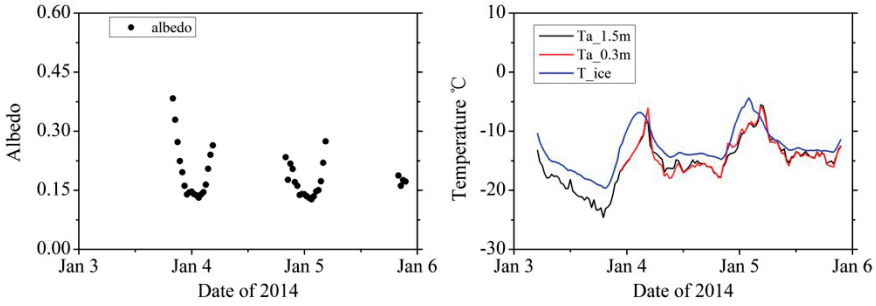

(a) (b)

Fig. 4 Observed albedo and temperature of ice and 0.3 m, 1.5m high over frozen lake

3.2 UNSTABLE ATMOSPHERE OVER OPEN WATER LAKE

3 years observations over lake show that the unfrozen lake water close to lake surface was almost always warmer than air (Fig. 5). It is similar with characteristics of tropical lakes, different with that of temperate lakes with low elevation in spring and early summer. The lake surface skin temperature calculated from radiation over lake also was higher than air temperature (Fig. 6a). The observed sensible heat flux in LS and LBS are positive (Fig. 6b). The observed warmer lake surface should be true. The lake water warming phenomenon corrsponded to the strong solar radiation, low pressure and dry air. And most of wind speed is less than 6 m/s over lake (Fig. 7).

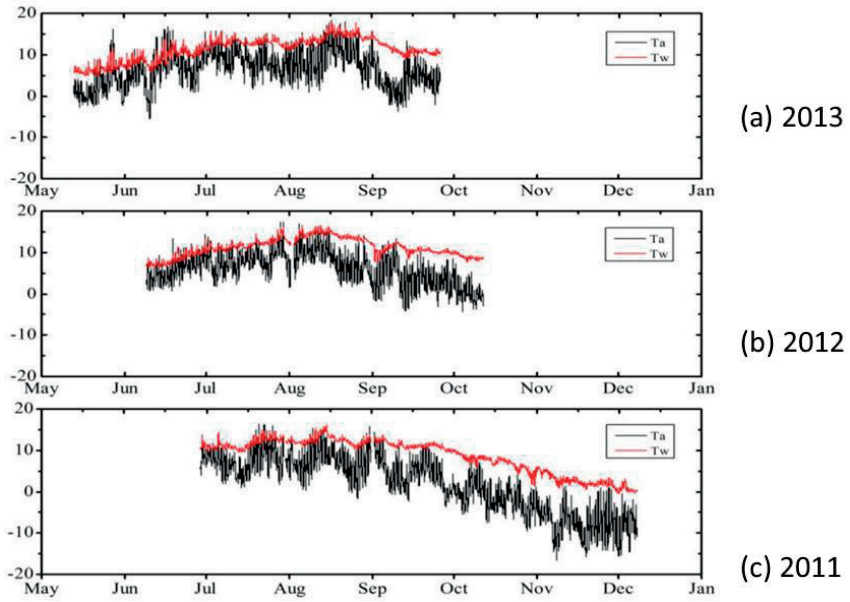

Fig. 5 Observed air temperature with 30-minute interval and lake water temperature with 0.5cm depth under the surface

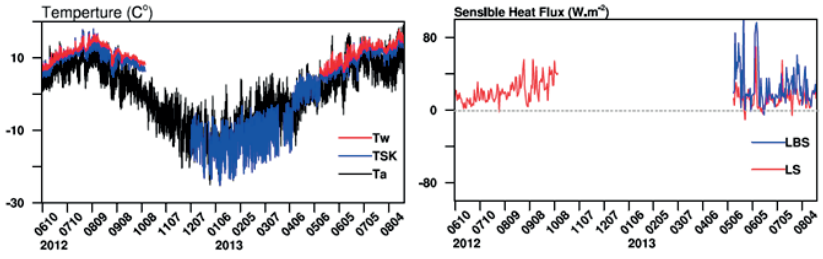

(a) (b)

Fig. 6 Combined surface temperature, lake water temperature and air temperature

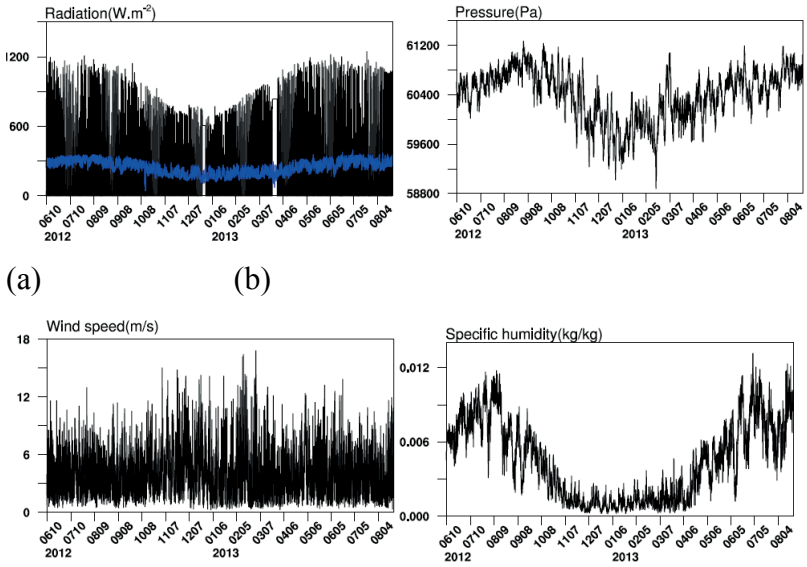

(a) (b)

(c) (d)

Fig. 7 Combined meteorological data

3.3 SIMULATION WITH CLM4.5

Owing to the difference mainly appeared in the Spring and summer, the observation in 2011 almost start in summer, and there was no observation in the winter from 2011 to 2012, we focus on the 2012 and 2013 in the following. There was no winter observation in LS, data in Fig. 7 from October 2012 to May 2013 are observed in LBS, other are observed in LS. These data will be used as forcing to drive the CLM4.5. The offline simulation is called CTL (the control run). To see the impact of winter observation from LBS on the simulation, we performed another run, called LSF (lake station forcing), which started from May 2013 with forcing data only from LS.

CLM model could provide realistic reproduction of surface observations (Fig. 8). The simulated lake surface temperature, lake water temperature, sensible heat flux and latent heat flux are similar to observations. The model can represent the temperature difference between lake surface and atmosphere in ice-free period. There is almost no difference between the simulated lake surface temperature in CTL and LSF. The combined data could be used for the simulation study.

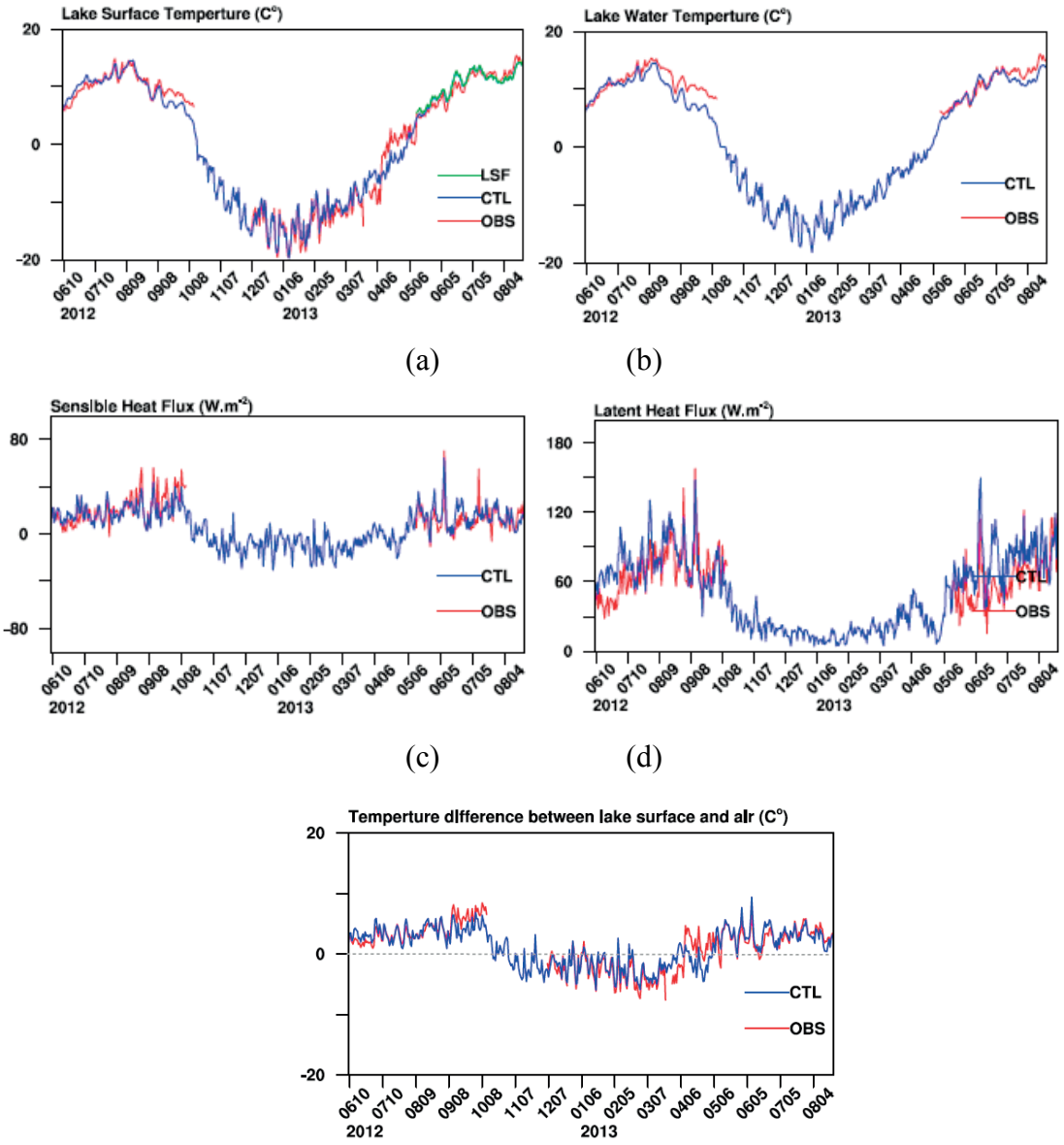

Fig. 8 Simulation with CLM4.5

3.4 EFFECTING FACTORS FOR UNSTABLE ATMOPHERE OVER ICE-FREE LAKE

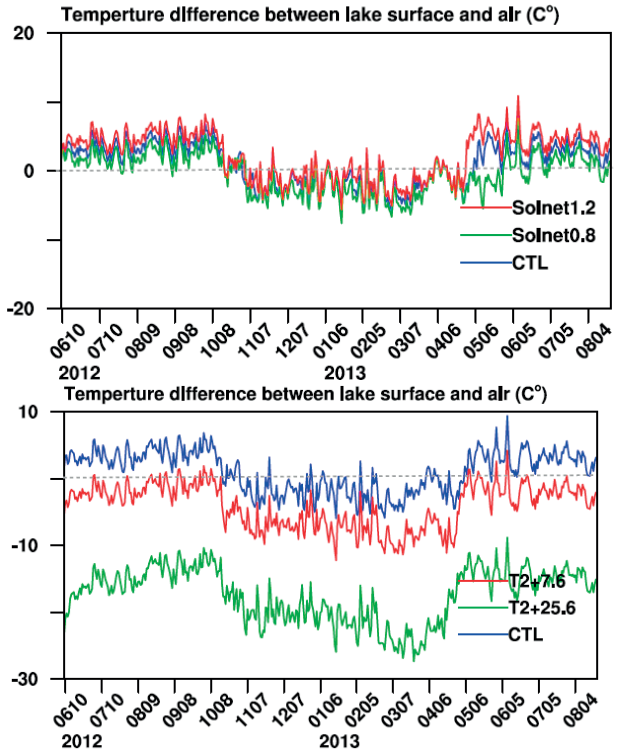

(a) (b)

Fig. 9 Simulation with changed aie temperature and net solar radiation

To investigate which factors induce the warming lake water in spring and early summer, the sensitivity experiments are carried out with change of each forcing data.

Decreasing solar radiation will reduce sensible heat flux and latent heat flux, low lake surface temperature and the lake difference. But with 20% change, the impact is not very significant (Fig. 9a).

According to the adiabatic rate, the air temperature changed from more than 4200m (4274m) altitude to 3000m altitude and sea level will significantly increse the lake surface skin temperature and latent heat flux (Fig. 9b), but low the positive temperature difference and sensible heat flux, even change to negative.

Increase of downward longwave radiation will enlarge the positive temperature difference between lake and air. Its influence magnitude is bigger than that with the same percentage change of downward solar radiation.

The increase of wind speed will decrease the positive temperature difference between lake and air, and the increase of specific humidity will supress the positive temperature difference.

Influence of pressure is small and can be ignored. The lake freezing preocess in winter can prevent heat loss and benefit to the warm lake water after ice-melting.

4. CONCLUSIONS

- Lake has warmer effect without snow in winter and cold effect with snow.
- Three years' observation show that Ngoring Lake water was warmer than air over it in the ice-free period.
- CLM model could provide realistic reproduction of surface observations
- The main contribution for the warmer temperature is from the low air temperature owing to the high altitude.
- Freezing process contribute to the unstable atmosphere to some extent.

ACKNOWLEDGMENT

The study was supported by National Natural Science Foundation of China (41475011 and 41130961). We acknowledge the support for using the computing resources at Supercomputing Center of Cold and Arid Regions Environmental and Engineering Research Institute, Chinese Academy of Sciences.

REFERENCES

Haginoya, S., Fujii, H., Kuwagata, T., Xu, J.Q., Ishigooka, Y., Kang, S.C., Zhang, Y.J., 2009. Air-Lake Interaction Features Found in Heat and Water Exchanges over Nam Co on the Tibetan Plateau. Sola 5, 172-175, DOI 10.2151/sola.2009-044.

Hostetler, S.W., Bates, G.T., Giorgi, F., 1993. Interactive coupling of a lake thermal model with a regional climate model. J. Geophys. Res. 98(D3), 5045-5057.

Jacobs, J.D., Grondin, L.D., 1988. The Influence of an Arctic Large-Lakes System on Mesoclimate in South-Central Baffin Island, Nwt, Canada. Arctic and Alpine Research 20(2), 212-219, Doi 10.2307/1551499.

Jiang, J., Huang, Q., 2004. Distribution and variation of lakes in Tibetan Plateau and their comparison with lakes in other part of China. Water Resources Protection 4(6), 24-27 (in Chinese with English Abstract).

Lauwaet, D., Van Lipzig, N.P.M., Van Weverberg, K., De Ridder, K., Goyens, C., 2012. The precipitation response to the desiccation of Lake Chad. Quarterly Journal of the Royal Meteorological Society 138(664), 707-719, DOI:10.1002/qj.942.

Li, X., Wang, L., Chen, D., Yang, K., Wang, A., 2014. Seasonal evapotranspiration changes (1983–2006) of four large basins on the Tibetan Plateau. Journal of Geophysical Research: Atmospheres 119(23), 13,079-013,095, 10.1002/2014jd022380.

Li, Z., Lyu, S., Ao, Y., Wen, L., Zhao, L., Wang, S., 2015. Long-term energy flux and radiation balance observations over Lake Ngoring, Tibetan Plateau. Atmos. Res. 155, 13-25, DOI:http://dx.doi.org/10.1016/j.atmosres.2014.11.019.

Long, Z., Perrie, W., Gyakum, J., Caya, D., Laprise, R., 2007. Northern lake impacts on local seasonal climate. Journal of Hydrometeorology 8(4), 881-896.

MacKay, M.D., Neale, P.J., Arp, C.D., Domis, L.N.D., Fang, X., Gal, G., Johnk, K.D., Kirillin, G., Lenters, J.D., Litchman, E., MacIntyre, S., Marsh, P., Melack, J., Mooij, W.M., Peeters, F., Quesada, A., Schladow, S.G., Schmid, M., Spence, C., Stokesr, S.L., 2009. Modeling lakes and reservoirs in the climate system. Limnol. Oceanogr. 54(6), 2315-2329.

Mishra, V., Cherkauer, K.A., Bowling, L.C., Huber, M., 2011. Lake ice phenology of small lakes: Impacts of climate variability in the Great Lakes region. Global and Planetary Change 76(3-4), 166-185.

Oleson, K.W., Dai, Y., Bonan, G., Bosilovich, M., Dickson, R., Dirmeyer, P., Levis, S., Niu, G.-Y., Thornton, P., Vertenstein, M., Yang, Z.-L., Zeng, X., 2004. Technical description of the Community Land Model (Access online via http://www.cgd.ucar.edu/tss/clm/distribution/clm3.0/index.html).

Ricko, M., Carton, J.A., Birkett, C., 2011. Climatic effects on lake basins. Part I: Modeling tropical lake levels. Journal of Climate 24(12), 2983-2999.

Samuelsson, P., Kourzeneva, E., Mironov, D., 2010. The impact of lakes on the European climate as simulated by a regional climate model. Boreal Environ. Res. 15(2), 113-129.

Steiger, S.M., Hamilton, R., Keeler, J., Orville, R.E., 2009. Lake-effect thunderstorms in the lower Great Lakes. J. Appl. Meteorol. Climatol. 48(5), 889-902.

Stepanenko, V.M., Goyette, S., Martynov, A., Perroud, M., Fang, X., Mironov, D., 2010. First steps of a Lake Model Intercomparison Project: LakeMIP. Boreal Environ. Res. 15(2), 191-202.

Subin, Z.M., Riley, W.J., Mironov, D., 2012. An improved lake model for climate simulations: Model structure, evaluation, and sensitivity analyses in CESM1. Journal of Advances in Modeling Earth Systems 4, DOI:Artn M02001.10.1029/2011ms000072.

Verburg, P., Antenucci, J.P., 2010. Persistent unstable atmospheric boundary layer enhances sensible and latent heat loss in a tropical great lake: Lake Tanganyika. J. Geophys. Res. 115, DOI:10.1029/2009JD012839.

Yang, X., Lü, Y., Ma, Y., Wen, J., 2015. Summertime thermally-induced circulations over the Lake Nam Co region of the Tibetan Plateau. Journal of Meteorological Research 29(2), 305-314, 10.1007/s13351-015-4024-z.

Summer and Winter Flows of a Large Northern River: The Mackenzie of Canada

Ming-ko Woo* and Robin Thorne

School of Geography and Earth Sciences, McMaster University, Hamilton, Ontario, CANADA L8S4K1
**woo@mcmaster.ca*

ABSTRACT

Like other large northern rivers, Mackenzie River of Canada traverses temperate, subarctic and Arctic latitudes, with diverse topography and landforms River flows in summer and winter are governed by atmospheric processes that regulate water gains and losses (precipitation, evaporation), and basin processes that affect storage and release (snow and ice, lakes and groundwater). Within the Mackenzie system, the flow of tributaries reflects the controlling factors noticeably during the open water season while in winter most rivers acquire an ice cover that isolates the flow from atmospheric influences. Main trunk Mackenzie integrates and modifies the flow characteristics of its tributaries. Summer flow far exceeds the winter total and in both of these seasons, mountain region produces large runoff while lowlands yield the least. The storage and release of lakes importantly alleviate the low flows of summer and winter, and the signature of human activities can be detected through the flow of Peace River that is out of phase with the natural rhythm.

KEYWORDS

winter flow; summer flow; Mackenzie River; streamflow regime; northern river

1. INTRODUCTION

Draining an area of 1.8 million km^2, Mackenzie River is the fourth largest circumpolar river in the world and the largest northern river in North America. In addition to serving significant roles in the northern aquatic ecosystem, the river provides water for human usage that ranges from community water supply to hydro-power production, and enables summer navigation along the main river course. Peak flows, especially those produced by spring snowmelt, pose recurrent and serious flood hazards. Much works have been done on snowmelt freshets of the Mackenzie Basin (Prowse & Carter 2002; de Rham et al. 2008). However, less attention has been paid on comparing the flows of the summer and the winter seasons, the former contains both low flow events and high flows produced by late snowmelt and by rainfall; the latter is dominated by low flow conditions. Low flows are of particular concern as they create problems for water supply, navigation and ecological wellbeing (Peters et al. 2006; Sung et al. 2006; Burn et al. 2008; Bradford & Heinonen 2008). This study addresses the factors that influence river flow and the major flow characteristics in winter and in summer, as well as the spatial variation in flow contribution within the Mackenzie drainage system.

2. STUDY AREA AND DATA

Circumpolar areas that support rivers of the Arctic drainage can be broadly distinguished into five hydro-physiographical regions, viz. Arctic tundra, boreal plains, mountainous terrain, Precambrian shields and temperate grasslands (Figure 1). All these regions are represented in the Mackenzie Basin. Rivers from different parts of the vast Basin acquire flow characteristics according to the diverse climate, geology, topography and vegetation of the hydro-physiographic regions they pass through.

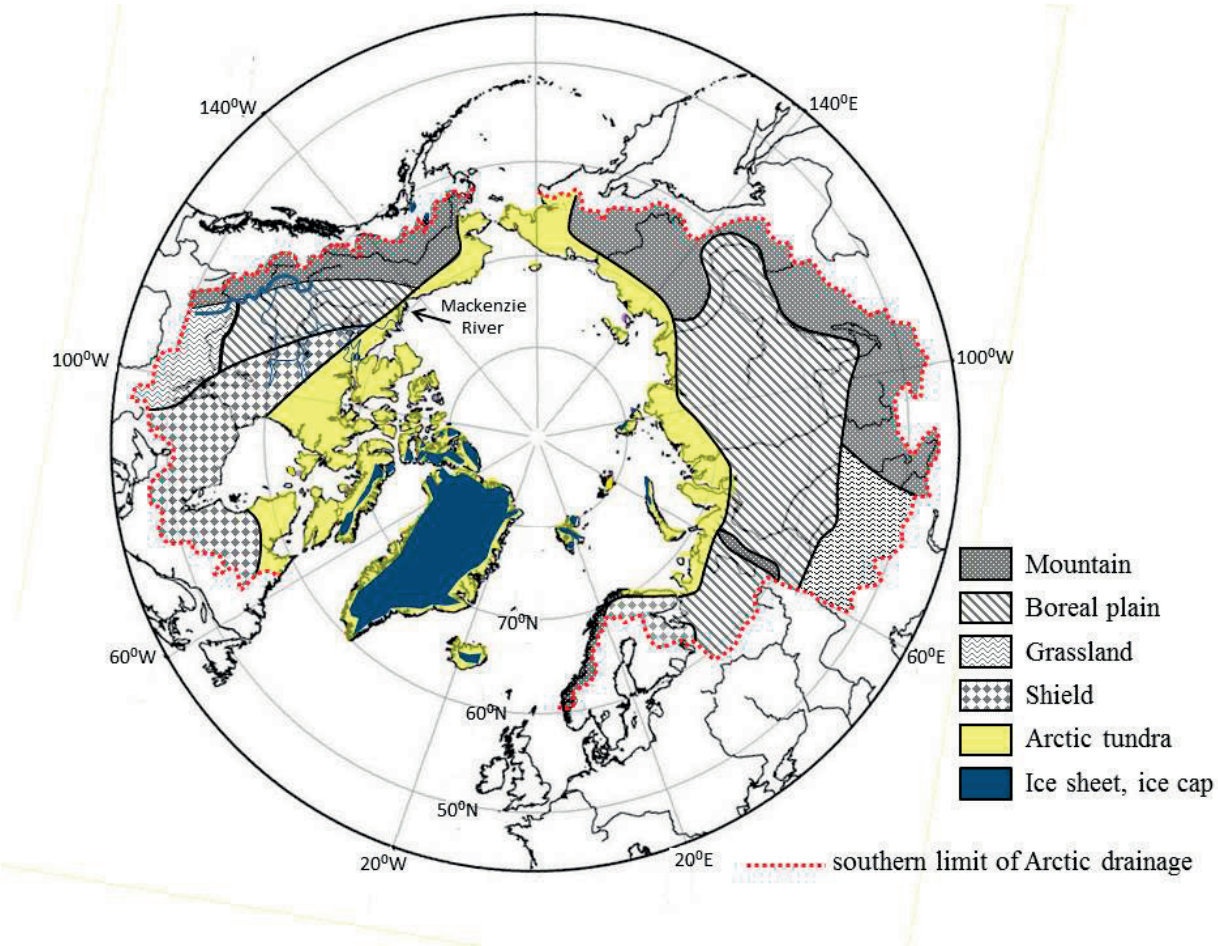

Figure 1.Hydro-physiographic regions of the Arctic drainage.

Mountains, intermontane plateaus and dissected valleys of the Western Cordilleras dominate the western third of the Mackenzie Basin, with snow, glaciers and rainfall providing large amounts of runoff to feed the spring and summer flow. In the east lies the Canadian Shield with rolling topography consisting of outcrops of mostly crystalline bedrock and soil-filled valleys occupied by many lakes and wetlands. Between the Shield and the Cordillera are the Interior Plains that stretch from the Arctic tundra at its northern extremity, through the boreal forests and wetlands, to the temperate grasslands of the Canadian prairies at the southern fringe. Permafrost underlies the northern parts of the Basin but all rivers and lakes are prone to the formation of an ice cover. Winter arrives later but spring comes earlier in the south than in the north (Woo & Thorne 2003). Owing to their time difference that can be weeks or even months, common time frames are adopted in this study to define summer (taken as June to September) and winter (from November 1 to the end of March) to allow comparison of flow conditions among rivers in various parts of the Basin.

Two groups of rivers are selected for this study, including the major tributaries with drainage areas in the range of 10^5 km^2 and the main trunk of Mackenzie River with stations that collect flows from areas in the order of 10^6 km^2. The selected hydrometric stations have daily streamflow records obtainable from the HYDAT database, the National Water Data Archive compiled by Water Survey of Canada. The study period is from 1972 to 2012.

3. WINTER AND SUMMER FLOW: FACTORS AND PROCESSES

Three sets of factors exert varying influences on flow generation in the summer and winter seasons. Essentially, they are the atmospheric, terrestrial and human elements.

1. Atmospheric processes:

Heat and moisture gains and losses have direct and indirect impacts on river flow. The loss of heat in autumn leads to river freeze-up and the formation of river ice (unless the river dries up) and warming up in spring causes snowmelt, followed by river ice decay and eventual breakup of the ice cover through thermal and mechanical processes (Beltaos 2003). The presence of a winter ice cover isolates the water bodies from interactions with the atmosphere other than heat loss and the growth and persistence of the ice. Within the drainage basin, spring melt releases the accumulated snow from winter storage to produce a substantial flood. Summer heat enables melting of late-lying snow and glaciers, to generate high runoff. Open water condition occurs in the summer and the drainage network (river channels, lakes, wetlands) is exposed to direct atmospheric activities. The river basins receive rainfall inputs and experience evaporation losses, which together exert control on the amount of water available for summer flow.

2. Environmental factors:

Topography and geology affect surface and groundwater storage and the delivery of water to rivers through surface and subsurface routes. Steep terrain offers large gradients that facilitate surface runoff in the summer and groundwater discharge throughout the year. Permafrost as a factor is inert in winter, but modifies runoff production and delivery in the thaw season. Evapotranspiration is suppressed in the winter but depending on vegetation growth conditions, summer water loss tends to be high in the southern parts of the Basin, decreasing towards the tundra zone. The Basin is host to myriad lakes, which during the open water season lose much of their water to evaporation. Additionally, lake storage delays the timing and modifies the magnitude of flow response, often overwhelming and distorting any discharge pattern imposed by other flow generating processes.

3. Human interference:

Most northern rivers exhibit a nival regime that is dominated by spring peakflow from snowmelt, followed by a declining summer flow spiked by rain events and recede to low flow in the winter months (Woo & Thorne 2003). Human interference in the form of hydroelectric power production, modifies the natural flow rhythm to suit its seasonal water demands (Peters & Prowse 2001). Other activities such as agriculture, mineral exploitation and community water use, have minimal effects on the flow of the Mackenzie system.

4. FLOW CHARACTERISTICS

Flow of the main trunk Mackenzie receives contributions from its tributaries, most of which come from the several major sub-basins, including the Athabasca, the Peace, the Liard and Great Bear. Here, we focus on the flow characteristics of these principal tributaries and along the Mackenzie main stem.

4.1 Principal Tributaries

Headwater rivers of the Mackenzie Basin inherit runoff attributes of the hydro-physiographical regions that they drain, to manifest several types of streamflow regime. They include the nival (with high flow dominated by snowmelt contribution), proglacial (glacier melt being an important consideration), prolacustrine (lake influence prevails), wetland (flow modified by the presence of wetlands), spring-fed (mostly in carbonate rock terrain) and regulated (flow managed according to human demands) regimes, all of which are described in Woo (2012). The flow characteristics of headwater rivers are conveyed downstream, the strength of the imprint depends on the magnitude and the timing of inflow received by the principal tributaries.

Summer flow for most rivers is far more varied than winter flow, as shown by the examples given in Figure 2. Summer high flows of the Athabasca at Fort McMurray are influenced by snowmelt, rainfall and glacier melt events. The Liard summer discharge is supported mainly by recession from spring and early summer snowmelt and by summer rain. The Peace is notably affected by hydro-power generation from the artificial Williston Lake at its upper course, combined with the natural flow rhythm (like that of the Liard) from below the reservoir. Great Bear basin is dominated by the huge Great Bear Lake, the eighth largest in the world. The pronounced lake effect gives rise to a prolacustrine regime that suppresses individual inflow events, yielding relatively uniform outflow throughout the year.

Winter flows generally represent a long recession from the autumn, sustained by groundwater discharge. Exceptions are for the prolacustrine and regulated flow regimes, which supply substantially more winter discharge than from the non-lake areas. In early winter, river ice formation leads to temporary blockage of discharge and abstraction of the flow by the ice, leading to a drop in the hydrograph. Water retained through this hydraulic storage (Prowse & Carter 2002) is released with the breakup in spring.

4.2 Main Stem Mackenzie

The main stem of Mackenzie integrates inflow from its tributaries. In addition, the flow along the Mackenzie is transformed by storage and release mechanisms, notably of the lakes and winter ice processes.

Large lakes and chains of small lakes modify downstream transmission of flow through their storage function that delays the timing and distorts the magnitude of inflow.The storage effect of large lakes along the main course of Mackenzie River can be seen by comparing outflow with inflow hydrographs. After passing through Lake Athabasca, the flow of Slave River (Figure 3) bears little resemblance with the individual or the combined hydrographs of Athabasca and Peace

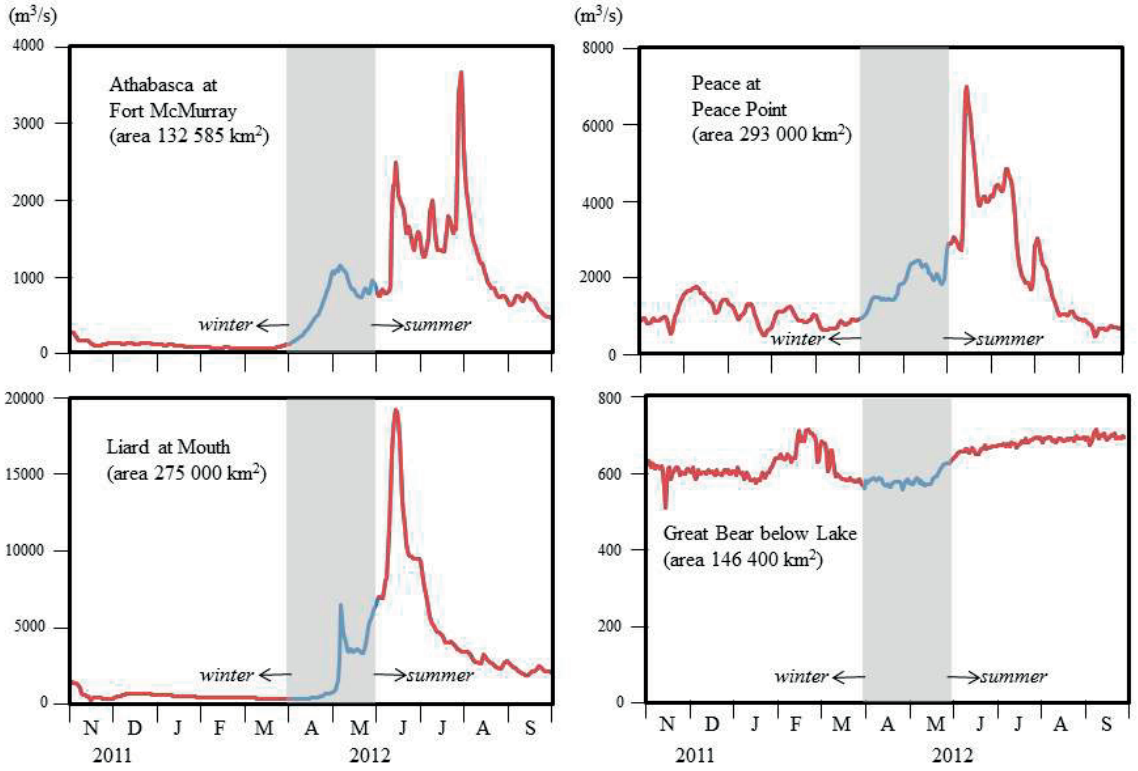

Figure 2. Examples of 2011-12 hydrographs from four principal tributaries in Mackenzie Basin.

(Figure 2). Similarly, after passing through Great Slave Lake, the hydrograph of the Slave becomes much smoothen for the Mackenzie at Strong Point. Further down the Mackenzie past Fort Simpson, the flow of Mackenzie River is conspicuously altered by inflow from Liard River (cf. Figures 2 and 3).

Both summer and winter flows recede from peak to low magnitudes, the former from spring melt and the latter from the autumn high. Whereas the general decline in summer is interrupted by multiple small rises, the winter recession can contain abrupt drops due to hydraulic storage. An exception to the steady winter decline is the Slave River that receives episodic flow releases from the reservoir of Williston Lake on Upper Peace River. The effect of Lake Athabasca is again evident: after the lake, fluctuations in Slave River hydrograph are subdued at Strong Point.

Of interest is the sudden drop in the hydrograph of Mackenzie at Strong Point on January 1. This may be truly attributed to hydraulic storage but may also be an artifact of data uncertainly, an indication of the complexity in obtaining winter discharge (see Rosenberg & Pentland 1966).

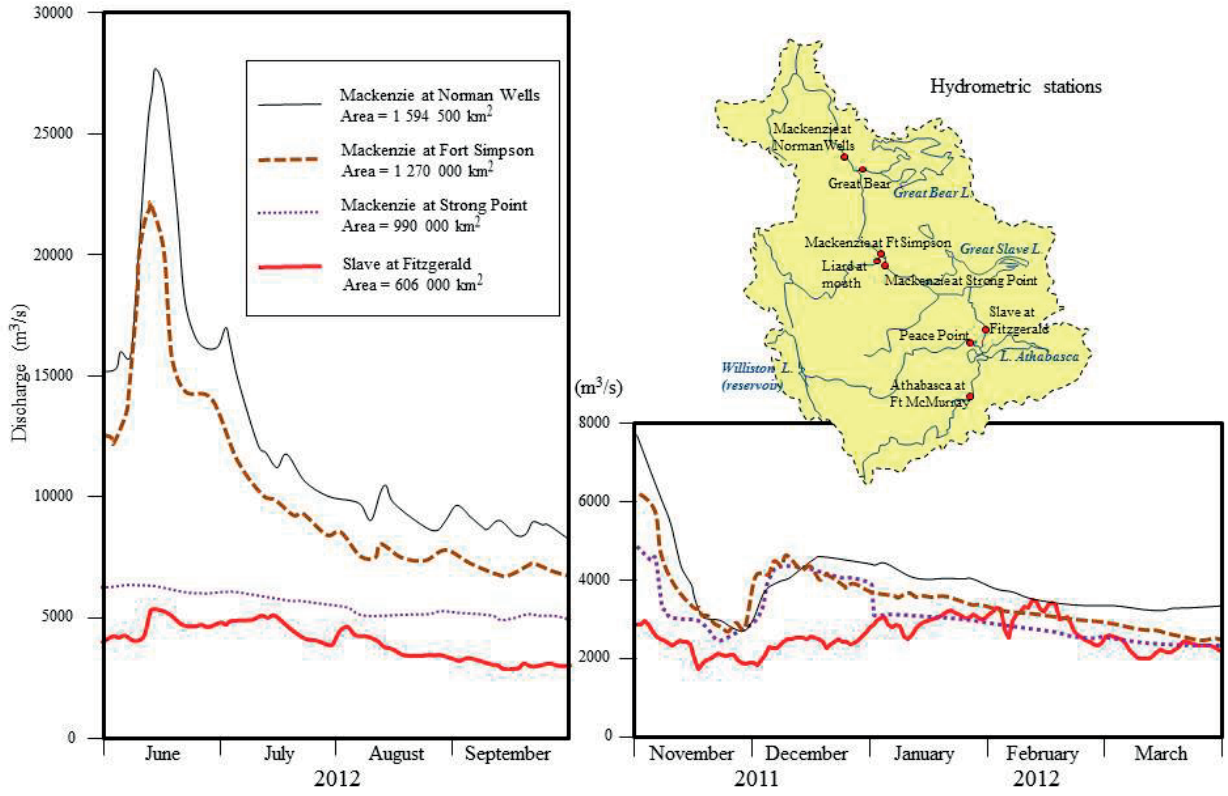

Figure 3.Summer and winter hydrographs from four hydrometric stations along the main stem of Mackenzie River. Inset shows location of stations and large lakes in the Basin.

5. SUB-BASIN CONTRIBUTIONS TO SUMMER AND WINTER FLOW

The relative contribution of sub-basins to overall Mackenzie flow varies considerably among them and can differ substantially between winter and summer (Table 1). For the Basin at Arctic Red River, summer flow totals 167 km^3 and it is 53 km^3 for the winter months. Overall, the Liard provides about one-third of the Mackenzie summer flow at Arctic Red River, and over one-quarter comes from the section between the mouth of Liard and Arctic Red River. The Peace yields about 15% and the rest comes from the eastern section and the southern edge of the Basin that are dominated by plains, Shield and lakes. In winter, the role of Peace and Liard reverses, with the Peace yielding about 40% of the Mackenzie flow and the Liard offers about 15%. Thus, the Liard dictates the summer flow of the Mackenzie while the Peace governs its winter flow. The areas containing Lake Athabasca and Great Bear Lake issue slightly more flow in the winter than in the summer, each contributing about 15% of total Mackenzie winter flow. This pattern does not hold for Great Slave Lake drainage, however, as its winter flow contribution is just 6% though its summer contribution reaches 13% of the Mackenzie total.

Table 1. Summer and winter flow contribution (km^3) of various parts of Mackenzie Basin to the total flow at Arctic Red River station (area at Arctic Red River =1 679100 km^2, 1972-2012 mean ± standard deviation). Also shown is runoff (flow/area), expressed in mm.

Flow contribution zone	**Area (km^2)**	**Summer Flow (km^3)**	**Summer Runoff (mm)**	**Winter Flow (km^3)**	**Winter Runoff (mm)**
Athabasca River at Ft McMurray	132 585	11.3±2.7	85.0±20.4	2.60±0.7	19.6±5.3
Peace River at Peace Point	293 000	27.0±8.4	92.0±28.8	20.45±2.7	69.8±9.2
Ft McMurray to Fitzgerald	180 415	7.9±4.5	43.8±24.9	8.57±3.7	47.5±20.6
Liard River at mouth	275 000	52.7±10.3	191.5±37.3	7.60±1.4	27.6±5.1
Fitzgerald to Ft Simpson	420 435	21.3±7.6	50.7±18.1	3.05±4.2	7.3±10.0
Great Bear River	146 400	5.98±0.6	40.8±4.1	6.69±0.7	45.7±4.8
Ft Simpson to Norman Wells	146 665	24.1±7.4	164.1±50.5	1.36±4.4	9.3±29.7
Norman Wells to Arctic Red R.	84 600	16.9±6.2	199.8±73.3	2.96±4.8	35.0±56.8
Total flow:					
*Mackenzie at Arctic Red R.**	1 679 100	166.6±21.4	99.2±12.8	52.7±7.5	31.4±4.5

**summer data available for 1973-2012; and only 30 years of winter data are available*

Sub-basin contribution depends on its drainage area and runoff (expressed in mm per unit area), the latter is indicative of the hydro-physiographic influence on flow production. With large snowmelt in early summer followed by much rainfall, mountain regions northward from the Liard and its tributaries are significant producers of summer runoff (>100 mm). The Athabasca also has high runoff in its mountain headwaters, especially with runoff from glacier melt; but runoff rate is diluted as the river encounters the Interior Plains downstream. The Peace lies mostly in the mountain areas but its discharge is highly regulated, so that its summer runoff can be rather variable, though still on the high side. Rivers from the Interior Plains and the Canadian Shield yield the lowest amount of runoff, partly attributable to much evaporation loss from their wetlands and lakes.

In the winter months, the mountain region generates more runoff through groundwater discharge, compared with the Plains. Most prominently, the regulated Peace discharges substantial winter runoff that averages 70 mm over the years, and two large lakes maintain continuous outflow in winter and due to storage effect. The combined amount of water released from Lake Athabasca and the Peace, and from Great Bear Lake is >45 mm and their runoff is about equal in both winter and summer. However, Great Slave Lake behaves differently, and its drainage area yields low winter runoff.

There are large yearly differences in the contribution of tributary flow to the main trunk of Mackenzie. To illustrate, such differences are summarized by the standard deviation values (Table 1). There is a tendency for the standard deviation to increase with the mean summer flow such that, for example, the Liard Basin with >50 km^3 of mean summer flow is accompanied by a standard deviation of >10 km^3whereas their respective values for Athabasca are about 11 and <3 km^3. However, this apparent relationship collapses completely in the winter. The Liard is no longer the largest flow contributor but the Peace River winter flow is the highest (20 km^3) despite its moderate amount of summer flow (27 km^3) relative to the Liard (53 km^3). The Peace has summer and winter standard deviations of about 8 and 3 km^3, which translate to coefficients of variations (CV) of 0.38 and 0.13. The low winter CV

may be due to relatively stable level of flow release for hydro-power production. In contrast, both the sections between Fitzgerald and Fort Simpson, and between Norman Wells and Arctic Red River have CV much exceeding 1.0 for winter flow, the former is boosted by several winters of fairly high winter outflow from Lake Athabasca (e.g. 1997, 1998) and the latter may be due to the baseflow that oscillated over the decades. The lowest CV of 0.1 for both seasons is reserved for Great Bear River, above which the substantial lake provides steady outflow.

6. CONCLUSIONS

The Mackenzie is the fourth largest circumpolar river, traversing a diversity of regions with different hydro-physiographical conditions. Seasonality brings about strong contrasts in the hydrological behaviour of this northern drainage system. In summer, streamflow responds directly to atmospheric forcing and basin environment, including evaporation, melt and rain events, adjusted locally by topography, vegetation, wetlands and lakes. Rivers that cross different hydrological provinces of the vast basin exhibit distinctive seasonal pattern of flow characteristic of the areas that they drain, though departures from the usual flow patterns do occur in some years. The flow of most rivers in wintertime is dominated by baseflow sustained mainly by groundwater, with ice condition that decouples hydrologic from atmospheric activities. Surface outflow is also maintained below sizable lakes and so the myriad lakes of the Canadian Shield and large lakes like the Great Bear contribute significantly. Human interference in the form of reservoir regulation yields recognizable effects, notably in the winter flow even of the main Mackenzie River.

In general, the largest difference between winter and summer flow processes is the dominance of subsurface flow under intense winter coldness and the switch to a prevalence of surface flow under open water conditions. In parts of the Mackenzie Basin, lake storage is a major modifier of the winter-summer flow contrasts, rendering the outflow to be more even during the year.

7. REFERENCES

Beltaos S. 2003 Threshold between mechanical and thermal breakup of river ice cover. *Cold Reg. Sci. Tech.* 37, 1–13.

Bradford, M.J. & Heinonen, J.S. 2008 Low flows, instream flow needs and fish ecology in small streams. *Can. Water Resour. J.* 33, 165-180.

Burn, D.H., Buttle, J.M., Caissie, D., MacCulloch, G., Spence, C. & Stahl, K. 2008 The processes, patterns and impacts of low flows across Canada. *Can. Water Resour. J.* 33, 107-124.

deRham, L.P., Prowse, T.D. & Bonsal, B.R. 2008 Temporal variations in river-ice break-up over the Mackenzie River Basin, Canada. *J. Hydrol.* 349, 441-454.

Peters, D.L. & Prowse, T.D. 2001 Regulation effects on the lower Peace River, Canada. *Hydrol. Proc.* 15, 3181–3194.

Peters, D.L., Prowse, T.D., Marsh, P., Lafleur, P.M. & Buttle, J.M. 2006 Persistence of water within perched basins of the Peace-Athabasca Delta, Northern Canada. *Wetl Ecol Manag.* 14, 221-243.

Prowse, T.D. & Carter, T. 2002 Significance of ice-induced storage to spring runoff: a case study of the Mackenzie River. *Hydrol. Proc.* 16, 779–788.

Rosenberg, H,B. & Pentland, R.L. 1966 Accuracy of winter streamflow records. Proceedings *23rd Eastern Snow Conference, Hartford, Connecticut, Feb. 10-11*, pp. 51-72.

Sung, R.Y-J., Burn, D.H. & Soulis, E.D. 2006 A case study of climate change impacts on navigation on the Mackenzie River. *Can. Water Resour. J.* 31, 57-68.

Woo, M.K. 2012. *Permafrost Hydrology*. Springer-Verlag, Berlin & Heidelberg.

Woo, M.K. & Thorne, R. 2003 Streamflow in the Mackenzie Basin, Canada. *Arctic* 56, 328-340.

Woo, M.K. & Thorne, R. 2014 Winter flows in the Mackenzie drainage system. *Arctic* 67, 238-256.

Symposium Abstracts

Lake-ice conditions as a control of under-ice productivity and oxygen levels in the Canadian Arctic: a review

David Barrett*[1], Terry Prowse[1 2], Fred Wrona[1]

[1]*Water and Climate Impacts Research Centre, Department of Geography, University of Victoria, Victoria, British Columbia, V8W 2Y2, CANADA*
[2]*Water and Climate Impacts Research Centre, Environment Canada, Victoria, British Columbia, V8W 2Y2, CANADA*
**dcbarrett@gmail.com*

ABSTRACT

The Canadian Arctic is experiencing heightened rates of environmental change at the current time. These changes in hydrologic and climate regimes have a direct impact on both a) the duration of ice-cover and b) the composition of the ice cover on Arctic lakes. Previous studies have examined the relationship between lake cover conditions, the quantity of photosynthetically active radiation (PAR) transmitted through to underlying freshwater and the consequences of PAR levels on oxygen levels throughout winter. During ice-on periods, underlying water is partially segregated from atmospheric conditions and this can have an impact on primary productivity by limiting oxygen diffusion and PAR availability. While some previous, simplistic models have been developed to look at under-ice oxygen levels, they have yet to be employed or validated to any great extent in this region. In an effort to lay the groundwork for ongoing future studies, this paper examines the current state of knowledge around under-ice lacustrine productivity through a systematic review of literature. Following the review of pertinent literature, we propose a method for developing a more accurate model of under-ice oxygen levels through a combination of controlled field experiments and the deployment of a remote lake monitoring system.

KEYWORDS

Under-ice productivity; PAR; dissolved oxygen; arctic limnology; light transmissivity;

Contextualizing Precipitation and Runoff Response over 20 Year: The Wolf Creek Experience

Sean K. Carey[1]*, Weigang Tang[1], J. Richard Janowicz[2]

[1]*School of Geography and Earth Sciences, McMaster University, Hamilton*, ON, L8S4K1 *CANADA*
[2]*Water Resources Branch, Yukon Department of Environment, Whitehorse, YT, Y1A2C6, CANADA*
**careysk@mcmaster.ca*

ABSTRACT

High latitude environments are particularly sensitive to climate change due to the importance the zero-degree isotherm plays in controlling precipitation phase, storage, and the nature of frozen ground. Precipitation-runoff patterns in mountainous subarctic watersheds are typically described to have nival regimes and where present, permafrost exhibits a strong control on the timing, volume and pathways of runoff. However, under warming conditions, a shift from a snowmelt to a more rainfall dominated flow regime is underway, and the sensitivity of individual catchments to this change is dependent upon their intrinsic watershed features and extrinsic climate factors. The objective of this paper is to evaluate approximately 20 years of meteorological and hydrometric data from Wolf Creek Research Basin (WCRB), Yukon, and assess its sensitivity to change in a comparative framework. Over 100 precipitation-runoff hydrographs are analyzed among three WCRB watersheds for common characteristics using a new automated hydrograph analysis toolbox. The nature of individual precipitation-runoff events are placed in the context of a catchment thermal and wetness state and patterns identified. On an annual basis, the sensitivity of streamflow timing and volume to precipitation fraction as snow or rain and seasonal delivery is evaluated. Results indicate that of precipitation timing as opposed to phase has a more profound influence on runoff in WCRB. Finally, comparing WCRB with other northern Canadian research watersheds suggests a common pattern where rainfall is becoming increasingly important both on event and annual scales of streamflow response.

KEYWORDS

Runoff; hydrograph analysis; precipitation; climate change; subarctic

Arctic-HYCOS: a hydrological cycle observing system for improved monitoring of freshwater fluxes to the Arctic Ocean

David Gustafsson[1], Al Pietroniro[2], Johanna Korhonen[3], Ulrich Looser[4], Jórunn Hardardóttir[5], Morten Johnsrud[6], Valery Vuglinsky[7], Berit Arheimer[1], Harry F. Lins[8], Jeffrey S. Conaway[9], Richard Lammers[10], Bruce Stewart[11], Tommaso Abrate[11], Paul Pilon[11], Daniel Sighomnou[11]

[1]*Swedish Meteorological and Hydrological Institute, Norrköping, SWEDEN*

[2]*Meteorological Service of Canada, National Hydrology Research Centre, Saskatoon, CANADA*

[3]*Finnish Environment Institute, Helsinki, FINLAND*

[4]*Global Runoff Data Centre, Federal Institute of Hydrology, Koblenz, GERMANY*

[5]*Icelandic Meteorological Office, Reykjavik, ICELAND*

[6]*Norwegian water and energy directorate, Oslo, NORWAY*

[7]*State Hydrological Institute, St Petersburg, RUSSIA*

[8]*U.S. Geological Survey, Reston, VA, USA*

[9]*U.S. Geological Survey, Anchorage, Alaska, USA*

[10]*University of New Hampshire, Durham, NA, USA*

[11]*World Meteorological Organization, Geneva, SWITZERLAND*

ABSTRACT

The Arctic region is an important regulating component of the global climate system, and is also experiencing a considerable change during recent decades. More than 10% of world's river-runoff flows to the Arctic Ocean and there is evidence of changes in its fresh-water balance. However, about 30% of the Arctic basin is still ungauged, with differing monitoring practices and data availability from the countries in the region. A consistent system for monitoring and sharing of hydrological information throughout the Arctic region is thus of highest interest for further studies and monitoring of the freshwater flux to the Arctic Ocean.

The purpose of the Arctic-HYCOS project is to allow for collection and sharing of hydrological data, and to make possible the following scientific goals: 1) to evaluate freshwater flux to the Arctic Ocean and Seas, 2) to monitor changes and enhance understanding of the hydrological regime and 3) to estimate flows in ungauged regions and develop models for enhanced hydrological prediction in the Arctic region. The project is intended as a component of the WMO WHYCOS (World Hydrological Cycle Observing System) network, covering the area of the expansive transnational Arctic basin with participation from Canada, Denmark, Finland, Iceland, Norway, Russian Federation, Sweden and United States of America. The overall objective is to regularly collect, manage and share high quality data from a defined basic network of hydrological stations in the Arctic basin, focusing on daily discharge and daily water temperature data. Data should be provisional in near-real time if available, whereas time-series of historical data should be provided once quality assurance has been completed.

The initial stages of the project will focus on collecting data on discharge and revise station selection criteria. For monitoring freshwater flow to oceans, stations close to the mouths of rivers and immediately inland for back-up purposes will be preferred. For studies of change the working group placed emphasis on hydrological regime stations located in headwaters

small sub-catchments, including pristine basins. Stations outside the Arctic Ocean basin, such as at the mouth of the Yukon River, Baltic Sea and Hudson Bay, can also be considered to allow a better understanding of hydrological processes occurring in the general region. Countries shall facilitate, to the extent possible, access to their data currently published online, and also access to those not yet regularly published on the web. At a later stage data exchange standards such as WaterML2.0 will be implemented. The project will also perform pan-Arctic hydrological modelling (geo-statistical, deterministic and probabilistic methods) for the assessment and integration of observational and modelled data to improve estimates of ungauged discharge and the overall estimates of freshwater flux to the Arctic Ocean, as well as understanding of hydrological processes. A first version of the Arctic-HYPE model has been set-up with some 32 000 subbasins for the entire Arctic basin.

Atmospheric Circulation Patterns Influencing Duration of Oulu-Hailuoto Ice Road in Finland

Masoud Irannezhad* and Bjørn Kløve

Water Resources and Environmental Engineering Research Group, Faculty of Technology, 90014 University of Oulu, FINLAND
**masoud.irannezhad@oulu.fi*

ABSTRACT

In Finland, Oulu-Hailouto ice road, with a total length of 9 km, links Oulu city in Northern Ostrobothnia and Hailuoto Island in the province of Oulu. The ice road was usually used 4-5 months a year, while now only 4-5 weeks. To explain such changes, growing attention has been recently paid on relationships between atmospheric circulation patterns manifesting natural climate variability over a region and annual anomalies of ice road opening time. Hence, this study analysed interannual variations, periodicity and trend in the duration of Oulu-Hailuoto ice road during 1973-2013 and its relationships with well-known atmospheric circulation patterns (ACPs) over the Northern Hemisphere. The Mann-Kendall non parametric test was used to detect statistically significant ($p<0.05$) trend in the duration of Oulu-Hailuoto ice road; Fourier series fitting method to determine a possible cyclic pattern; and Spearman rank correlation to measure relationships with ACPs. In average, the duration of Oulu-Hailuoto ice road was about 71 days over the study period (1973-2013). The longest duration was 128 days in 1987 and the shortest was 6 days in 2001. At 5% significance level, trend analysis determined a shortening of 1.54 days per year in the duration of ice road over the period 1973-2013. The Fourier series estimated a time cycle of 45 years ($R^2=0.40$) for a long-short mode of Oulu-Hailuoto ice road duration. Arctic Oscillation (AO), recognizing as most influential ACP on temperature in Finland, was also the most significant ACP affecting variations in the duration of Oulu-Hailuoto ice road in Finland ($rho=-0.35$, $p<0.05$).

KEYWORDS

Atmospheric circulation; climate variability; ice road; Finland

Links between Changes in Ratio of Snow to Total Precipitation in Finland and Atmospheric Teleconnection Patterns

Masoud Irannezhad*, Anna-Kaisa Ronkanen and Bjørn Kløve

[1]*Water Resources and Environmental Engineering Research Group, Faculty of Technology, 90014 University of Oulu, FINLAND*

**masoud.irannezhad@oulu.fi*

ABSTRACT

As a sensitive hydrologic indicator to climate variability, ratio of snow to total precipitation (S/P) can be used to detect climate change, particularly in boreal regions. This study used simulated daily (S/P) ratio in water years (September-August) during 1909-2008 at Kaisaniemi, Kajaani and Sodankylä stations in southern, central and northern Finland, respectively, based on temperature-index snowmelt model. The Mann-Kendall non parametric test was used to detect statistically significant ($p<0.05$) trends in annual S/P ratio time series. The Spearman rank correlation was applied to measure links between the S/P ratio and well-known atmospheric teleconnection patterns (ATPs) over the Northern Hemisphere. In average, 27% of total precipitation at Kaisaniemi, 46% at Kajaani and 52% at Sodankylä occurred as snow during 1909-2008. The S/P showed a decrease of 5% at Kaisaniemi during the period 1909-2008, but no clear trend at Kajaani and Sodankylä. Variability of the S/P ratio was most significantly associated with Arctic Oscillation (AO) at Kaisaniemi (rho = -0.56, $p<0.05$), while with Polar (POL) pattern at Kajaani (rho = 0.36, $p<0.05$) and Sodankylä (rho = 0.22, $p<0.1$). These highlighted that increased precipitation over northern Europe has played an important role in offsetting snow resource declines resulted from changes in precipitation falling form from snow to rain under climate warming.

KEYWORDS

S/P ratio; trend analysis; teleconnection; Finland

National Scale Assessment of Growing Season Climate in Finland in Relation to Atmospheric Circulation Patterns, 1961-2011

Masoud Irannezhad* and Bjørn Kløve

[1]*Water Resources and Environmental Engineering Research Group, Faculty of Technology, 90014 University of Oulu, FINLAND*
**masoud.irannezhad@oulu.fi*

ABSTRACT

Interannual variability and trends in growing season (GS) climate in terms of sum daily temperature (GST) and precipitation (GSP) on a national scale of Finland during 1961-2011 were analysed using daily temperature and precipitation datasets from regular grid points (10*10 km^2). To detect statistically significant ($p<0.05$) trends in GST and GSP, the Mann-Kendal non-parametric test was applied. The Spearman rank correlation was used to measure correlations of GST and GSP with some of well-known atmospheric circulation patterns (ACPs) over the Northern Hemisphere. The length of GS in Finland naturally increases from north to south, in association with earlier GS start and later GS end days. On nation-wide of Finland, the results determined that long-term average value for GST was 1538°C and for GSP was 223.2 mm. GST and GSP on a national-scale of Finland were significantly ($p<0.05$) increased by 0.40 (°C/day) and 1.39 (mm/day) during 1961-2011. On a nation-wide of the country, the most significant influential ACP on GST variability was the East Atlantic (EA) pattern (rho = 0.40), while on GSP variability was the East Atlantic/West Russia (EA/WR) pattern (rho = -0.54). The results provide a detailed national scale changes in GS climate over Finland during 1961-2011 and reveal that the interannual variations in GSS and GSP in Finland are strongly controlled by the EA and EA/WR patterns.

KEYWORDS

Growing season climate; sum daily temperature; precipitation; trend; atmospheric circulation; Finland

Trends and Regime Shift in Snow Days in Finland, 1909-2008

Masoud Irannezhad* and Bjørn Kløve

Water Resources and Environmental Engineering Research Group, Faculty of Technology, 90014 University of Oulu, FINLAND

**masoud.irannezhad@oulu.fi*

ABSTRACT

Snow days (SD) as the number of days with snow water equivalent (SWE) larger than a given threshold play a key role in climate system and hydrological cycle by interacting spatio-temporally with surface thermal energy, soil thermal conditions and atmospheric dynamics. This study used long-term (1909-2008) simulated daily SWE time series based on temperature-index snowmelt model at Kaisaniemi, Kajaani and Sodankylä stations in south, centre and north of Finland, respectively. Days with simulated SWE > 0 mm were defined as possible SD (PSD), > 2.5 mm as shallow SD (SSD) and > 7.5 mm as deep SD (DSD). The Mann-Kendall (MK) non parametric test to detect statistically significant ($p<0.05$) trends at each station and the sequential t-test analysis of regime shift (STARS) to determine possible transitions in annual PSD, SSD and DSD over Finland were used. In average, PSD, SSD and DSD were about 161, 143 and 132 days at Kaisaniemi; 200, 193 and 184 days at Kajaani; and 227, 219 and 212 days at Sodankylä, respectively. At both Kaisaniemi and Sodankylä, all PSD, SSD and DSD showed statistically significant ($p<0.05$) decreasing trends (ranging from -0.45 to -0.27 days/year) during 1909-2008. At Kajaani, PSD decreased by 0.12 (days/year, $p<0.05$), while no clear trend was found in SSD and DSD. In Finland, 1926 was a positive shift point for PSD by 21 days, SSD by 18 days and DSD by 16 days; but 2006 was a negative shift point by 22, 27 and 32 days for PSD, SSD, and DSD respectively.

KEYWORDS

Trend; regime shift; snow day; Finland

Impacts of Climate Warming on the Hydrologic Response of River Ice, Permafrost and Glacier Regimes of Northwestern Canada

J Richard Janowicz

Water Resources Branch, Yukon Department of Environment, Whitehorse, YT, Y1A2C6, CANADA
**richard.janowicz@gov.yk.ca*

ABSTRACT

Hydrologic response in Northwestern Canada is largely a nival process with secondary summer rainfall influences, which may produce the annual peak flow on smaller streams. Early spring snowmelt driven discharge events initiate river ice break-up, which may produce ice jams and associated flooding, which often produce the annual peak water level. Minimum annual discharge occurs in March or April, coinciding in timing to minimum annual groundwater inputs. Western regions of the study region have significant glacier and ice cap coverage. Unlike nival regimes which experience their peak flow in May or June due to snowmelt, peak flows in glacierized basins are delayed until later in the summer due to supplemental inputs from glacier melt.

Permafrost has a dominant control over hydrologic response in northern regions by producing short pathways to the stream channel with little interaction with subsurface processes. A thicker active layer increases residence time and promotes a longer pathway to the stream channel, as compared to a more rapid response of near surface flow. The hydrologic response of northwestern Canada follows this principle, and is closely tied to the underlying permafrost. While precipitation decreases in higher latitudes, the ratio of runoff to precipitation generally increases due to the increasing dominance of the underlying permafrost. The exception is observed in glacierized basins of the study region. Since glacial regimes originate in mountainous regions with high annual precipitation amounts, they also tend to have the highest annual streamflow volumes. The opposite trend generally applies to minimum winter flows which decrease moving northwards as a result of lesser groundwater contributions due to the increasing control exerted by the underlying permafrost. In Arctic regions, only large rivers have any appreciable winter flows, while in discontinuous permafrost regions, even small streams may display extended streamflow throughout the winter due to continued groundwater contributions.

Annual, winter and summer air temperatures have generally increased throughout the study region in the last few decades, with greater increases observed in central and northern areas. Annual precipitation trends are not consistent. Winter precipitation has generally increased in northern regions and decreased in southern regions. Summer precipitation has generally increased slightly throughout, with greater increases observed in southeast and central regions.

Higher winter and spring air temperatures are producing an earlier onset of, and more rapid snowmelt events, resulting in a compressed runoff period with higher peak flows in some regions. The warming climate is also having a significant impact on ice regimes with earlier occurrence of break-up, later freeze-up and a shorter ice cover period. Mid-winter break-up events and associated flooding is becoming more common, especially in transitional areas. Some break-up water level trends suggest that break-up severity is increasing. In addition examples of combined break-up and freshet generated water level peak stages have been observed.

The warming climate also appears to be resulting in a change in the permafrost and glacier distributions of the study region. Permafrost warming and the associated thaw results in a thicker active layer and permafrost loss in favourable areas. As permafrost properties change with climate warming, hydrologic response appears to be changing as well. Degrading permafrost increases the thickness of the active layer, decreases the overall thickness of the permafrost and in certain areas eliminates the presence of underlying permafrost entirely. These actions place a greater reliance on the interaction between surface and subsurface processes. The impact of climate warming on glacial regimes has been observed to be significant. On a regional basis glaciers throughout western North America have generally retreated since the Little Ice Age. Melting glaciers and ice caps are likewise altering hydrologic response by increasing runoff and altering its distribution.

Observations of the last few decades indicate that annual mean flows have increased within most permafrost zones, with some variability within sporadic permafrost regions. Annual peak flows have decreased within some continuous permafrost regions, and lesser so within discontinuous regions with variable trends within sporadic permafrost zones. Winter low flows have experienced significant increases within continuous and discontinuous permafrost regions over the last three decades with variable trends within sporadic permafrost regions.

Streamflow response trends of the glacierized drainage basins within the sporadic and discontinuous permafrost zones of southwestern Yukon indicate an increasing trend of both mean and minimum annual discharge throughout the study region, while trends of annual maximum discharge are more variable, with the majority of streams exhibiting an increasing trend while some have significant decreasing trends. Glacierized basins with little permafrost seem to exhibit classic glacial response trend characteristics, while those with significant amounts of permafrost seem to exhibit more classic permafrost response trends. Other glacierized basins with variable amounts of permafrost have overlapping signals exhibiting mixed streamflow trends which are difficult to interpret.

KEYWORDS
nival processes; permafrost regimes; glacierized basins; river ice break-up; climate warming

Long-term historical data on hydrological cycle in small watersheds in Siberia as a key to understand runoff formation in permafrost environment

Lebedeva L.[1*], Semenova O.[2, 3]

[1]*Laboratory of Permafrost Groundwater and Geochemistry, Melnikov Permafrost Institute, Yakutsk, 677010, RUSSIA*
[2]*Gidrotehproekt Ltd., St. Petersburg, 194223, RUSSIA*
[3]*St. Petersburg State University, St. Petersburg, 199178, RUSSIA*

**lyudmilaslebedeva@gmail.com*

Heat and water fluxes are inherently linked in Arctic river basins. Dynamic position of freezing/thawing front that usually behaves as aquifuge controls water exchange between subsurface, subsurface and ground flow. Ground ice could play role of additional storage of water in the basin and affect flow distribution between seasons and years. Diversity and temporal non-stationarity of hydrological processes in cold regions is not well-understood yet. Continuous long-term data on hydrological variables and permafrost characteristics is especially valuable for development of process-based models that could explain present-day situation and project future changes.

The goal of the study was to apply process-based hydrological model Hydrograph to two sets of small research watersheds situated in continuous and discontinuous permafrost zone. The Hydrograph model describes not only all essential processes of land hydrological cycle but also explicitly accounts for soil heat dynamics and water phase changes. Main model parameters refer to observable soil and vegetation properties. It brings the advantage to the Hydrograph model in comparison to parameters calibration approach.

Observational data and related soil and vegetation information collected at the Kolyma and Bomnak research sites representing continuous and discontinuous permafrost environments were used to develop and verify the parameter sets for typical (representative) permafrost landscapes. Kolyma and Bomnak stations are unique research spots for Russian permafrost zone in terms of both length and comprehensiveness of hydrology-related observations. They were monitored for 1948-1990 and 1934-1968 years respectively. Each station includes a set of nested and adjacent gauged watersheds with an area ranging from 0.017 km^2 to 21.8 km^2. Smaller watersheds are homogeneous in terms of meteorological input and landscapes; larger ones combine several land surface types and are representative for surrounding regions. Besides discharge and basic meteorological measurements ground freeze/thaw depths, groundwater levels, soil, water and snow evaporation, hydrochemistry were monitored at the Kolyma and Bomnak water-balance stations.

The model was tested against river discharges and point observations of above-listed characteristics in bare rocks, mountain tundra, sparse larch forest, wet larch forest, birch forest and bogs.

Data analysis and modelling results showed that interactions between permafrost and hydrology depend on predominant landscapes that are highly variable in the permafrost environments.

At Kolyma station groundwater flow is formed in thawed active layer in summer period only. In winter ground is completely frozen with exception of near-channel talik. Permanent

groundwater flow occurs in summer in river valley and low parts of the slopes where the ground thawing depth reaches 0.5-1 m. At higher slopes and bare rocks plateau ground thaws up to 1.5-2 m depth and groundwater flow occurs sporadically after intense precipitation only. At Bomnak site unmerged permafrost is formed when ground freezing depth in winter is shallower than permafrost surface. Since thawing depth in summer reaches talik active layer water has a direct connection with talik groundwater. As a consequence river flow in the second half of the summer in watersheds with unmerged permafrost is much less than at the adjacent permafrost-covered basin due to water losses to deep groundwater horizons.

Seasonal dynamics of groundwater is controlled by precipitation, snowmelt, evaporation and seasonal thawing and freezing. Active layer development causes aquifuge deepening and groundwater level decrease. Such mechanism is a specific for permafrost zone.

Modelled and observed SWE, thawing/freezing depths and hydrographs satisfactorily agree in all studied watersheds. Modelling results show that surface flow occurs when the ground is frozen and ice-saturated.

Robust parameterization and separately validated process-based model algorithms using long-term historical data series serve as a base for understanding of current state and projecting of future changes of hydrological system in Arctic basins.

The reported study was partially supported by RFBR, research project No. 15-35-21146.

High Resolution Snowdrift Simulations: Application to Polar Bears and Arctic Hydrology

Glen E. Liston

Cooperative Institute for Research in the Atmosphere (CIRA), Colorado State University, Fort Collins, Colorado, 80523-1375, USA
**Glen.Liston@ColoState.Edu*

ABSTRACT

Throughout the Arctic most pregnant polar bears (*Ursus maritimus*) construct maternity dens in seasonal snowdrifts that form in wind-shadowed areas. We developed and verified a spatial snowdrift polar bear den habitat model (SnowDens-3D) that predicts snowdrift locations and depths along Alaska's Beaufort Sea coast. SnowDens-3D integrated snow physics, weather data, and a high-resolution digital elevation model (DEM) to produce predictions of the timing, distribution, and growth of snowdrifts suitable for polar bear dens. SnowDens-3D assimilated 18 winters (1995 through 2012) of observed daily meteorological data and a 2.5 m grid-increment DEM covering 337.5 km^2 of the Beaufort Sea coast, and described the snowdrift depth distributions on 30 November of each winter to approximate the timing of polar bear den entrance. In this region of Alaska, winds that transport snow come from two dominant directions: approximately NE to E (40°T to 110°T) and SW to W (210°T to 280°T). These wind directions control the formation and location of snowdrifts. In this area, the terrestrial, coastal mainland and barrier island banks where polar bears den are often ≤ 3 m high, limiting snowdrift depths to ≤ 2 m deep. We compared observed den locations (n=55) with model-simulated snow-depth distributions for these 18 winters. For the 31 den locations where position accuracy estimates were available in the original field notes, 29 locations (97%) had a simulated snowdrift suitable for denning within that distance. In addition, the model replicated the observed inter-annual variability in snowdrift size and location at historical den sites, suggesting it simulates interactions between the terrain and annual weather factors that produce the snowdrifts polar bears use for dens. The area of viable den habitat ranged from 0.0 ha to 7.6 ha (0.00% to 0.02% of the 337.5 km^2 simulation domain), depending on the winter. SnowDens-3D is available to help management agencies and industry improve their prediction of current polar bear den sites in order to reduce disturbance of denning bears by winter recreational and industrial activities.

KEYWORDS

Den habitat; model; polar bear; SnowDens-3D; snowdrift; weather

Trends in ice phenology of Estonian rivers

Tiia Pedusaar[1*], Tiina Nõges[2], Peeter Nõges[2], Liidia Klaus[1]

[1] *Estonian Environment Agency, Hydrology Department, Mustamäe tee 33, 10616 Tallinn, ESTONIA*

[2] *Estonian University of Life Sciences, Centre for Limnology, Institute of Agrigultural and Environmental Sciences, 61117, Rannu, Tartu County, Estonia*

**tiia.pedusaar@envir.ee*

ABSTRACT

This study was initially motivated by changes in the national hydrometric network. Due to automatization, several manual observations, including ice conditions, stopped. Therefore, there is time to analyse and summarize collected homogenous data series. At the same time, long term records of ice phenology, the timing of freeze and breakup, and ice cover duration have proven to be useful indicators of climate change. Ice phenology is sensitive to both water body-specific characteristics and broader scale meteorological variables.

Documentation of ice conditions in Estonia started with first systematic hydrological observations in the 1920s. Observers of hydrometric stations made visual ice observations at agreed sites and time every day since the first ice phenomena in autumn until the last ice phenomena in spring. The methodology for summarizing ice observations has been the same providing highly valuable long-term ice time-series for eighty years or longer.

The aim of the study is to show long-term and most recent trends in ice phenology of Estonian rivers from different hydrogeological areas and find relationship with air and water temperature.

The initial data analysis has shown decreasing trends in the duration of ice cover caused by both – an earlier ice-off and a later ice-on – which are consistent with recent findings about the northern hemisphere ice regime.

An Overview of the 2013 Yukon River Flood and the Resulting Development of River Ice and Flood Extent Products Derived from Suomi NPP VIIRS Satellite Data

Edward Plumb[1*], Sanmei Li[2], Melissa Kreller[1], Eric Holloway[3]

[1]*National Oceanic and Atmospheric Administration, National Weather Service, Fairbanks, AK, 99775, USA*
[2]*Dept. of Geography and Geo-Information Science, George Mason University, Fairfax, VA, 22030, USA*
[3]*National Oceanic and Atmospheric Administration, Alaska-Pacific River Forecast Center, Anchorage, AK, 99502, USA*
**edward.plumb@noaa.gov*

ABSTRACT

The 2013 spring ice breakup of the Yukon River in Alaska resulted in destructive flooding in several communities. Large ice jams dammed the Yukon River and created massive lakes as the river inundated the surrounding floodplain. The village of Galena experienced record flooding as water and ice surged overbank and damaged or destroyed much of the community. The lack of river ice data during spring break-up creates many forecast challenges for National Weather Service (NWS) hydrologists in Alaska. Limited and infrequent ice condition observations are provided by river observers, community officials, pilots, and the public. Although these observations are invaluable, there are extensive spatial and temporal data gaps across Alaska during spring break-up. Suomi NPP Visible Infrared Imaging Radiometer Suite (VIIRS) satellite imagery was found to be a highly effective tool to identify flooding as a result of ice jams along the Yukon River. The VIIRS imagery provided critical decision making information to NWS forecasters responsible for issuing flood warnings for the region. The 2013 flooding initiated the development of real-time, satellite derived river ice and areal flood extent products available to NWS forecasters. Since 2013, the NWS in Alaska continues to evaluate the potential use of these new and innovative products in an operational forecast setting.

KEYWORDS

Forecasting; hydrology; flooding; ice jam; river breakup; satellite remote sensing

Using an Iridium Satellite Telemetered Gage (iGage) for Hydrologic, Snowfall, and Coastal Storm Surge Measurements to Support Forecast Operations in Alaska

Edward Plumb[1*] and Crane Johnson[2]

[1]*National Oceanic and Atmospheric Administration, National Weather Service, Fairbanks, AK, 99775, USA*
[2]*National Oceanic and Atmospheric Administration, Alaska-Pacific River Forecast Center, Anchorage, AK, 99502, USA*
**edward.plumb@noaa.gov*

ABSTRACT

Data sparseness in Alaska poses a challenge for National Weather Service (NWS) meteorologists and hydrologists responsible for the forecasting of hazardous weather and flooding conditions. Reliable real-time hydrometeorlogic data is critical information needed by forecasters when issuing warnings to the public for river or coastal flooding, heavy snow events, and other hazardous weather.

In cooperation with the U.S. Army Corps of Engineers and the State of Alaska, the NWS developed and tested a compact, low cost, ultrasonic iridium satellite telemetered gage (iGage) that has been used to measure hourly snow depth, river stage, and coastal water levels. The iGage is battery and solar powered and can quickly be mounted to a static structure over a water or snow surface. The NWS has successfully installed the iGage on highway bridges across Alaska during the summer open-water season and now receives stage data on previously ungaged rivers and streams. The iGage is removed from the bridges in the autumn and deployed elsewhere to provide forecasters with hourly snowfall and snow depth in the winter. In addition, iGages have been mounted on bridges over estuaries in coastal Alaska and provide tidal and storm surge data during the fall Bering Sea storm season. During the summer of 2015, the NWS will test an iGage that will take oblique river stage measurements from a stationary position on a riverbank.

The operational use of the iGage by the NWS in Alaska has improved forecaster situational awareness, decision support services for customers and stakeholders, and verification of hazardous weather events.

KEYWORDS

Forecasting; meteorology; hydrology; flooding; coastal floods; decision support services

The Arctic Freshwater Synthesis (AFS): Foci, Results and Future Research Priorities

Prowse, T.[1*], Bring, A.[2], Carmack, E.[3], Karlsson, J.[4]

[1] *Water and Climate Impacts Research Centre, Environment Canada/University of Victoria, Victoria, BC, CANADA*
[2] *Institute for the Study of Earth, Oceans and Space, University of New Hampshire, Durham, New Hampshire, USA*
[3] *Institute of Ocean Sciences, Fisheries and Oceans Canada, Sidney, BC, CANADA*
[4] *Department of Physical Geography, Stockholm University, Stockholm, SWEDEN*
**Terry.Prowse@ec.gc.ca*

ABSTRACT

There is increasing scientific recognition that changes to the Arctic freshwater systems have produced, and could produce even greater, changes to bio-geophysical and socio-economic systems of special importance to northern residents and also produce some extra-Arctic effects that will have global consequences. In recognition of such concerns, three international organizations, the World Climate Research Program's Climate and Cryosphere Project (WCRP-CliC), the International Arctic Science Committee (IASC), and the Arctic Council's Arctic Monitoring and Assessment Program (AMAP), jointly initiated a scientific assessment entitled the "*Arctic Freshwater Synthesis* (AFS)", which focused on assessing the various Arctic freshwater sources, fluxes, storages and effects. The AFS was organized into 6 major Components including: i) Oceans; ii) Atmosphere; iii) Terrestrial Hydrology; iv) Terrestrial Ecology; v) Resources and vi) Modelling. Each Component was led by two co-Leads and supported by a team of international co-authors. Notably, at the 19th NRB in Alaska, a NRB Working Group was identified that could contribute to the goals of the AFS Resources Component and two NRB members subsequently became co-authors of this Component. In considering historical and projected future changes in the various freshwater components, synergistic roles among components, and the overall freshwater budget, the assessment also evaluated effects on: i) regional and global climate, ii) biological productivity and biodiversity, and iii) human and economic systems. This presentation reviews the major findings of each AFS Component, examines important synergistic processes/effects among Components, and identifies key priorities for future research.

KEYWORDS

Arctic freshwater; oceans; atmosphere; terrestrial hydrology; terrestrial ecology; resources; modelling; regional climate; global climate; biological productivity; biodiversity

Long-term Changes in Sea Ice in the Baltic Sea

Iina Ronkainen*, Jari Haapala and Byoung Woong An

Marine Research, Finnish Meteorological Institute, Helsinki, 00101, FINLAND
**iina.ronkainen@fmi.fi*

ABSTRACT

The duration of the ice season is 5-7 months in the Baltic Sea. The amount of seasonal ice varies significantly from year to year. However, in the last 100 years there has been a decreasing trend in the ice occurrence, which has resulted from the climate warming. In this study observations and model results were analyzed in order to find the long-term ice statistics, the changes in ice conditions and the underlying reasons for these changes. Three observation stations along the Finnish coast were chosen: Kemi, Utö and Loviisa. The used time series were 120 years long and included the dates of freezing and break-up, the length of ice season and the maximum annual ice thickness. The used model was NEMO/LIM-3 and the modeled time 1961-2007. The probability of ice occurrence has been decreasing in Utö and is now 81%. In Kemi and Loviisa the probability is still 100%. The freezing date has become 12-24 days later, while the break-up date has taken place 10-20 days earlier per century. The trend of maximum annual ice thickness is increasing in Kemi and decreasing in Loviisa. According to the model, the maximum annual ice thickness has decreased also in Kemi. The trend of modeled maximum annual ice volume is decreasing in the entire Baltic Sea and also in different basins. The modeled ice volume correlates well with the observed maximum annual ice extent even though the ice volume has bigger inter-annual variations.

KEYWORDS

Sea ice; Baltic Sea; climate change

The value of hydrological information – examples from the hydropower industry

Knut Sand*

Statkraft Energi AS, Trondheim, N-7005, NORWAY
**Knut.Sand@statkraft.com*

ABSTRACT

Statkraft, as the third largest power company in the Nordic, had during 2013 a production from hydropower in Norway and Sweden of 44 TWh. This is approximately 16% of the total energy production in the two countries. The generation of hydropower comes from 330 hydropower plants with installed capacity varying from 3 to 1240 MW.

The inflow forecasting system consists of 147 individual HBV-models which provide daily updates of the hydrological conditions in the drainage basins as well as inflow forecasts for the hydropower reservoirs. During the entire period of snow on the ground, regular, representative and accurate hydro-meteorological data are crucial in order to simulate an accurate development of the drainage basin water budgets. For updating the HBV-models Statkraft uses observation of precipitation and temperature from more than 200 strategically located weather stations. Erroneous or missing observations will cause false input to the HBV-models and give wrong estimates of snow storage, soil moisture and groundwater storage in the models. Consequently, the long term inflow forecasts to the hydropower reservoirs may be considerably wrong and the energy management will not be successful. Over the years, Statkraft has had some experiences with consequences of erroneous or missing observation causing fatal decisions in energy management. In order to visualise the value of hydrological observations the cost of some of these incidents have been analysed. Based on the knowledge gained from such examples Statkraft is now trying to develop general methods for assessing the value of hydrological data.

KEYWORDS

Hydrology; hydrological data; hydropower production; economic value

Hydrologic Observations of Low-gradient Alaskan Arctic Watersheds

Svetlana L. Stuefer*, Anna Liljedahl and Douglas L. Kane

Water and Environmental Research Center & Department of Civil and Environmental Engineering, University of Alaska Fairbanks, Fairbanks, Alaska 99775, USA
**sveta.stuefer@alaska.edu*

ABSTRACT

Broad coastal areas that drain into the Arctic seas have low-gradient drainages that are poorly gauged and rarely included in the estimates of the freshwater input into the Arctic Ocean. This study uses research observational dataset from Alaskan Arctic to quantify the freshwater input into the adjacent part of the Beaufort Sea and to document hydrologic runoff response of low-gradient drainages to snowmelt and warm season precipitation across different spatial scales. Four low-gradient drainages that are being studied range in watershed areas from 0.025 km^2 to 471 km^2. Streamflow observations for the largest stream go back to 1999 and continue to 2014, while other streams have shorter period of record starting in 2007. In addition to the discharge, a suite of supporting hydrometeorological information is analysed including precipitation, repeated snow surveys, ablation measurements, water levels within ice wedge polygonal terrain, air temperature, radiation, wind, soil moisture, soil temperature and active layer depths. As with the large Arctic Rivers, most of the surface runoff is delivered to the Beaufort Sea during the snowmelt period. Water balance partitioning shows that evapotranspiration remains the main loss of water during the summer months. Recent climate modelling studies relate future increases in Arctic precipitation to local evaporation and sea-ice retreat. Under this scenario, coastal low-gradient watersheds, presented here, emerge as a new region that is likely to undergo significant hydrological changes.

KEYWORDS

Arctic; low-gradient watersheds; snow; permafrost; precipitation

Glaciers and ice caps: A disappearing water resource?

Thorsteinn Thorsteinsson*, Tómas Jóhannesson and Árni Snorrason

Icelandic Meteorological Office, Bústaðavegur 7-9, 108 Reykjavík, ICELAND

**thor@vedur.is*

ABSTRACT

Glaciers and ice caps are present at high latitudes and/or high altitudes in most parts of the world. Glacier volumes have been declining since the late 19th century and melting rates have generally increased in the past 20 years. According to recent climate scenarios for the Nordic region, glaciers in Iceland and Scandinavia are projected to mostly disappear within the 21st and 22nd centuries, leading to a sea-level increase of 1 cm. The projected changes will lead to increased glacier runoff until the mid-21st century, but declining runoff levels at later stages. Hydropower production utilizing glacial meltwater will thus need to be adjusted during the coming decades according to the level of glacial melt available at any time. In some parts of the world, declining levels of spring snowmelt and summer glacial melt are projected to affect crop yields in mountain regions.

In order to monitor these important changes, the World Meteorological Organization (WMO) has initiated a new international mechanism for supporting in-situ and remote sensing observations of the cryosphere, including glaciers and ice caps. The WMO´s Global Cryosphere Watch (GCW) will provide data and analyses on the past, current and future state of the cryosphere. A key element of GCW is a network of surface-based stations, Cryonet, for the monitoring of single or multiple components of the cryosphere, including snow depth and glacier mass balance.

Winter limnology eutrophication process: investigation on two Nordic Lakes from Finland and northern China

Fang Yang*[1,2], Matti Leppäranta[1], Ioanna Merkouriadi[1]

[1]*Department of Physics, University of Helsinki, Helsinki 00014, FINLAND*
[2]*Water Conservancy and Civil Engineering College, Inner Mongolia Agricultural University, Hohhot 010018, CHINA*
**ffff.yyyy@sina.com*

ABSTRACT

Eutrophication problem has become the primary pollution facing global water environment today. Especially in Nordic area, ice cover turns to be important infector of eutrophication process in shallow lakes during winter time. The present study aims to evaluate the ice cover effects of lake evolutionary process and nutrients migration in eutrophic shallow lakes, Vanajavesi Lake (Hämeenlinna, Finland) and Ulansuhai Lake (Inner Mongolia, China). In this paper, we discussed heat flux and freezing-degree-day coefficients and ice growth of those two lakes, depending on snow and free-snow during winter time. Using field sampling data of ice cores and liquid water, it analyzed inter-relationship between ice cover and liquid water with nutrients balance, dissolved oxygen condition and primary production. This paper improves our understanding of ice cover is an essential element of water environment in boreal zoon, and will improve management methods for eutrophic lakes under cold climate.

Investigation of the climate impact on the snow and ice thickness in Lake Vanajavesi, Finland

Yu Yang[1]*, Matti Leppäranta[2], Bin Cheng[3], Zhijun Li[4], Ioanna Merkouriadi[2]

[1]*Department of Basic Sciences, Shenyang Institute of Engineering, Shenyang 110136, CHINA*

[2]*Department of Physics, University of Helsinki, Fi-00014 Helsinki, FINLAND*

[3]*Finnish Meteorological Institute, Fi-00101 Helsinki, FINLAND*

[4]*State Key Laboratory of Coastal and Offshore Engineering, Dalian University of Technology, Dalian 116024, CHINA*

**yangyang-0606@hotmail.com*

ABSTRACT

Global warming impacts on the snow and ice in high-latitude regions, and the presence (or absence) of ice cover has an impact on both regional climate and weather events in the winter-spring season. So, understanding the processes and interactions of lake ice and atmosphere is essential for numerical weather prediction and climate research. In this paper, we perform modeling investigations of the evolution of snow and ice thickness in Lake Vanajavesi (61.13°N, 24.27°E), which is located in southern Finland. Special attention was paid to the atmospheric and solar forcing on the snow and ice thickness. Model calibration was made for the mean climatological conditions with forcing based on the Jokioinen weather station data. The simulated snow, snow-ice and ice thickness showed good agreement with observations. A number of climate sensitivity simulations were carried out. The air temperature, wind speed, cloudiness and solar radiation were selected as the forcing factors, and in each experiment, one factor at a time was changed. The diurnal weather cycle gave significant impact on ice thickness in spring. Ice climatology was highly sensitive to snow conditions.

KEYWORDS

Lake snow and ice; climate impact; air temperature; surface balance

FEDERATION OF FINNISH LEARNED SOCIETIES
Delegation of the Finnish Academies of Science and Letters

Finnish Association for Geophysicists

ISBN 978-952-11-4512-4 (pbk.)
ISBN 978-952-11-4513-1 (PDF)